Electronic Supplementary Material (ESI) for ChemComm.

SUPPLEMENTARY INFORMATION

Engineered peptidic constructs metabolize Amyloid β by self-assembly driven reactions

Tanmay Mondal and Bhubaneswar Mandal*

Laboratory of Peptide and Amyloid Research, Department of Chemistry, Indian Institute of Technology Guwahati, Assam-781039, India

*To whom correspondence should be addressed: bmandal@iitg.ac.in

Table of contents: **Page no.**

1. Reagents and solvents …… 4
2. Procedure of peptide synthesis …… 4
3. Peptide sequences used for the current study…… 5
4. Liquid chromatography and Mass spectrometry …… 7
5. Methods…… 9
    5.1. Aβ sample preparation…… 9
    5.2. Th.T. Fluorescence assay…… 9
    5.3. Circular Dichroism (CD) …… 10
    5.4. Fourier Transformation Infra Red (FTIR) …… 10
    5.5. Transmission Electron Microscopy (TEM) …… 10
    5.6. Atomic Force Microscopy (AFM) …… 11
    5.7. Congo-Red stained Birefringence…… 11
    5.8. Dynamic Light Scattering (DLS) …… 11
    5.9. Large Unilamellar Vesicles…… 12
    5.10. DFT calculation…… 12
6. Characterization data of the peptides…… 13
7. Molecular Docking …… 19
8. Plausible routes of the proteolytic activity of AS1 on mAβ …… 24
9. Plausible routes of the proteolytic activity of AS2 on mAβ …… 30
10. Plausible routes of the proteolytic activity of AS3 on mAβ …… 36
11. Plausible routes of the proteolytic activity of AS4 on mAβ …… 40
12. Comparative map of the existence of mAβ …… 44
13. Plausible routes of self degradation of AS4 (SD-AS4)…… 44
14. Self degradation of mAβ …… 47
15. DFT calculation of the intermediate C'''' …… 49
16. Kinetics study by HPLC and ESI-Mass of mAβ in presence of AS2 …… 50
17. Plausible routes of the proteolytic activity of AS4 on $A\beta_{1-40}$ …… 54
18. MALDI mass spectra of $A\beta_{1-40}$ …… 58
19. Plausible routes of the proteolytic activity of AS4 on mutant DTP28 (negative control)…… 61
20. Self degradation of mutant DTP28 …… 64

21. Inhibition of Amyloid accumulation of $A\beta_{1-40}$ by AS4……..…….……..… 66

21.1. Th.T. Fluorescence assay and CD experiments of $A\beta_{1-40...}$…….……...… 66

21.2. FTIR spectra of $A\beta_{1-40}$…..……..……....… 66

21.3. TEM images and Congo-Red stained Birefringence images of $A\beta_{1-40}$……...67

22. Disruption of preformed $A\beta_{1-40}$ fibril by AS4……..…..…….…….…… 68

22.1. Th.T. Fluorescence assay and CD experiments of $A\beta_{1-40}$……..…….……...… 68

22.2. FTIR spectra of $A\beta_{1-40}$ ……...……....… 68

22.3. TEM images and Congo-Red stained Birefringence images of $A\beta_{1-40}$ ……..…69

23. DLS analysis of inhibiting $A\beta_{1-40}$ fibril formation by AS4……..…..69

24. Preparation of large unilamellar vesicles (LUVs) and carboxyfluorescein entrapment ... 70

25. Vesicle leakage study ……...…… 71

NOTE: AS stands for “artificial a-secretase” in the supporting information.

1. Reagents and solvents:

Rink amide MBHA resin was purchased from GL Biochem (Shanghai) (Loading 0.7 mmol/g). N, N-Diisopropylethylamine (DIPEA) was purchased from Spectrochem Pvt. Ltd. Dimethylformamide (DMF, extrapure grade), dichloromethane (extrapure grade) and acetonitrile of HPLC grade were obtained from Merck (India). Acetic anhydride (synthesis grade), N-methyl imidazole (extrapure), Trifluoroacetic acid (TFA) of extrapure grade were purchased from SRL (India). Milli-Q water at 18.2 Ω was used. All Fmoc (N- terminus protected) amino acids, BOP [(Benzotriazole-1-yloxy) tris (dimethylamino) phosphonium hexafluorophosphate] and human Alzheimer's β-amyloid ($A\beta_{1-40}$) peptide were purchased from GL Biochem (Shanghai).

2. Procedure of peptide synthesis:[1]

All the described peptides were synthesized by standard Fmoc/tBu solid phase peptide synthesis (SPPS) method.200 mg of Rink amide MBHA resin (loading 0.7 mmol) was taken in a 5 ml frit-fitted plastic syringe and was allowed to swell with DCM solvent first and then with DMF solvent. After that, Fmoc group that was attached with the resin was cleaved with 20% piperidine in DMF. The resin was then washed with DMF. Then, 2.5 equivalent of Fmoc Amino acid, 3.0 equivalent of BOP (coupling reagent) and 5.5 equivalent of DIPEA (base) were dissolved in DMF and added to the syringe. The syringe was allowed to rotate by a Stuart blood tube rotator for coupling. After that, the reaction mixture in the syringe was washed with DMF first followed by with DCM. It was then acetylated (capping) with 2 equivalent of acetic anhydride, 2 equivalent of N-methyl imidazole in DCM. The cycle of the cleavage of the Fmoc group of the terminal amino acid and coupling of the desired amino

acids was continued as mentioned above. Finally, cocktail cleavage was carried out with 2ml of TFA:DCM (8.5:1.5) and one drop of H_2O for 3h (or 5h where necessary) to cleave the C-terminus of the peptide from the Rink amide resin. After completion of the synthesis of the peptide sequence, the mixture was precipitated by cold diethyl ether to get the crude peptide that was purified and characterized as specified later.

In case of artificial α-secretases (ASs), side chain modification of lysine unit was carried out via coupling reaction of the crude peptide with mono-benzyl adipate in solution phase, using 1.2 equivalent of BOP (coupling reagent) and 2.5 equivalent of DIPEA (base) in DCM. Mono-benzyl adipate was synthesized also from coupling reaction between 5 equivalent of adipic acid and 1 equivalent of benzyl alcohol, using 2.5 equivalent of EDC.HCl, 14 equivalent of DIPEA, and 0.3 equivalent of HOBt in DCM for 12h followed by evaporation and performed silica gel column chromatography to get pure product.

3. Peptide sequences used for the current study are as follows:

3.1. Sequence of model Aβ peptide (mAβ): Ac-V-H-H-Q-K-L-V-F-F-G-G-NH_2

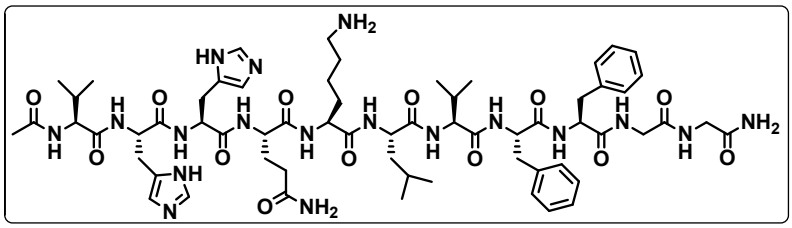

Figure S1: Chemical structure of the mAβ peptide.

3.2. Sequence of AS1:

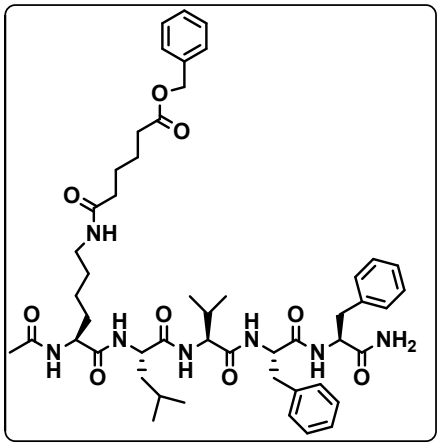

Figure S2: Chemical structure of the AS1.

3.3. Sequence of AS2:

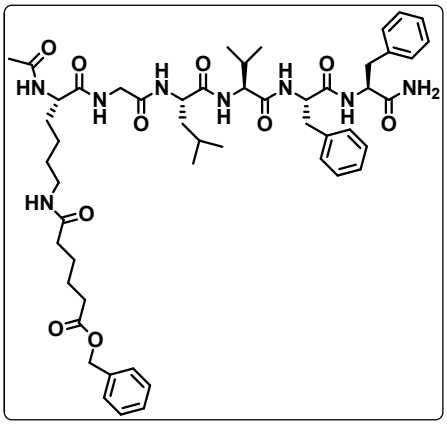

Figure S3: Chemical structure of the AS2.

3.4. Sequence of AS3:

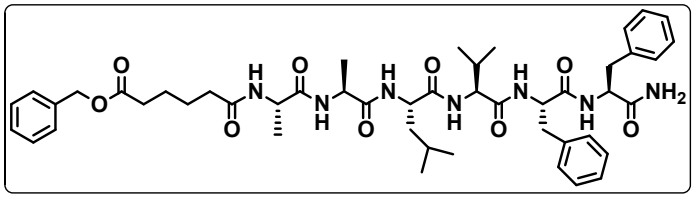

Figure S4: Chemical structure of the AS3.

3.5. Sequence of AS4:

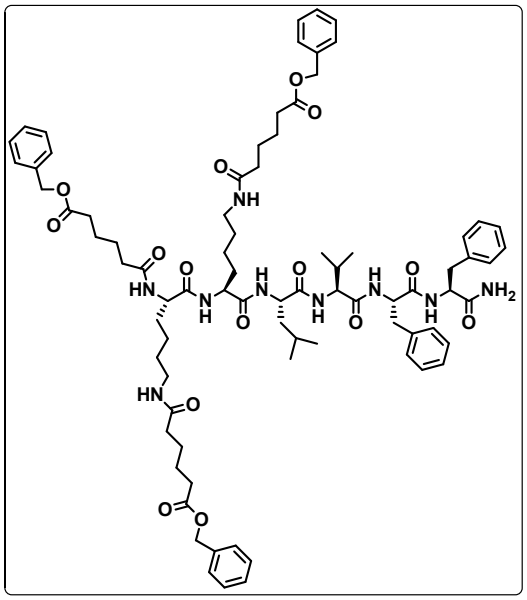

Figure S5: Chemical structure of the AS4.

3.6. Sequence of mutant DTP28 (negative control):
GSSDSIGPLGYGKTVDHTKVNSPLSLFG-NH_2

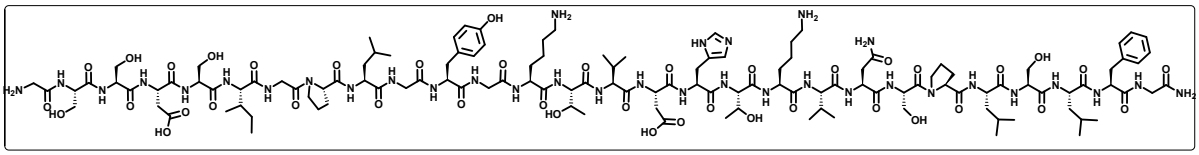

Figure S6: Chemical structure of the negative control peptide.

4.1. Liquid chromatography:

Crude peptides were dissolved in CH_3CN/H_2O mixture and purified by RP-HPLC (Waters 600E) using a C18-μ Bondapak column at a flow rate of 4 mL/ min. Binary solvent system [solvent A (0.1 % TFA in H_2O) and solvent B (0.1 % TFA in CH_3CN)] were used. Waters 2489 UV detector was used with dual detection at 214 and 254 nm. A total run time of 20 min. was used for purification and gradient was set as 5−100 % CH_3CN for 18 min followed by 100% CH_3CN till 20 min.

Purity of the peptides was confirmed using Waters 600E analytical HPLC system. An Ascentis C18 analytical column, flow rate of 1 ml/min, linear gradient of 5-100% CH_3CN over 18 minutes in a total run time of 20 min were used. Dual wavelength was selected at 214 nm and 254 nm.

Kinetics study was done using Waters 600E analytical HPLC system also. An Ascentis C18 analytical column, flow rate of 0.8 ml/min, linear gradient of 5-50-100% CH_3CN over 0-10-18 minutes in a total run time of 20 min were used. Dual wavelength was selected at 214 nm and 254 nm.

4.2. Mass spectrometry:

Mass of the peptide samples were analyzed on Agilent-Q-TOF 6500 instrument, in ESI positive mode, equipped with Mass hunter work station software.

Sample preparation for MALDI Mass analysis. Purified and lyophilized peptide samples of mAβ, AS1, AS2, AS3 and AS4 were dissolved in PBS (50 mM, pH 7.4) to obtain stock solutions of 200 μM. While mAβ was pretreated with TFA and HFIP, 6% Ethanol was added to PBS (50 mM, pH 7.4) solutions of ASs to get clear stock solutions. They were co-incubated appropriately at 37 °C on a water bath and tested in a time dependent manner.

MALDI mass of the peptide samples were analyzed using CHCA matrix on BRUKER autoflex speed instrument which consists of a MALDI ionization source for samples in the solid state and a TOF/TOF mass analyzer, equipped with Bruker daltonics flex analysis software. To prepare CHCA matrix, 1.0 mg of CHCA was dissolved in 100 μL of CH_3CN/H_2O (1:1) containing 0.1% TFA. Parameters used for MALDI mass analyses were as follows: Processing method: SC_Peptide_Cent, Method: RP_700-3500_Da.par, Reflector: 3x 2076v, Sample Carrier: Random walk - complete sample mode (off mode where necessary).

5. Methods:

5.1. Aβ sample preparation. $A\beta_{1-40}$ was purchased from GL Biochem Shanghai, China and directly used without purification. 2.1 mg of $A\beta_{1-40}$ was dissolved in 20 μL of TFA to get disaggregated $A\beta_{1-40}$. TFA was evaporated using nitrogen gas. To remove TFA completely, HFIP was added and evaporated using nitrogen gas to get disaggregated $A\beta_{1-40}$ peptide. This process was repeated twice. 2.0 ml of PBS (50 mM, pH 7.4) was added into the disaggregated material, followed by sonication and vortex to obtain transparent solution and the total solution was divided into 10 equal portion followed by addition of 800 μL of PBS to each portion to obtain a final concentration of 50 μM.

5.2. Thioflavin T Fluorescence Assay.[2] Thioflavin T (ThT) was purchased from Sigma Aldrich, and concentration of 50 μM in PBS (50 mM, pH 7.4) was prepared as a stock solution and stored at 4 °C with dark cover to prevent degradation from light. Purified solid peptide samples (mAβ and $A\beta_{1-40}$ after TFA, HFIP treatment; and, artificial α-secretases and negative control directly) were dissolved in PBS (50 mM, pH 7.4) to obtain a stock solution of variable concentrations (50 μM of $A\beta_{1-40}$, 200 μM of mAβ and different molar ratios of artificial α-secretases) and incubated at 37 °C on a water bath. In case of ASs, 6% Ethanol was used along with PBS (50 mM, pH 7.4) to get a clear stock solution. To perform the fluorescence study, 40 μL of peptide sample was taken out from the stock solution and was mixed with 200 μL of ThT solution (50 μM); final volume of 400 μL was made up with PBS (50 mM, pH 7.4). For a desired stock solution three different replicate solutions were prepared. For ThT fluorescence assay, emission was measured at 485 nm and excitation at 440 nm, using a slit of 5 nm on a Fluoromax-4, Horiba instrument. Text file was taken from the instrument and OriginPro 8 software was used to plot the graph. Three different sets of

replicate solutions were scanned separately for each data point and average was taken with observed standard deviation.

5.3. Circular Dichroism (CD).[3] Peptide stock solutions were prepared in the same way as described earlier for sample preparation of ThT fluorescence assay. To perform the CD study, stock solution was diluted with respective buffer solutions to obtain final concentration of 100 μM (50 μM for $A\beta_{1-40}$ peptide). 400 μL of the sample was taken in a cuvette (Model SPC-001) having bandwidth of 1 mm. Three measurements were collected. Spectra were recorded from 190 nm to 260 nm on a JASCO (Model J-1500) instrument. Observed ellipticity (mDeg) [obtained from Spectra Manager] was converted to mean residue molar ellipticity using the following equation:

$[\theta]$ (deg. cm^2 .$dmol^{-1}$) = Ellipticity (mdeg). 10^6 / Pathlength (mm). [Protein] (μM). N

5.4. Fourier Transformation Infra Red (FTIR).[2] Peptide stock solutions were prepared in the same way as described earlier for sample preparation of ThT fluorescence assay. 20 μL aliquot was taken from the stock, mixed with KBr and dried completely at 50ºC, and a pellet was prepared. For each sample, the spectrum was recorded after required time intervals (immediately after sample preparation, after 28 and 45 days). The background scan was subtracted from the sample scans and OriginPro 8 software was used to plot the graph from text files.

5.5. Transmission Electron Microscopy (TEM).[2] 10 μL aliquot from the stock peptide solution after incubation of 45 days (7 days, 28 days where necessary) was added over the carbon coated copper grid and allowed to float for 1 min. Then 2% uranyl acetate solution (10 μL) was added on the same grid for negative staining and allowed to float for a further 1 min. Blotting paper was used to remove excess solution. The sample was air-dried at room

temperature and kept in desiccators. TEM analyses were performed on JEOL instrument (Model: JEM 2100) at 200 kV.

5.6. Atomic Force Microscopy (AFM). To perform the AFM analysis, stock solution was diluted with water to obtain final concentration of 5 μM (1 μM for $A\beta_{1-40}$ peptide) after incubation of 45 days (7 days where necessary). 20 μL aliquot from the diluted peptide solution was added over the coverslips, washed with Milli-Q water and dried at room temperature and analysed on Agilent stm 5500 instrument.

5.7. Congo-Red Stained Birefringence.[2] Commercially available Congo red was purchased from Sigma Aldrich and dissolved in 80 % aqueous ethanol to prepare a saturated solution. Then sodium chloride solution (saturated) was added into the saturated Congo red solution and filtered to get needed Congo red solution for analysis.

After 45 days (28 days where necessary) of incubation, 20 μL aliquot of the required peptide solution was taken from the stock and placed over a glass slide followed by 40 μL of the saturated Congo red solution. Blotting paper was used to remove excess solution. The sample was dried at room temperature and kept in desiccators. Birefringence analyses were performed on Leica ICC50 HD polarizable microscope.

5.8. Dynamic Light Scattering (DLS).[4] The size distributions of $A\beta_{1-40}$ aggregates and AS4 were analysed using Zetasizer Nano-ZS90 (Malvern Instruments). To perform the DLS analysis, stock solutions were diluted with Milli-Q water to obtain final concentration of 100 μM (50 μM for $A\beta_{1-40}$ peptide), after different time interval of incubation upto 7 days. All the DLS results were reported as the average of three measurements.

5.9. Large Unilamellar Vesicles (LUVs) Studies.[5] Dye leakage studies were performed using carboxyfluorescein dye entrapped LUVs to check toxicity of the peptide fragments generated from $A\beta_{1\text{-}40}$ by proteolytic cleavage by AS4. Details are described later.

5.10. DFT Calculation. The most stable conformation of the intermediates was obtained after performing density functional theory (DFT) based methods using B3LYP as energy functional and 6-31G as basis set through Gaussian 5.0.9 program.

6. Characterization data of the peptides:

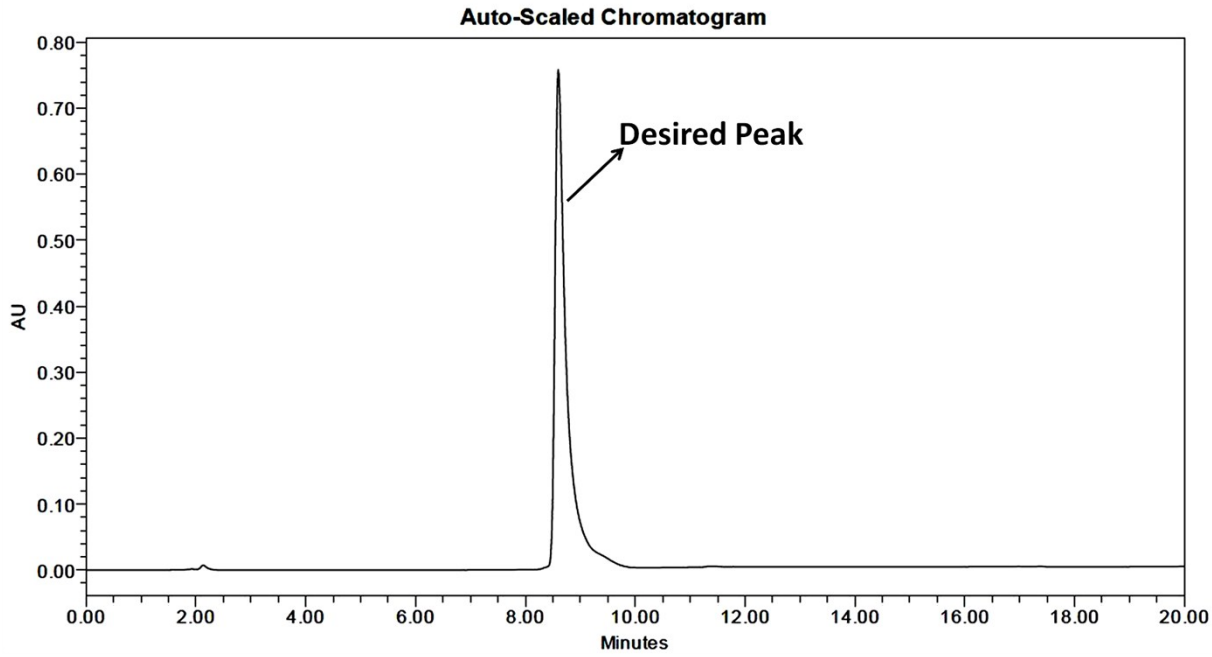

Figure S7: HPLC profile picture of the pure mAβ peptide.

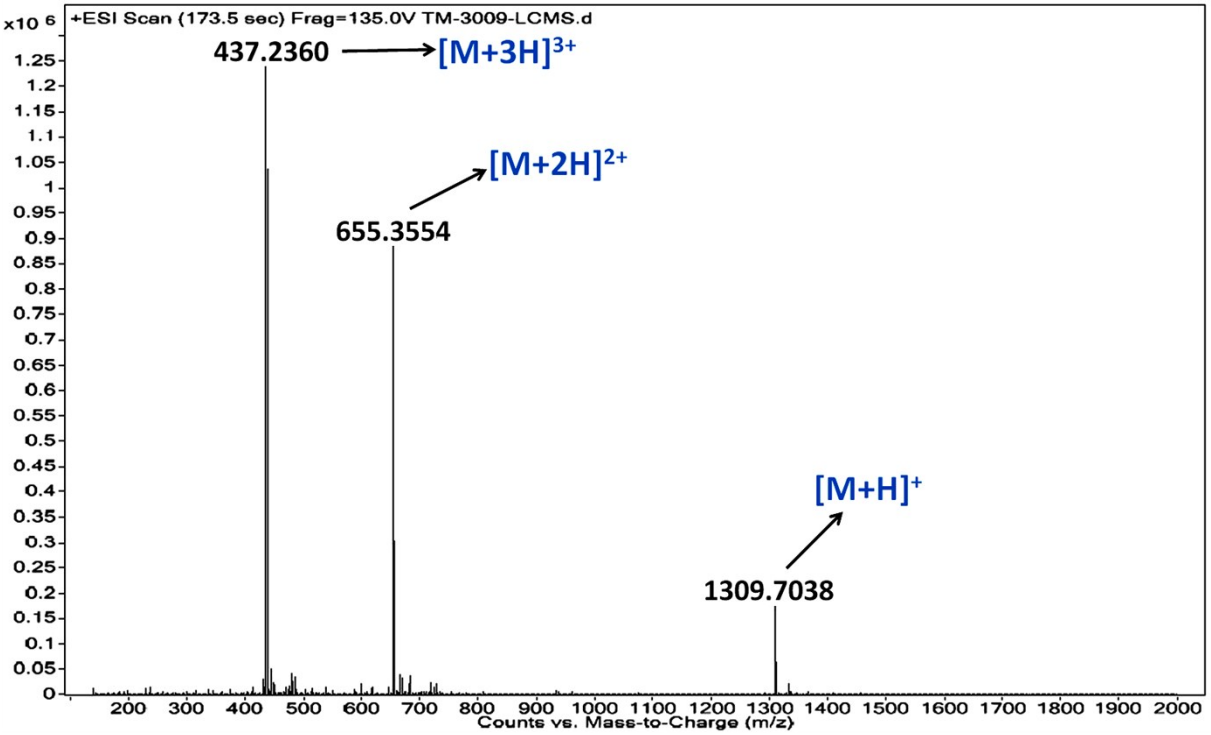

Figure S8: ESI-MS profile picture of the pure mAβ peptide. Calculated m/z for $C_{63}H_{92}N_{18}O_{13}$ $[M+H]^+$ is 1309.7097, observed 1309.7038, calculated m/z for $C_{63}H_{92}N_{18}O_{13}$ $[M+2H]^{2+}$ is 655.3548, observed 655.3554, calculated m/z for $C_{63}H_{92}N_{18}O_{13}$ $[M+3H]^{3+}$ is 437.2365, observed 437.2360.

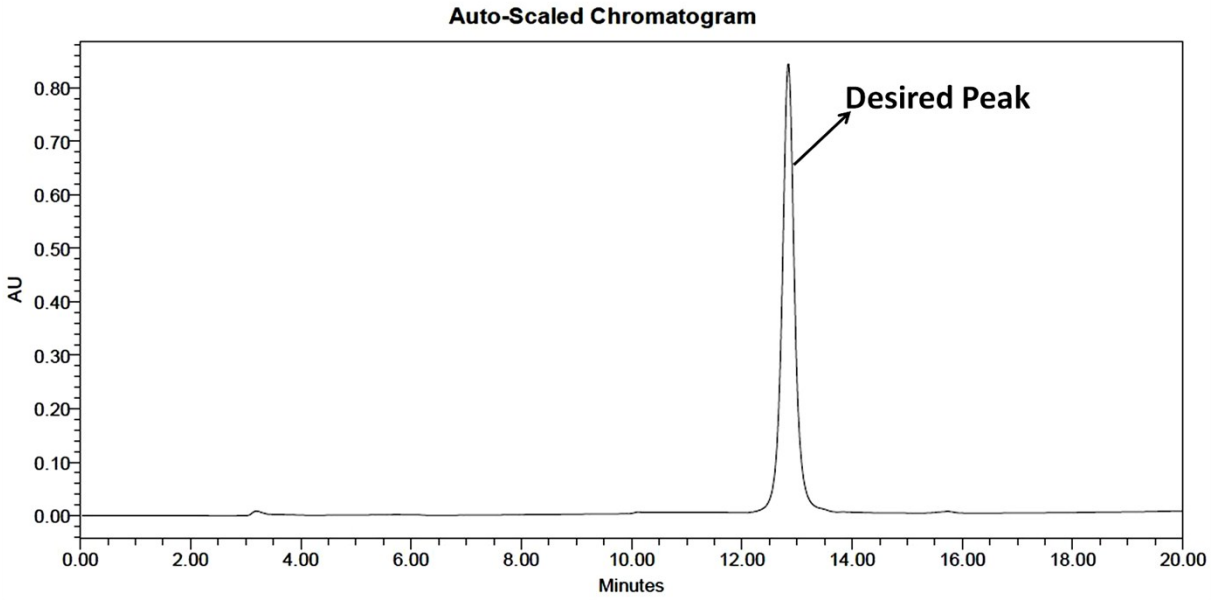

Figure S9: HPLC profile picture of the pure AS1.

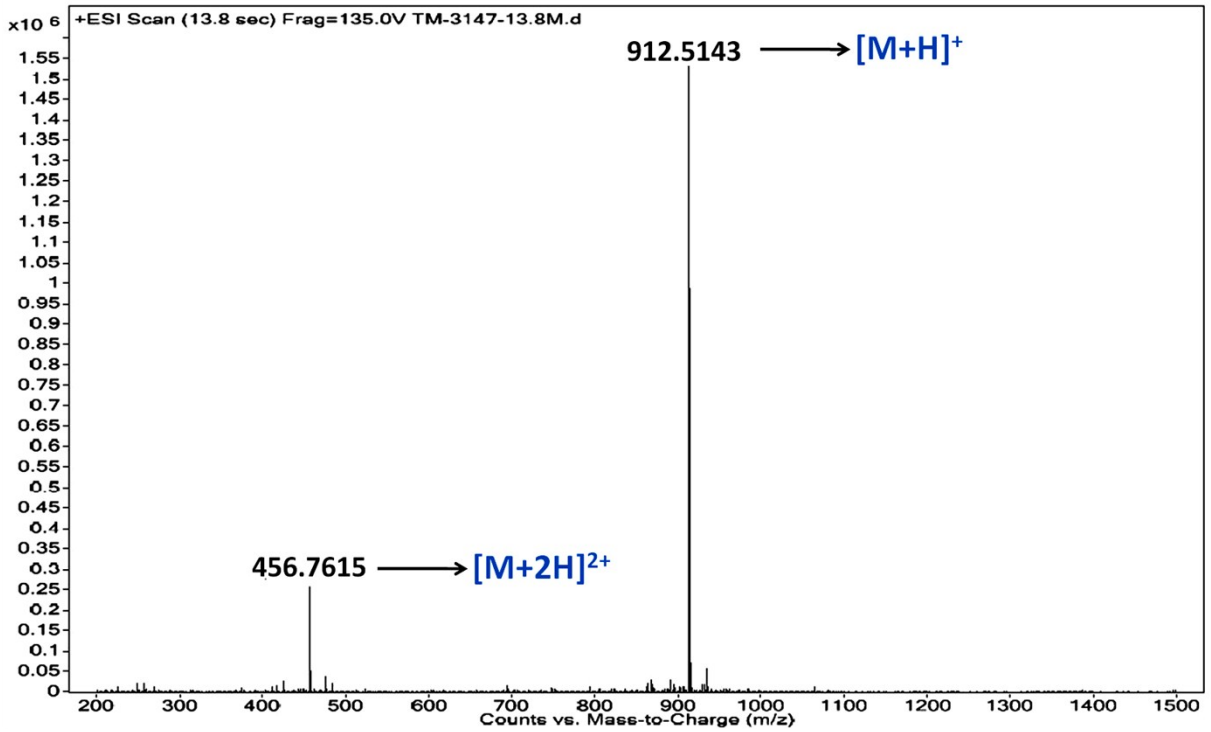

Figure S10: ESI-MS profile picture of the pure AS1. Calculated m/z for $C_{50}H_{69}N_7O_9$ $[M+H]^+$ is 912.5157, observed 912.5143, calculated m/z for $C_{50}H_{69}N_7O_9$ $[M+2H]^{2+}$ is 456.7578, observed 456.7615.

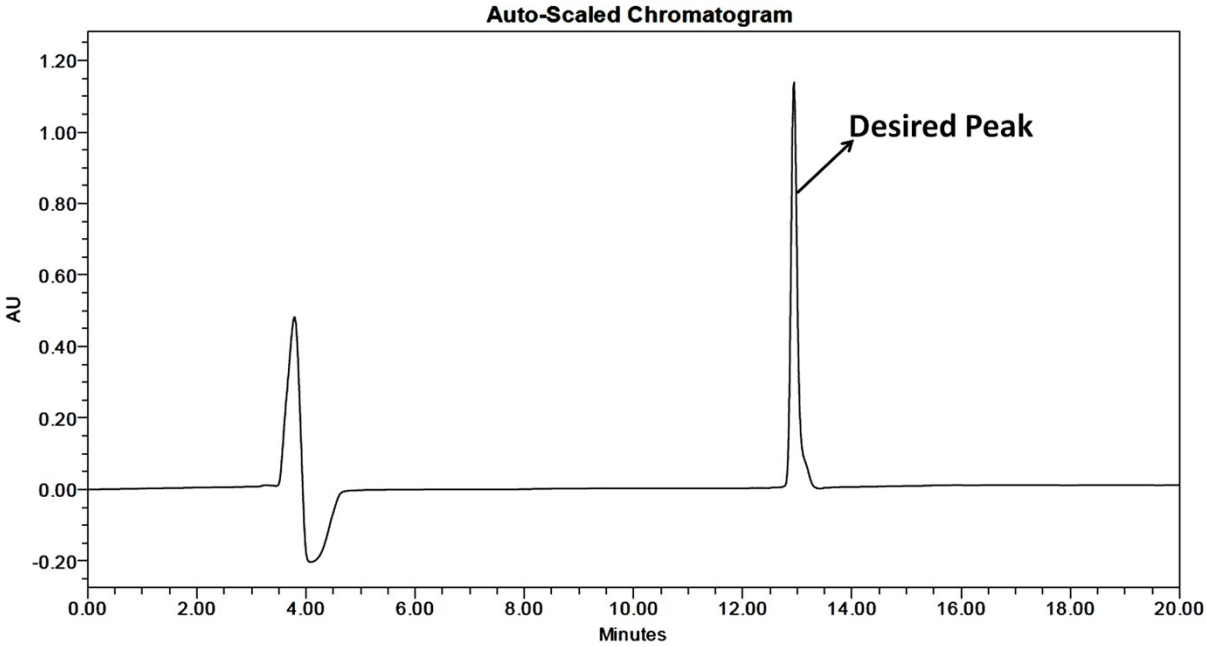

Figure S11: HPLC profile picture of the pure AS2.

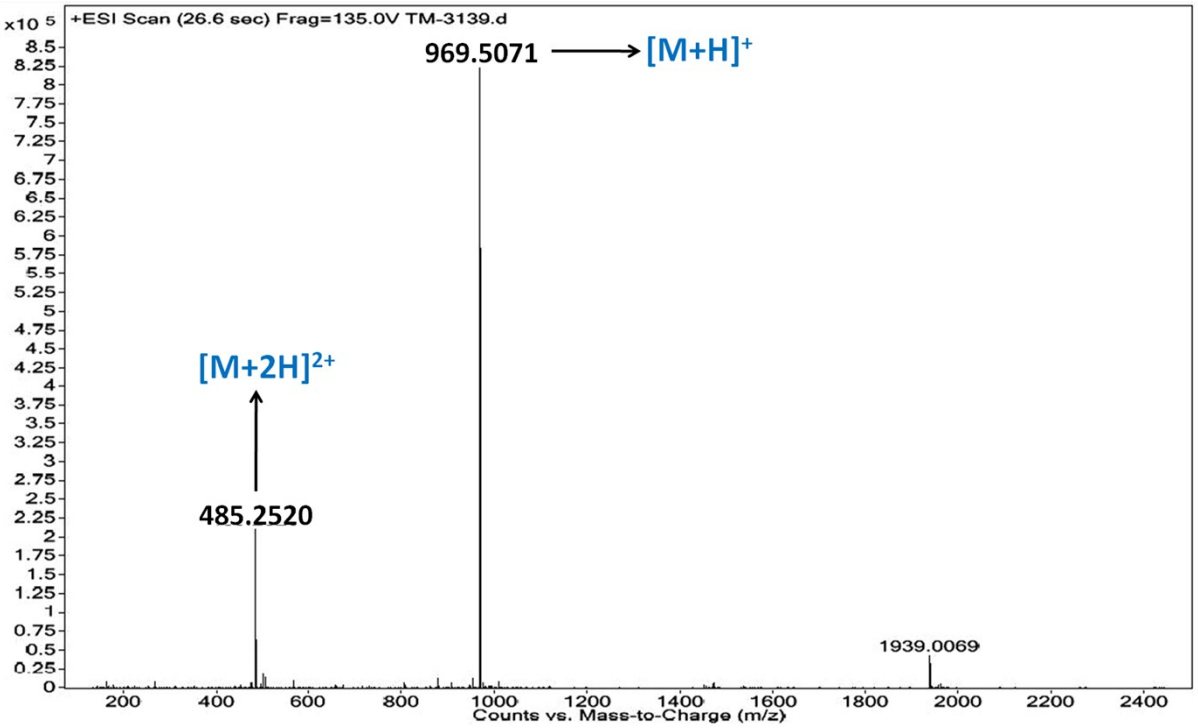

Figure S12: ESI-MS profile picture of the pure AS2. Calculated m/z for $C_{52}H_{72}N_8O_{10}$ $[M+H]^+$ is 969.5371, observed 969.5071, calculated m/z for $C_{52}H_{72}N_8O_{10}$ $[M+2H]^{2+}$ is 485.2685, observed 485.2520.

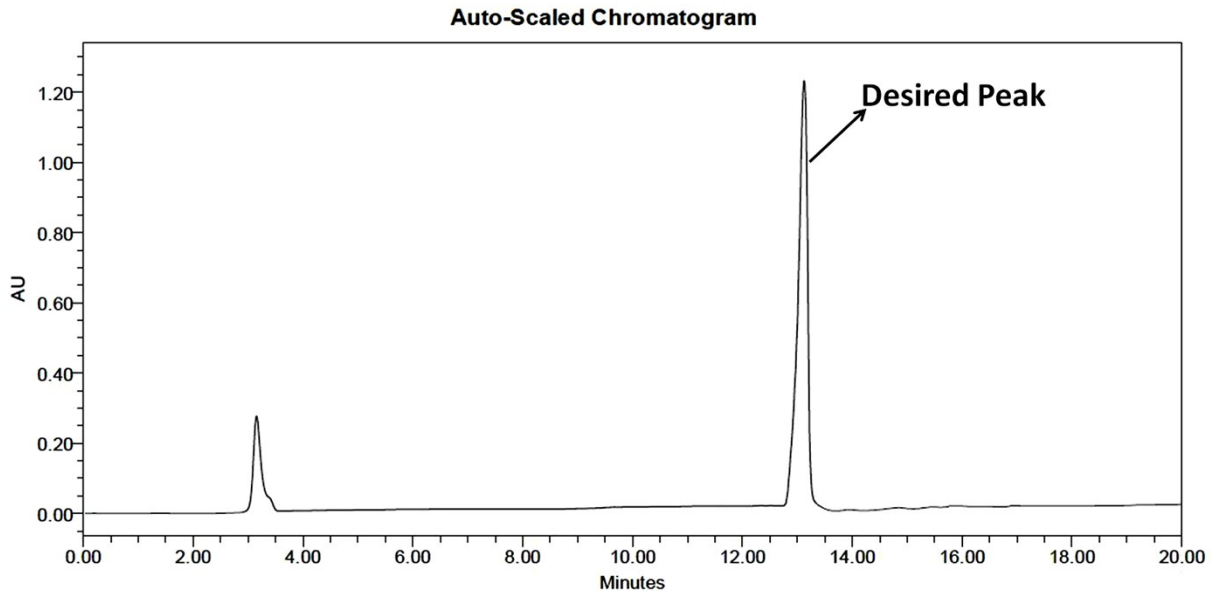

Figure S13: HPLC profile picture of the pure AS3.

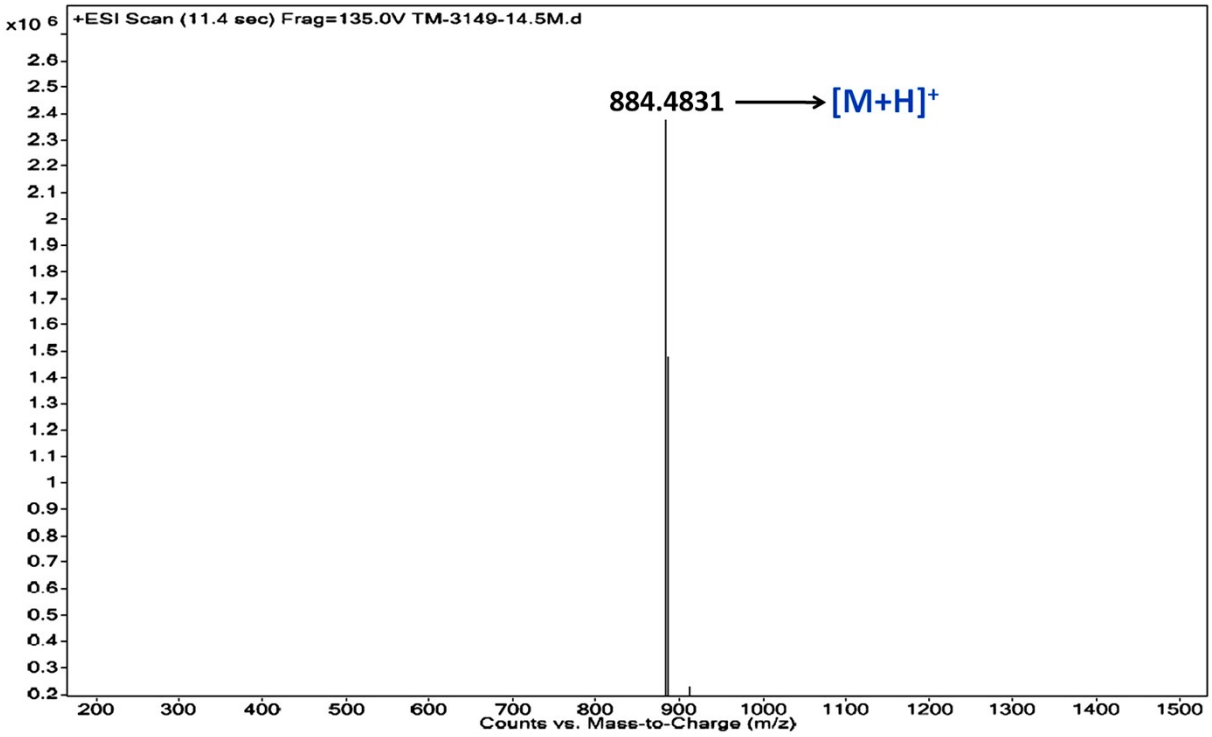

Figure S14: ESI-MS profile picture of the pure AS3. Calculated m/z for $C_{48}H_{65}N_7O_9$ $[M+H]^+$ is 884.4844, observed 884.4831.

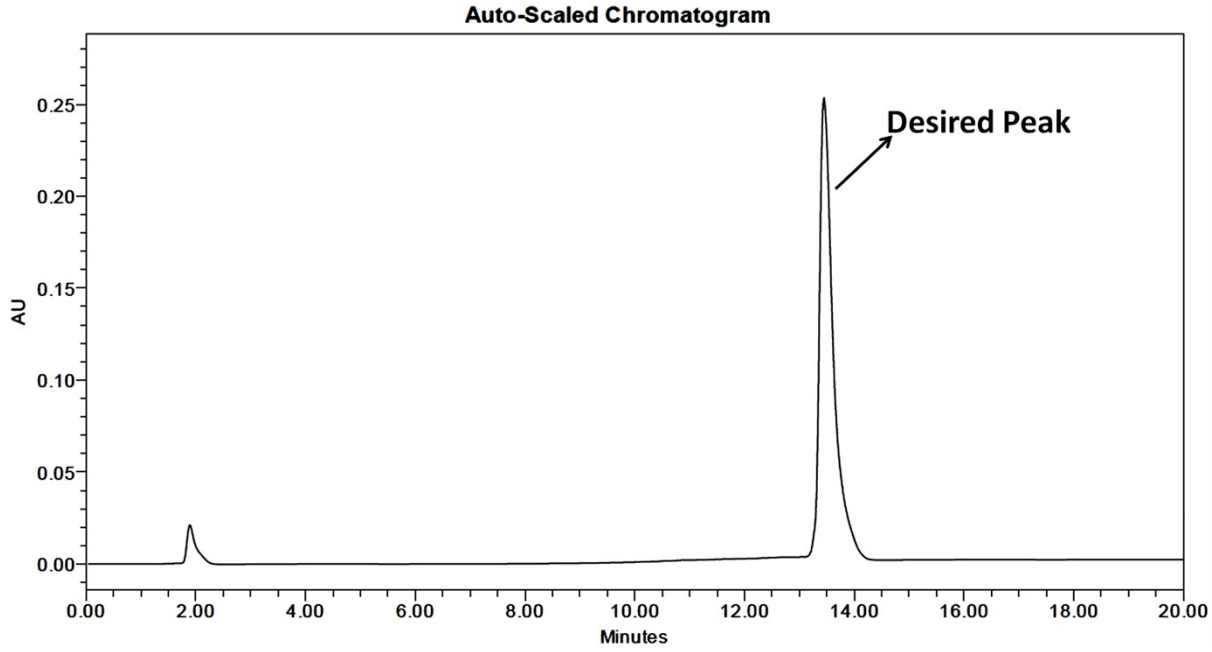

Figure S15: HPLC profile picture of the pure AS4.

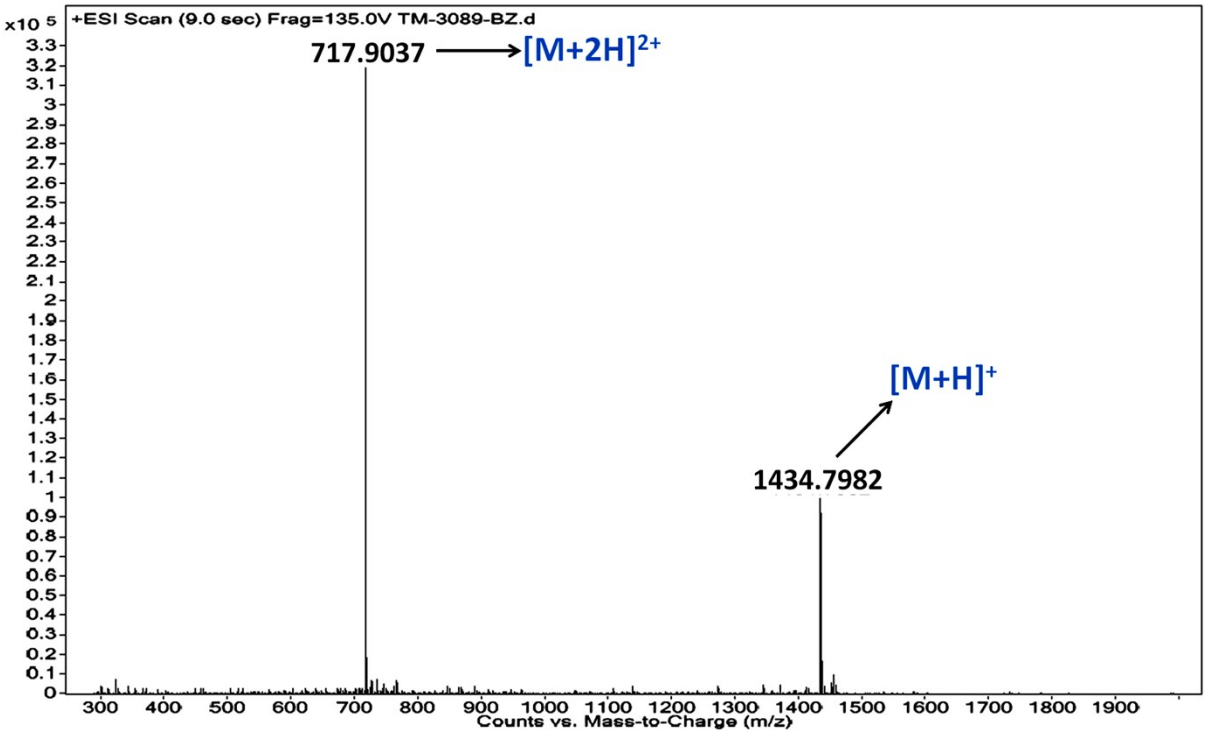

Figure S16: ESI-MS profile picture of the pure AS4. Calculated m/z for $C_{80}H_{107}N_9O_{15}$ $[M+H]^+$ is 1434.7900, observed 1434.7982, calculated m/z for $C_{80}H_{107}N_9O_{15}$ $[M+2H]^{2+}$ is 717.8950, observed 717.9037.

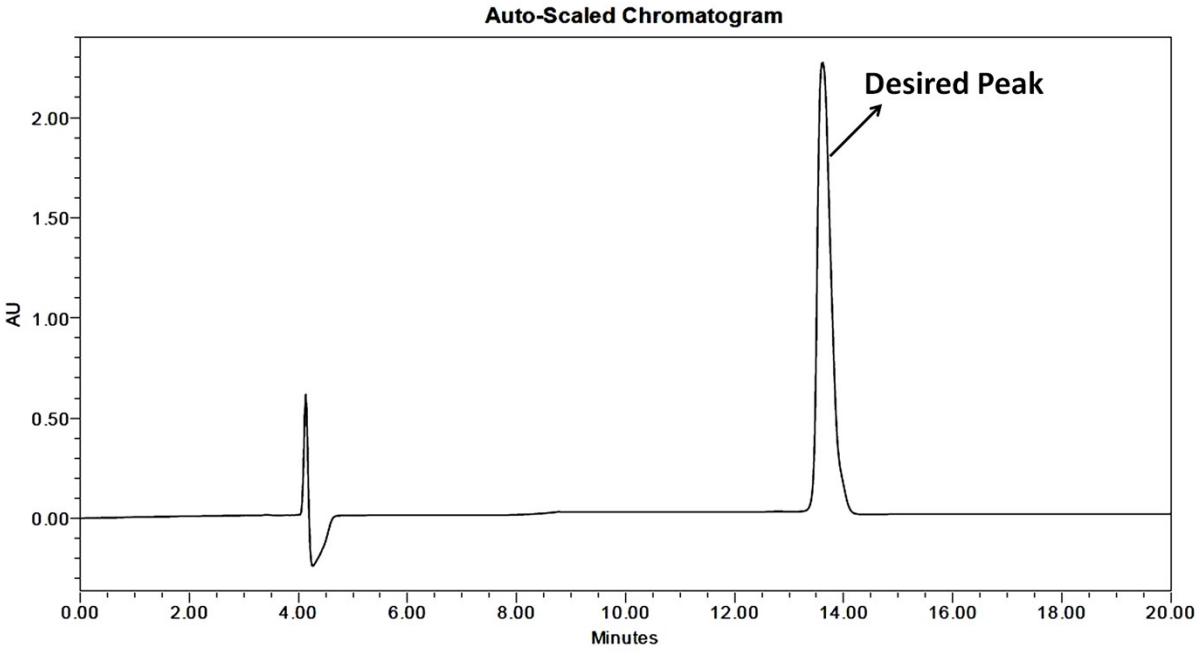

Figure S17: HPLC profile picture of the pure mutant DTP28.

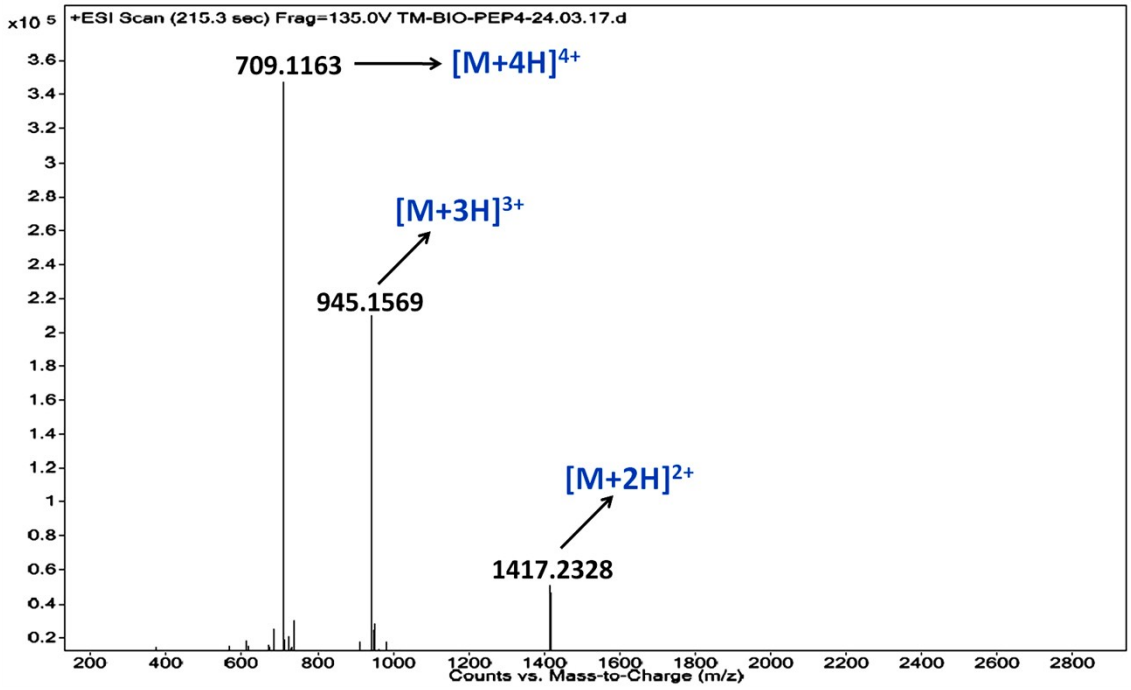

Figure S18: ESI-MS profile picture of the purified mutant DTP28. Calculated m/z for $C_{125}H_{198}N_{34}O_{41}$ $[M+2H]^{2+}$ is 1417.5564 and observed 1417.2328, calculated m/z for $C_{125}H_{198}N_{34}O_{41}$ $[M+3H]^{3+}$ is 945.3709 and observed 945.1569, calculated m/z for $C_{125}H_{198}N_{34}O_{41}$ $[M+4H]^{4+}$ is 709.2782 and observed 709.1163.

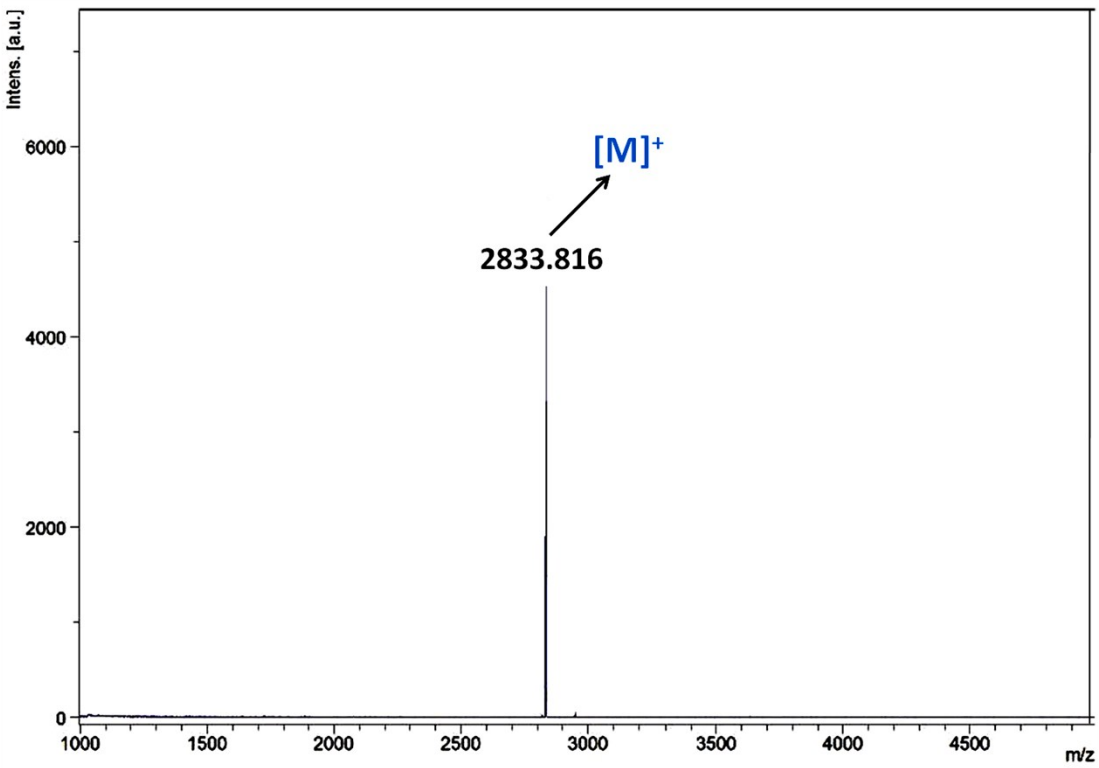

Figure S19: MALDI profile picture of the purified mutant DTP28. Calculated m/z for $C_{125}H_{198}N_{34}O_{41}$ $[M]^+$ is 2833.1128 and observed 2833.8160.

7. Molecular Docking:[6]

AutoDock Vina version 1.1.2 software was used for molecular docking study. At first, a segment of helical and fibril $A\beta_{1\text{-}40}$ were extracted from RCSB protein data bank (PDB ID: 4NGE and 2M4J respectively).[7] AutoDock 4.2 MGL Tools version 1.5.6 software package was used for protein preparation. Water molecules were removed to avoid error; polar hydrogen atoms were added to the protein; Gasteiger charges of the macromolecule were added and saved as PDBQT (for protein) format. OpenBabel version 2.4.1 software was used to convert ligand in PDB format after minimizing energy [obtained from DFT calculation; Calculation Method: B3LYP, Basis Set: 6-31G] and the PDB file was modified by addition of Gasteiger charges. PDBQT format of the ligand was generated to coordinate files, which includes atomic partial charges and atom types. Torsion angles were calculated to assign the

fixable and non-bonded rotation of molecules. Grid file was customized by using Auto Grid version 4.2 to calculate the grid parameters. Grid file is an imaginary box where within the range of volume, the given ligand can find the best possible binding site with lowest binding energy and higher binding affinity; short grid was generated to recognize the binding region of the protein molecule (receptor). We performed blind docking experiments of ASs with grid volume of 40x58x40 points (60x60x60 for AS4), grid spacing of 0.803 Å (1.000 Å for AS4) and centred (3.130, -3.283, -17.750) on the receptor helical $A\beta_{1-40}$ peptide (PDB ID: 4NGE). Also we performed blind docking experiments of AS4 (of different units) with fibril $A\beta_{1-40}$ peptide (PDB ID: 2M4J). In that case, grid volumes were (66x96x56 for 1 unit, 122x124x68 for 3 units, 112x112x78 for 4 units, 110x108x74 for 6 units), grid spaces were (0.814 Å for 1 unit, 0.900 Å for 3 units, 0.903 Å for 4 units, 1.000 Å for 6 units), centres were (3.655, -20.332, 101.713 for 1 unit; -8.891, -6.213, 101.870 for 3 units; -5.675, -9.676, 103.120 for 4 units; -8.735, -6.099, 104.448 for 6 units). After completion of docking, output file was generated as ligand_out.pdbqt format which contains binding affinity (in kcal/mol) and RMSD lower bound, RMSD upper bound. PyMOL version 1.7.4.5 software was used for molecular visualization and viewing the docking results. The active site regions were selected and labelled them as needed. It was observed that, ASs interact or bind well in the helical $A\beta_{1-40}$ binding pocket having binding affinity -5.9 kcal/mol (for AS1), -5.4 kcal/mol (for AS2), -6.2 kcal/mol (for AS3), and -6.6 kcal/mol (for AS4). Interestingly, AS4 is showing maximum binding among ASs. Also AS4 binds well in the fibril $A\beta_{1-40}$ binding pocket, whether the extracted $A\beta_{1-40}$ unit became one (binding affinity -4.8 kcal/mol), or three (binding affinity -3.9 kcal/mol), or four (binding affinity -5.0 kcal/mol), or even six (binding affinity -6.2 kcal/mol). We found that interacting amino acids in the $A\beta_{1-40}$ binding pocket are 17Leu, 18Val, 19Phe, and 20Phe, in most of the cases. Finally, AS4 was docked into helical C-terminal domain of APP (C99, residues 683-728) [PDB ID: 2LP1], and it was observed

that AS4 fitted well in the APP binding pocket having binding affinity -5.3 kcal/mol where the interacting amino acids in the pocket were ^{687}KLVF^{691}F.

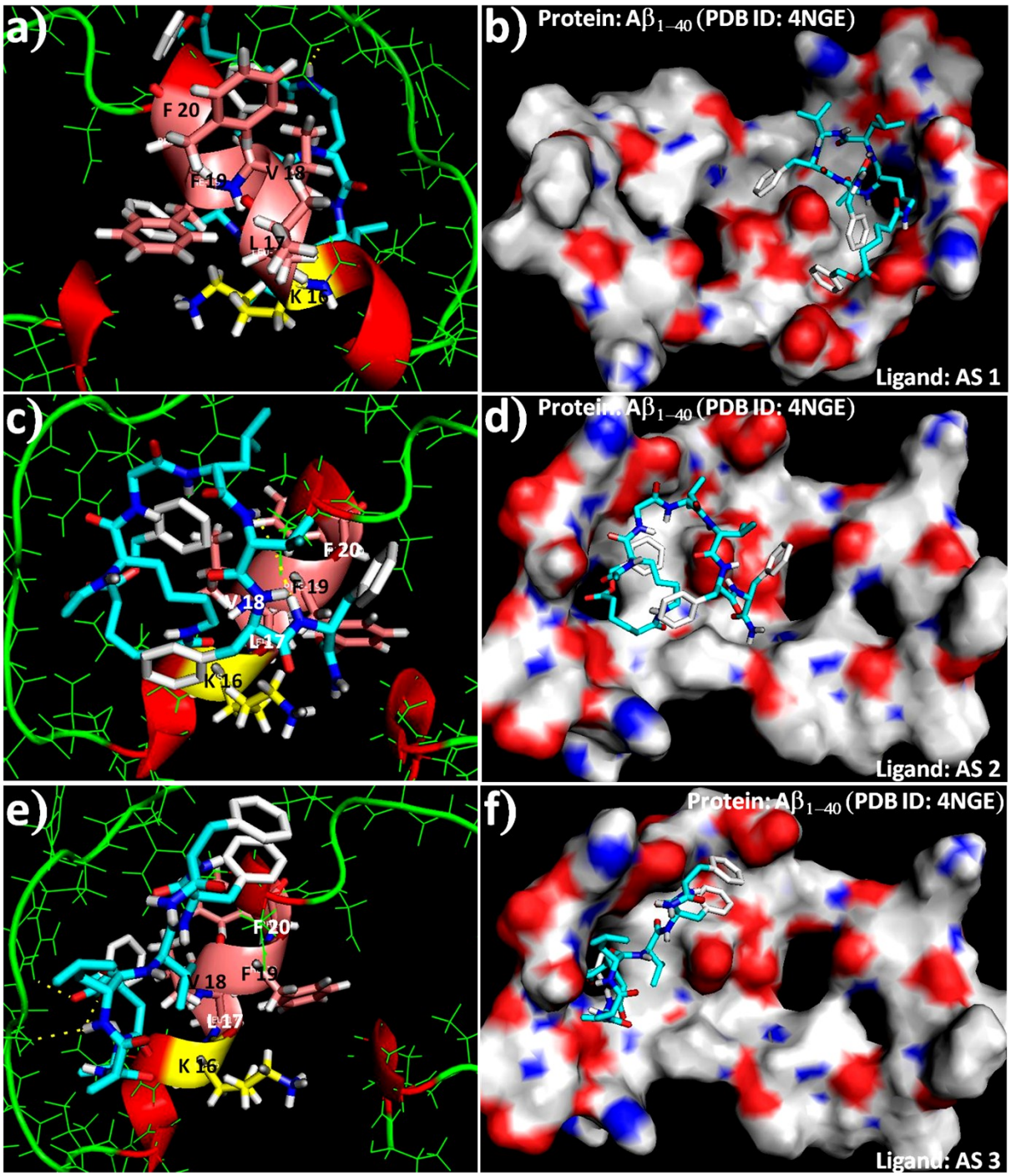

Figure S20: Molecular docking images of AS1 (a, b), AS2 (c, d), and AS3 (e, f) into helical $A\beta_{1-40}$ (PDB ID 4NGE) reveals that ASs binds at the binding site (^{16}KLVF^{20}F) with binding affinity -5.9 kcal/mol, -5.4 kcal/mol , and -6.2 kcal/mol, respectively. Structures are shown as line and cartoon representation (for a, c, e), and surface representation (for b, d, f). The surface of $A\beta_{1-40}$ is coloured according to the charges of the atoms where negatively and positively charged zones are represented in red and blue, respectively.

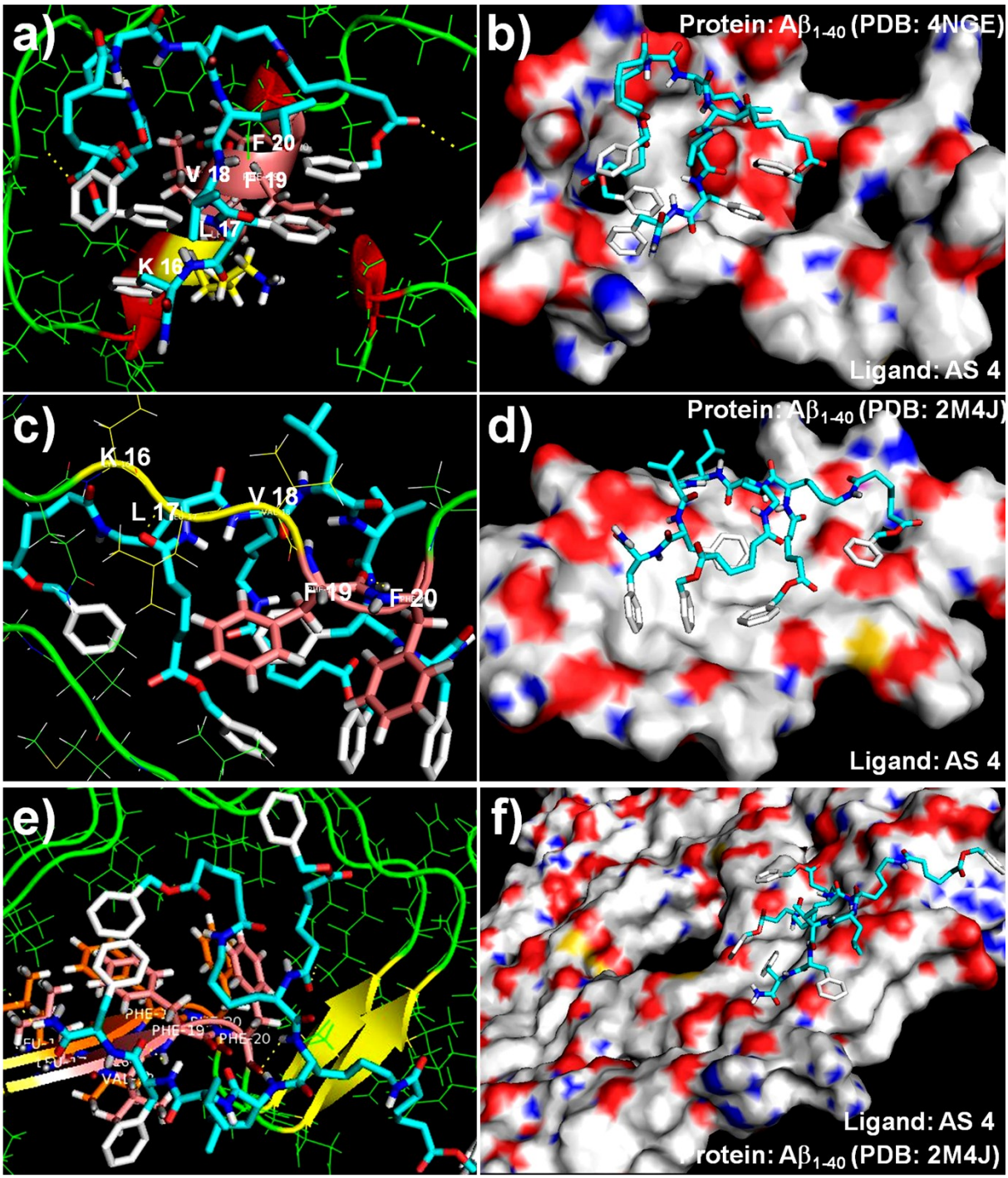

Figure S21: Molecular docking images of AS4 into helical (a-b), and fibril (c-f) $A\beta_{1-40}$ (PDB ID 4NGE for a, b and 2M4J for c-f) reveals that AS4 binds at the binding site (^{16}KLVF^{20}F) with binding affinity -6.6 kcal/mol, -4.8 kcal/mol, and -6.2 kcal/mol, respectively. Structures are shown as line and cartoon representation (for a, c, e), and surface representation (for b, d, f). The surface of $A\beta_{1-40}$ is coloured according to the charges of the atoms where negatively and positively charged zones are represented in red and blue, respectively.

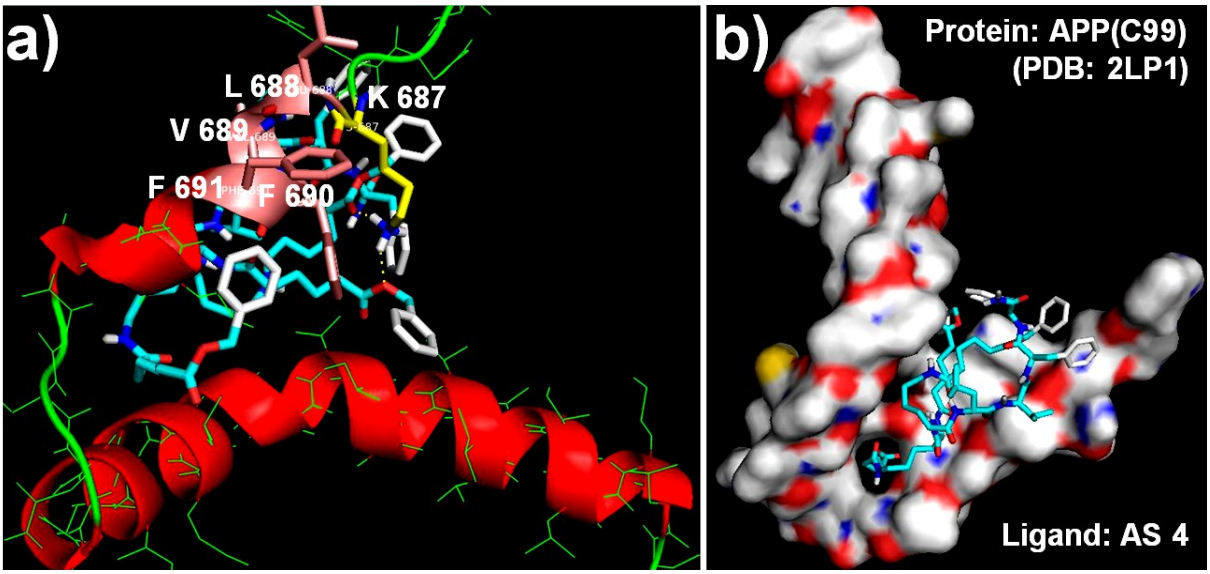

Figure S22: Molecular docking images of AS4 into (a-b) helical C-terminal domain of the amyloid precursor protein (C99) (PDB ID: 2LP1) reveals that AS 4 binds at the binding site (^{687}KLVF^{691}F) with binding affinity -5.3 kcal/mol. Structures are shown as line and cartoon representation (for a), and surface representation (for b). The surface of APP is coloured according to the charges of the atoms where negatively and positively charged zones are represented in red and blue, respectively.

8. Plausible routes of the proteolytic cleavage of mAβ by AS1:

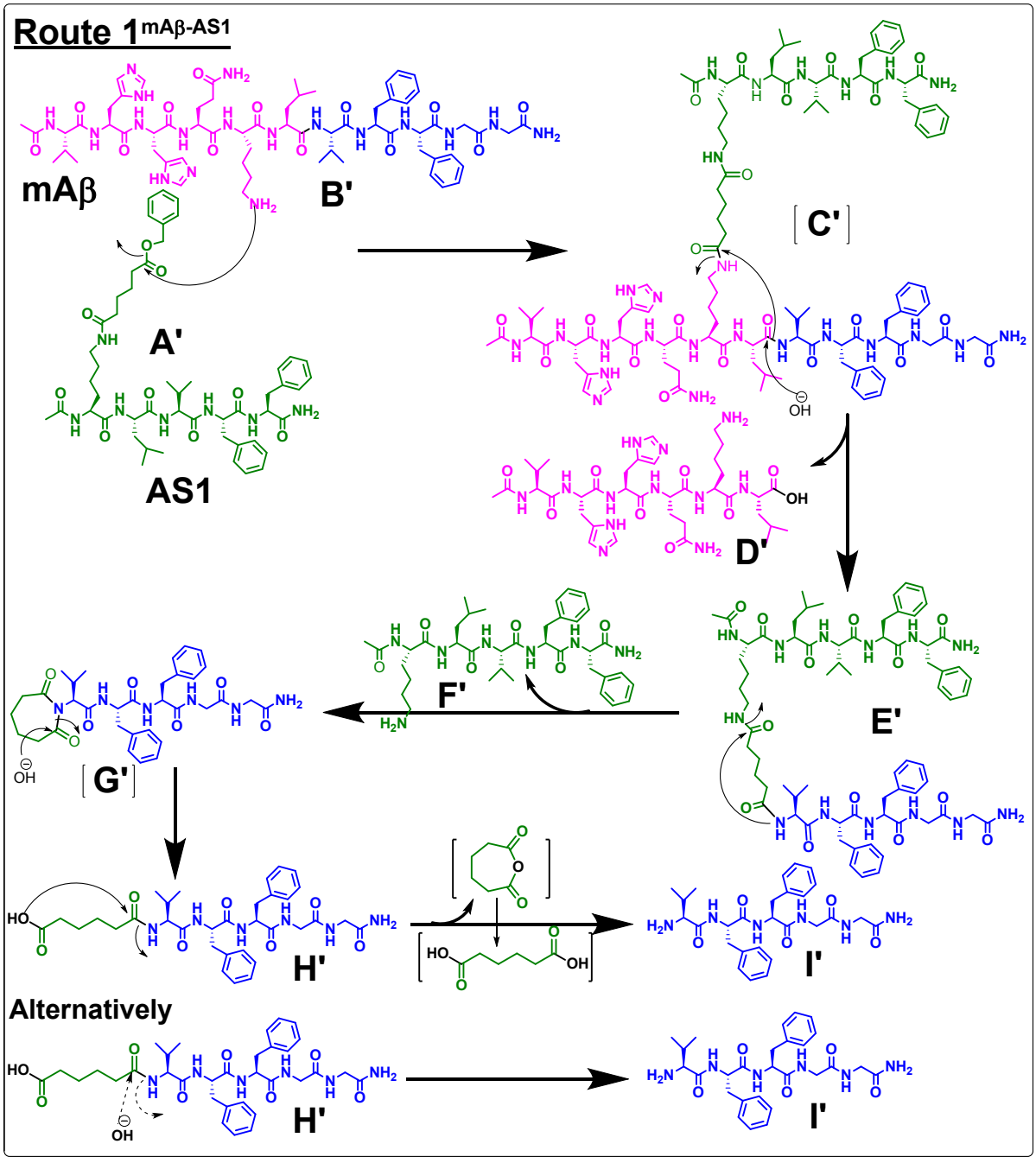

Figure S23. Plausible route for proteolysis of mAβ by AS1 into various fragments (Route 1$^{mAβ-AS1}$).

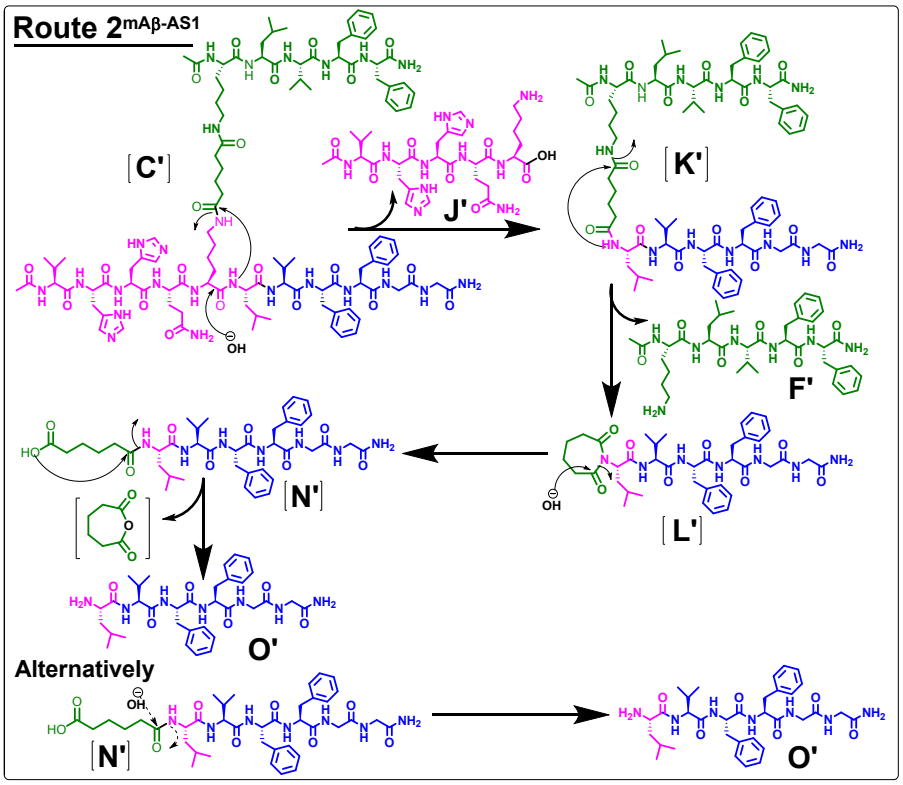

Figure S24. Plausible routes of cleavage of mAβ into various fragments by AS1 (Route 2$^{mAβ-AS1}$).

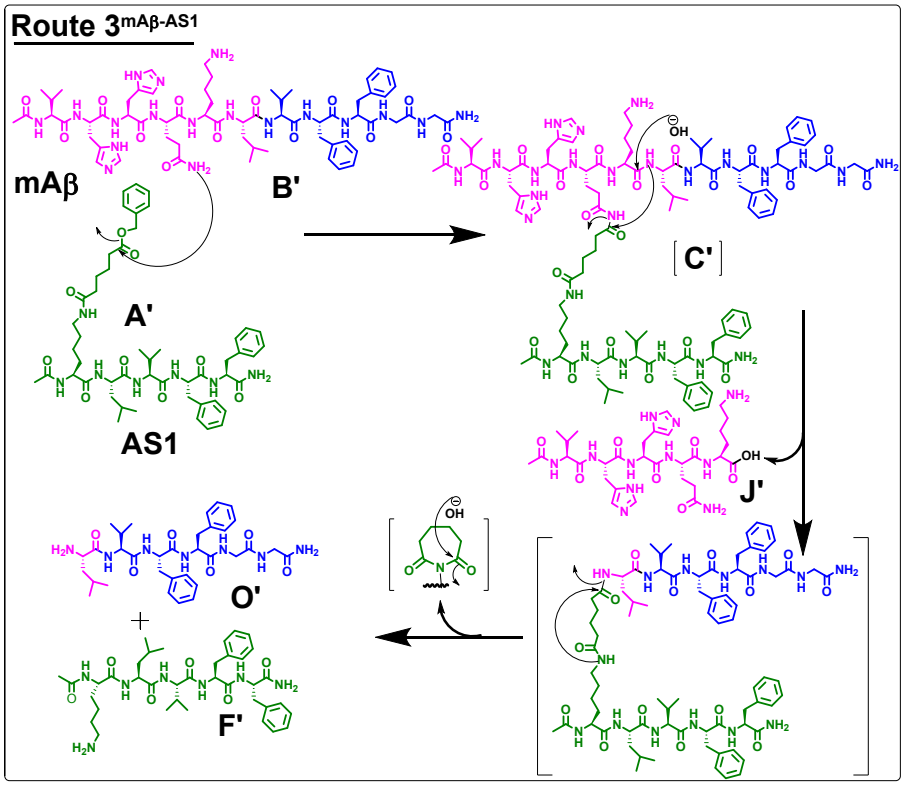

Figure S25. Plausible routes of cleavage of mAβ into various fragments by AS1 (Route 3$^{mAβ-AS1}$).

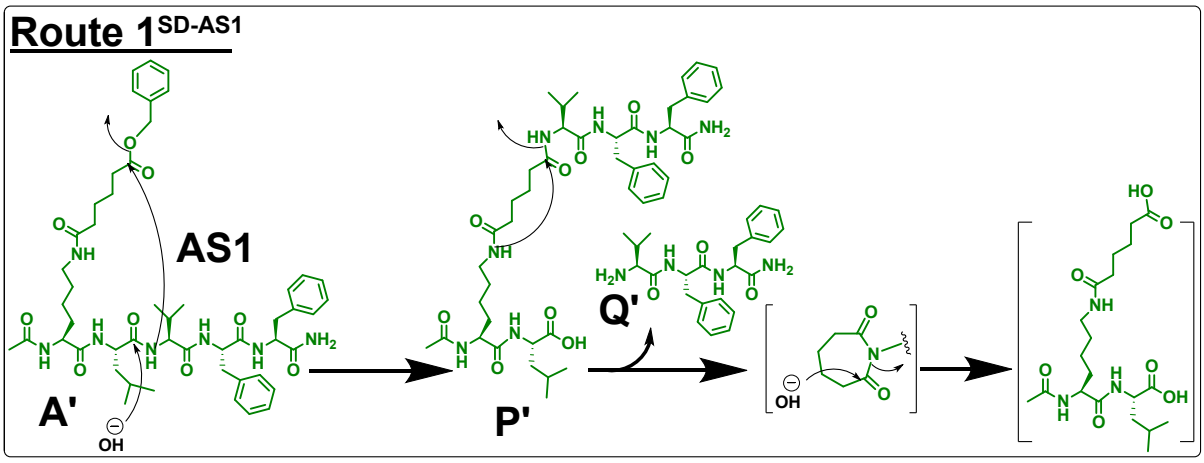

Figure S26. Plausible route of self degradation of AS1 in absence of mAβ (Route 1^{SD-AS1}).

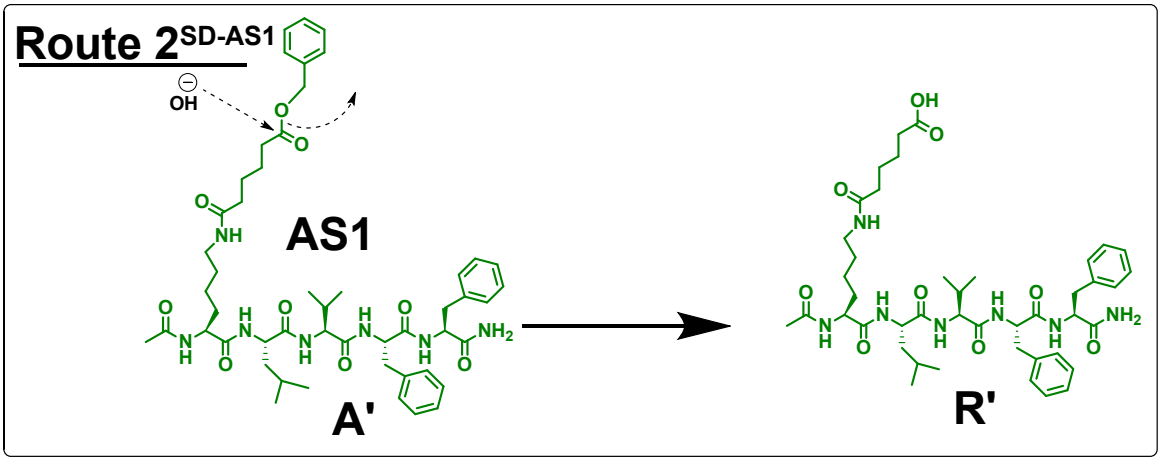

Figure S27. Plausible route of self degradation of AS1 in absence of mAβ (Route 2^{SD-AS1}).

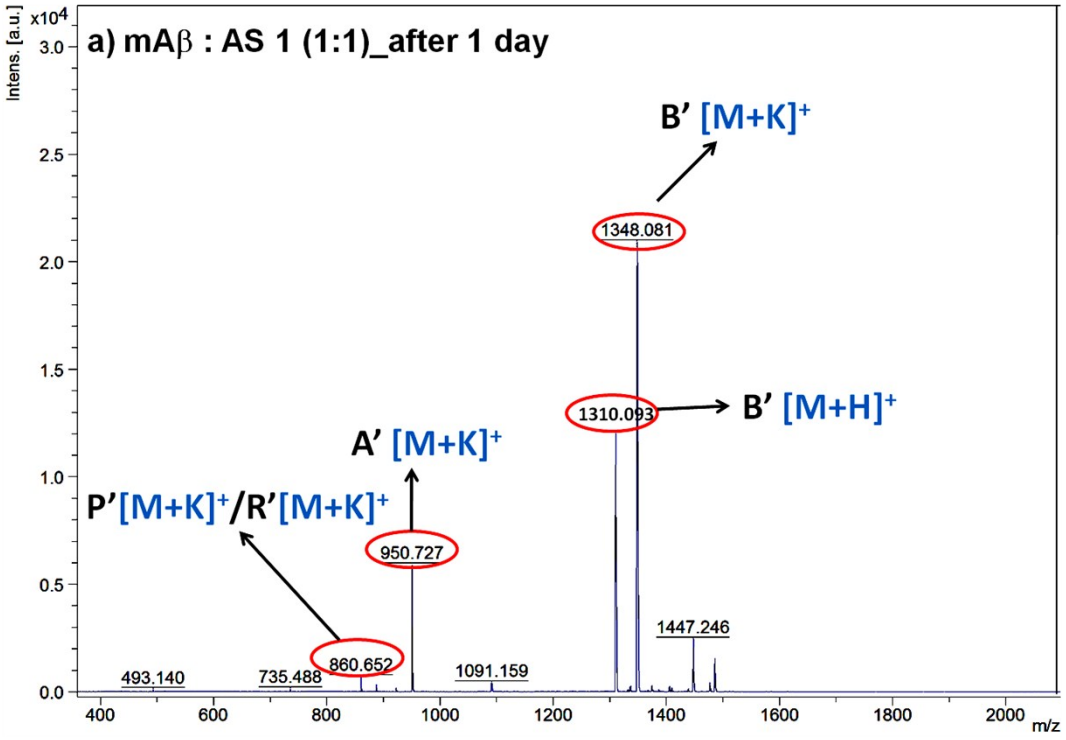

Figure S28. MALDI mass spectrum of mAβ in presence of AS1 (1:1) after 1 day of incubation in PBS pH 7.4 at 37°C. As P'and R' are positional isomers, they exhibit same m/z value.

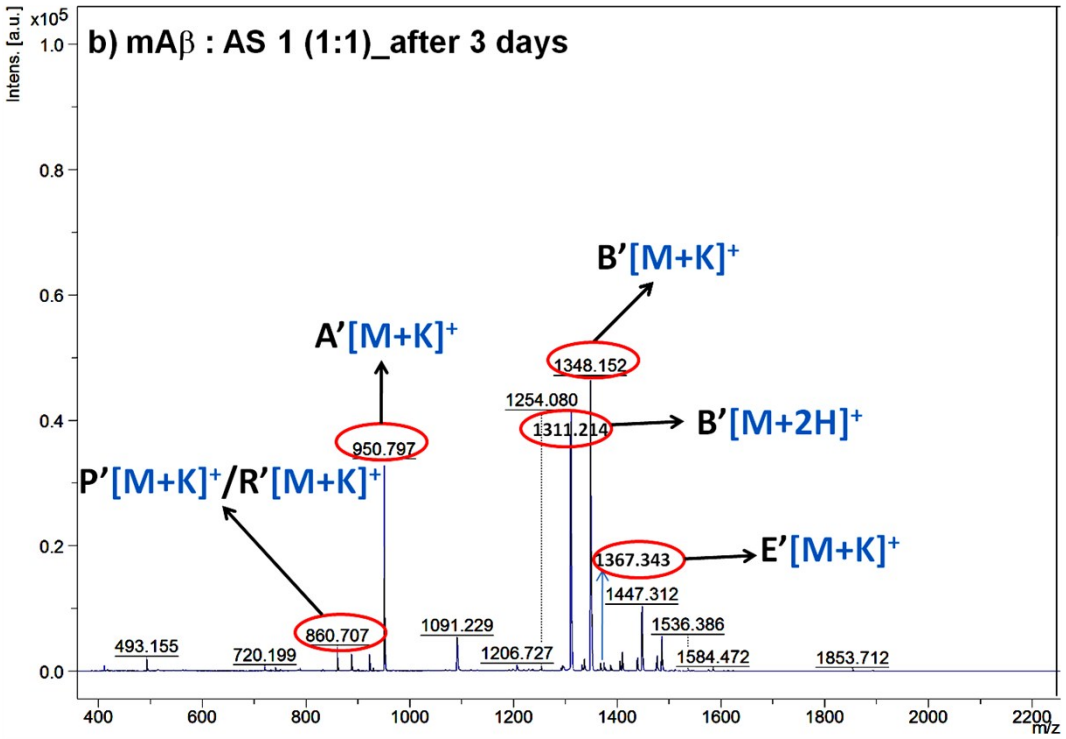

Figure S29. MALDI mass spectrum of mAβ in presence of AS1 (1:1) after 3 days of incubation in PBS. As P'and R' are positional isomers, they exhibit same m/z value.

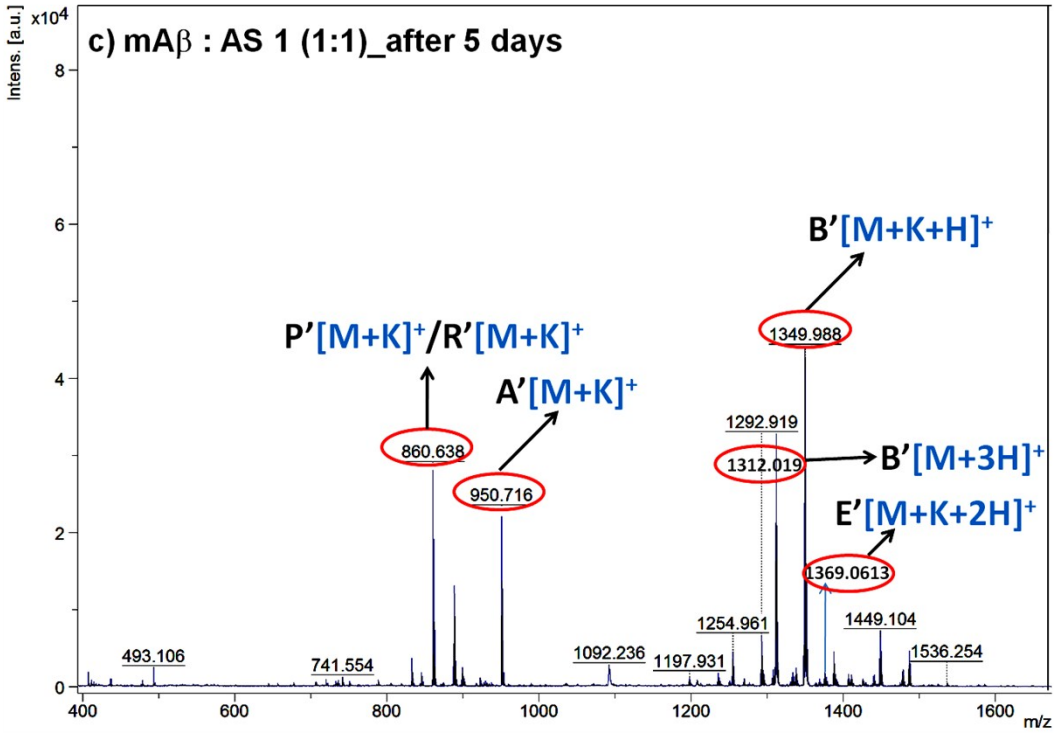

Figure S30. MALDI mass spectrum of mAβ in presence of AS1 (1:1) after 5 days of incubation in PBS. As P'and R' are positional isomers, they exhibit same m/z value.

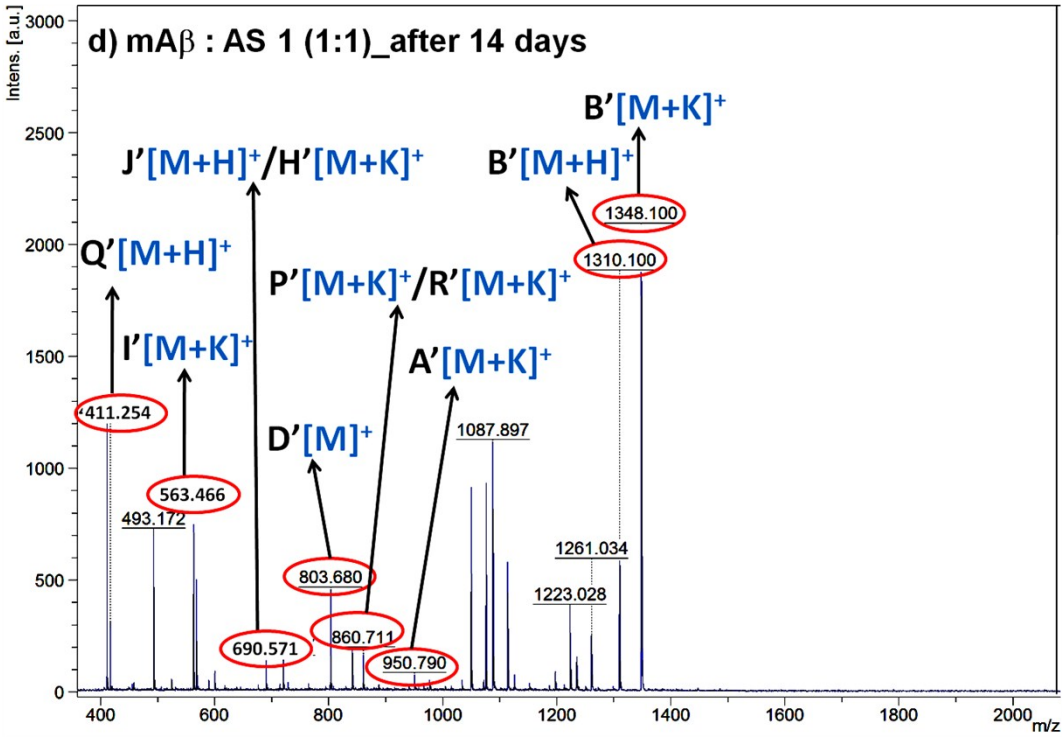

Figure S31. MALDI mass spectrum of mAβ in presence of AS1 (1:1) after 14 days of incubation in PBS. As P'and R' are positional isomers, they exhibit same m/z value.

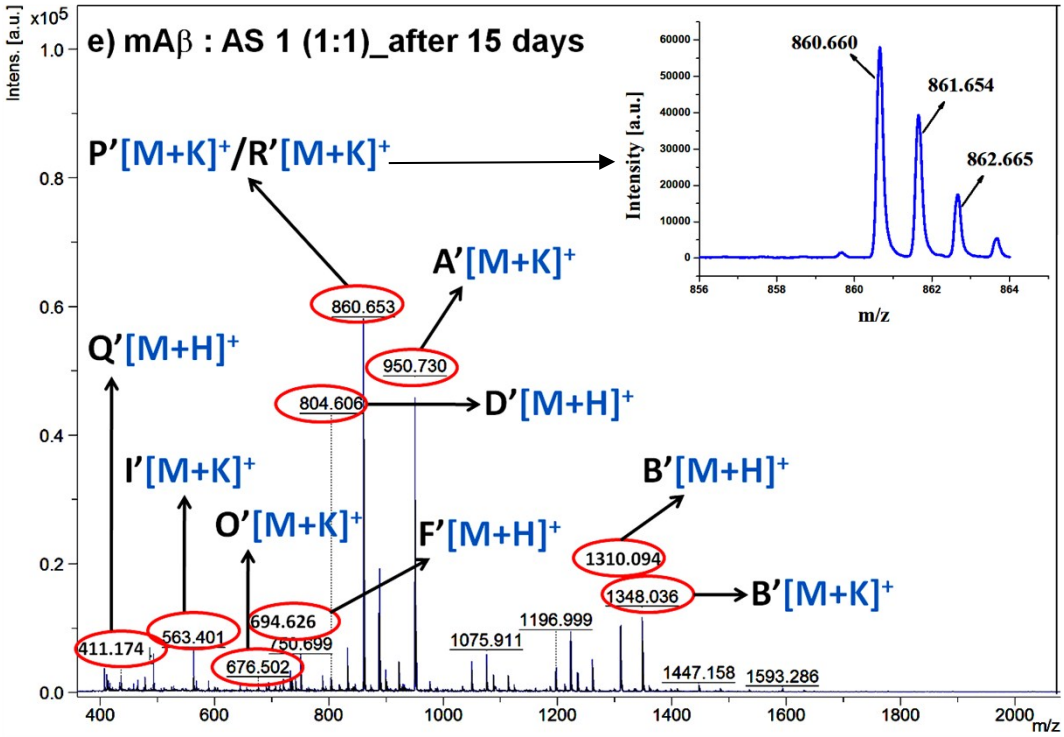

Figure S32. MALDI mass spectrum of mAβ in presence of AS1 (1:1) after 15 days of incubation in PBS. As P'and R' are positional isomers, they exhibit same m/z value.

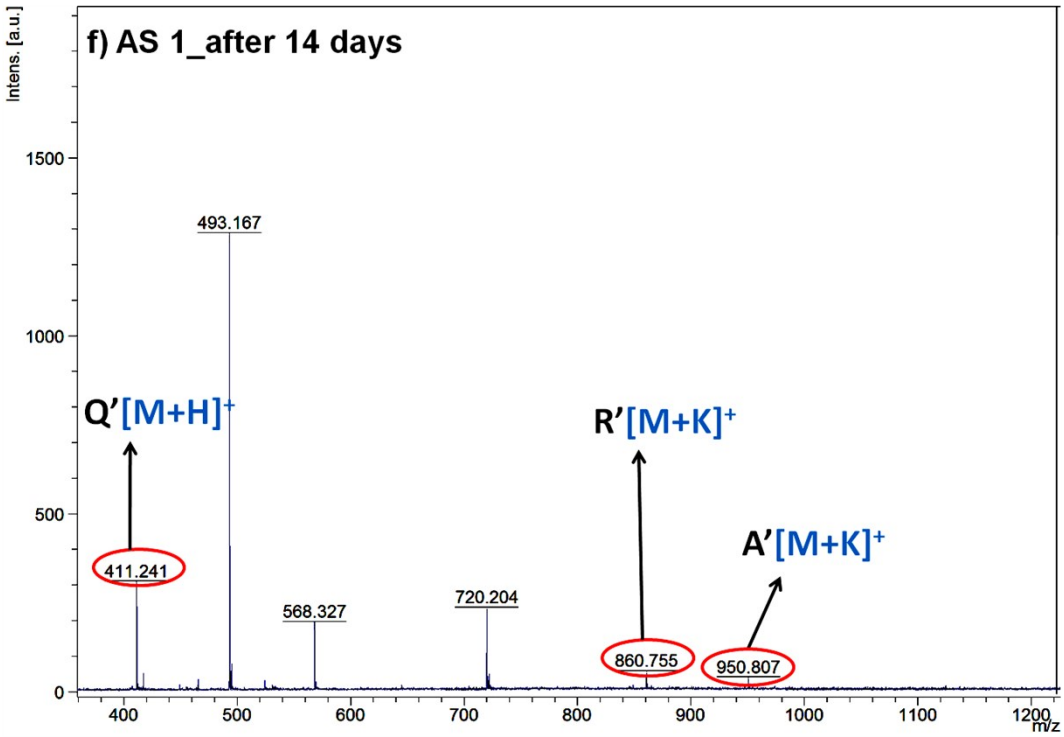

Figure S33. MALDI mass spectrum of AS1 in absence of mAβ after 14 days of incubation in PBS.

9. Plausible routes of the proteolytic activity of AS2 on mAβ:

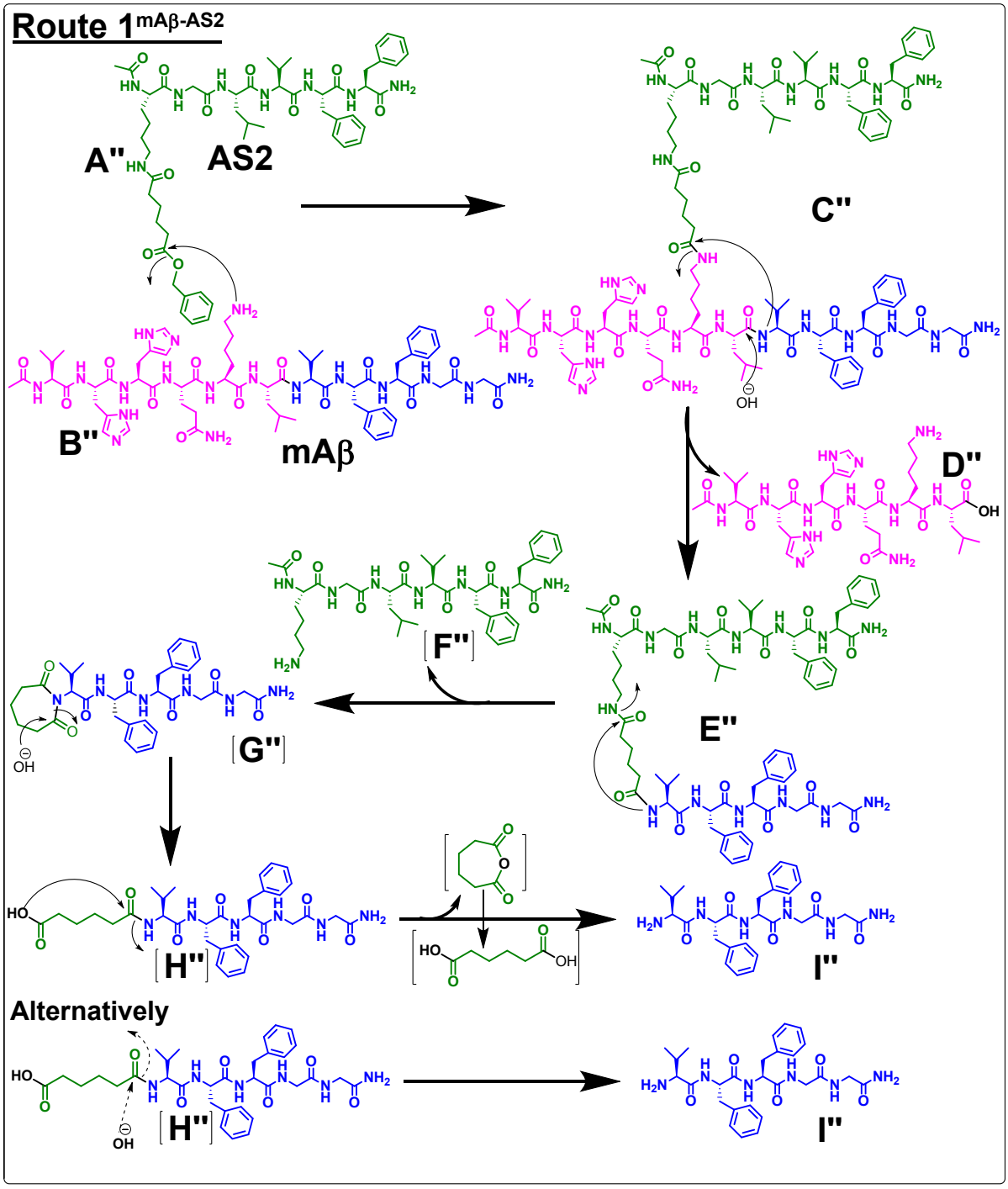

Figure S34. Plausible route of proteolysis of mAβ into various fragments by AS2 (Route 1$^{mAβ-AS2}$).

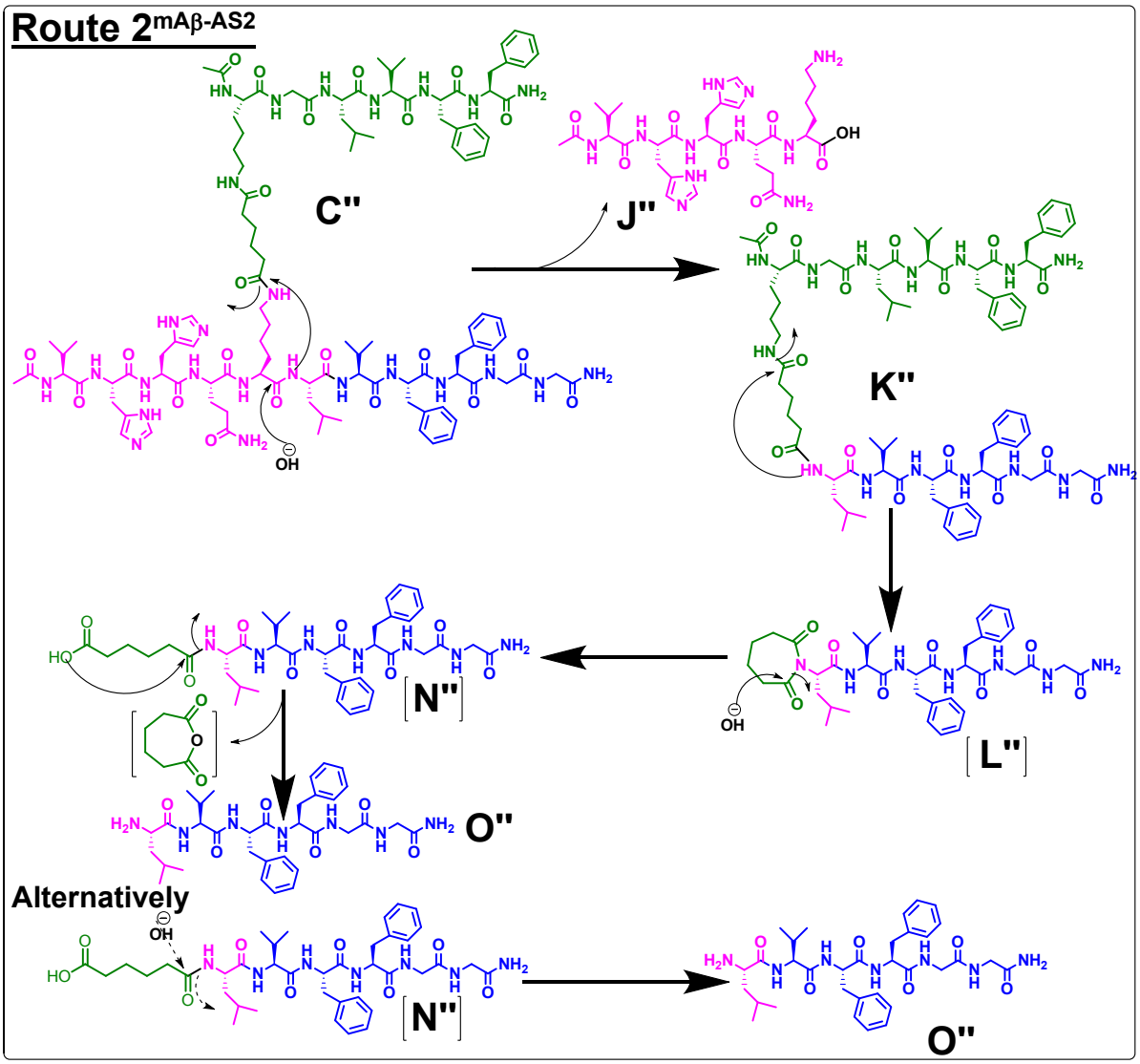

Figure S35. Plausible route of proteolysis of mAβ into various fragments by AS2 (Route 2$^{mAβ-AS2}$).

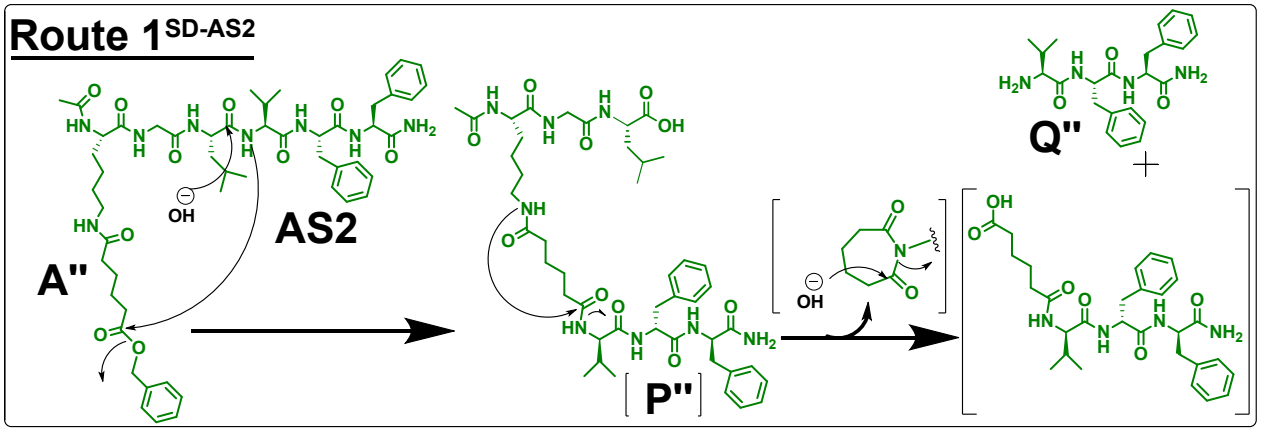

Figure S36. Plausible route of self degradation of AS2 (Route 1^{SD-AS2}).

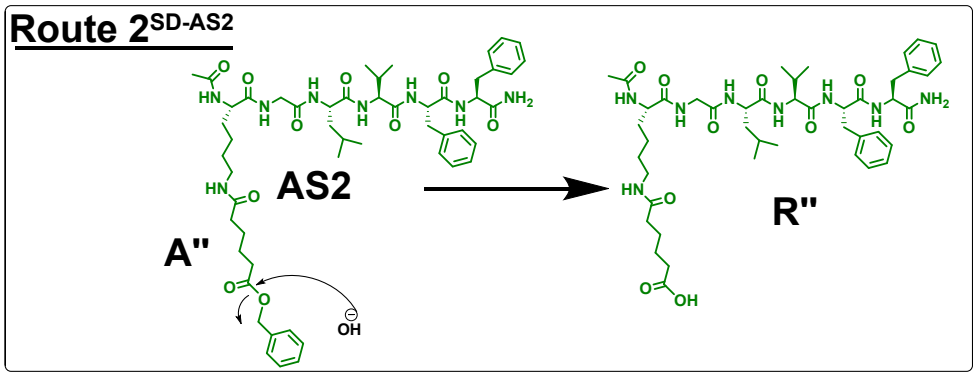

Figure S37. Plausible route of self degradation of AS2 (Route 2^{SD-AS2}).

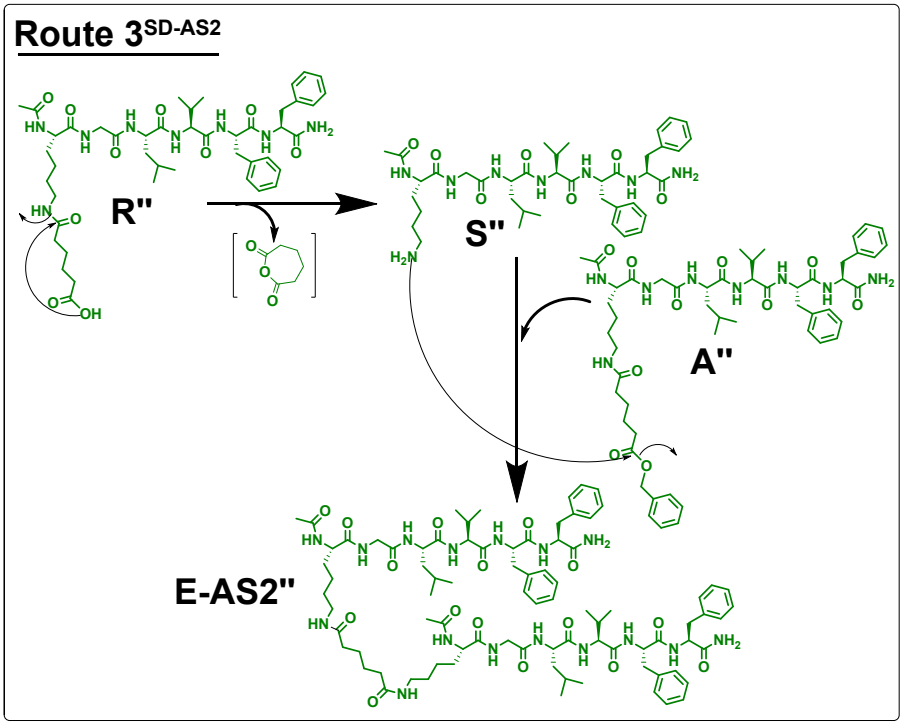

Figure S38. Plausible route of self degradation of AS2 (Route 3^{SD-AS2}).

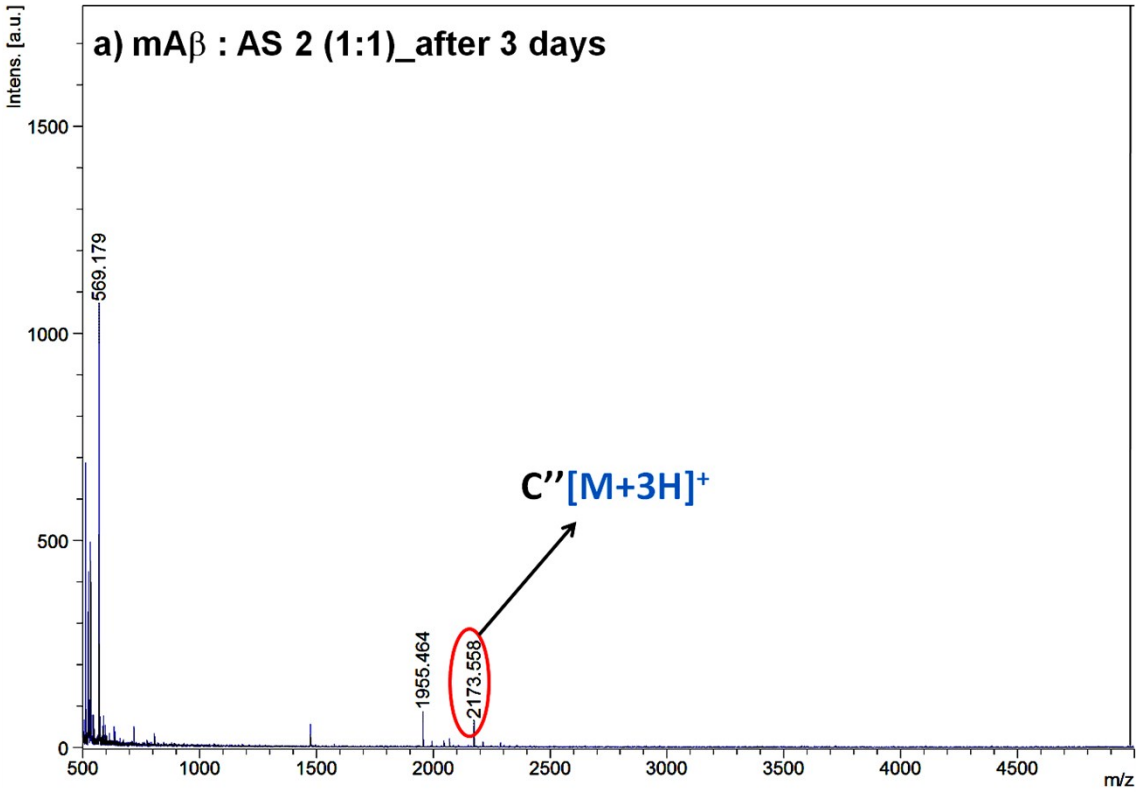

Figure S39. MALDI mass spectrum of mAβ in presence of AS2 (1:1) after 3 days of incubation in PBS pH 7.4 at 37°C.

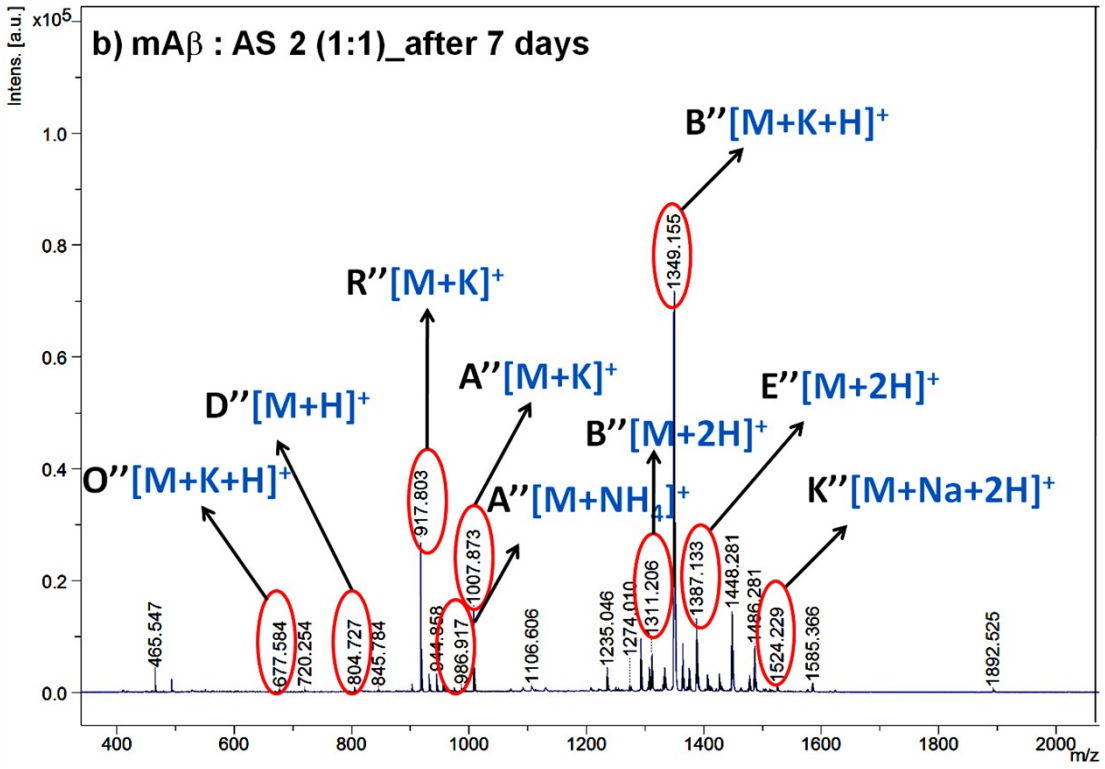

Figure S40. MALDI mass spectrum of mAβ in presence of AS2 (1:1) after 7 days of incubation in PBS.

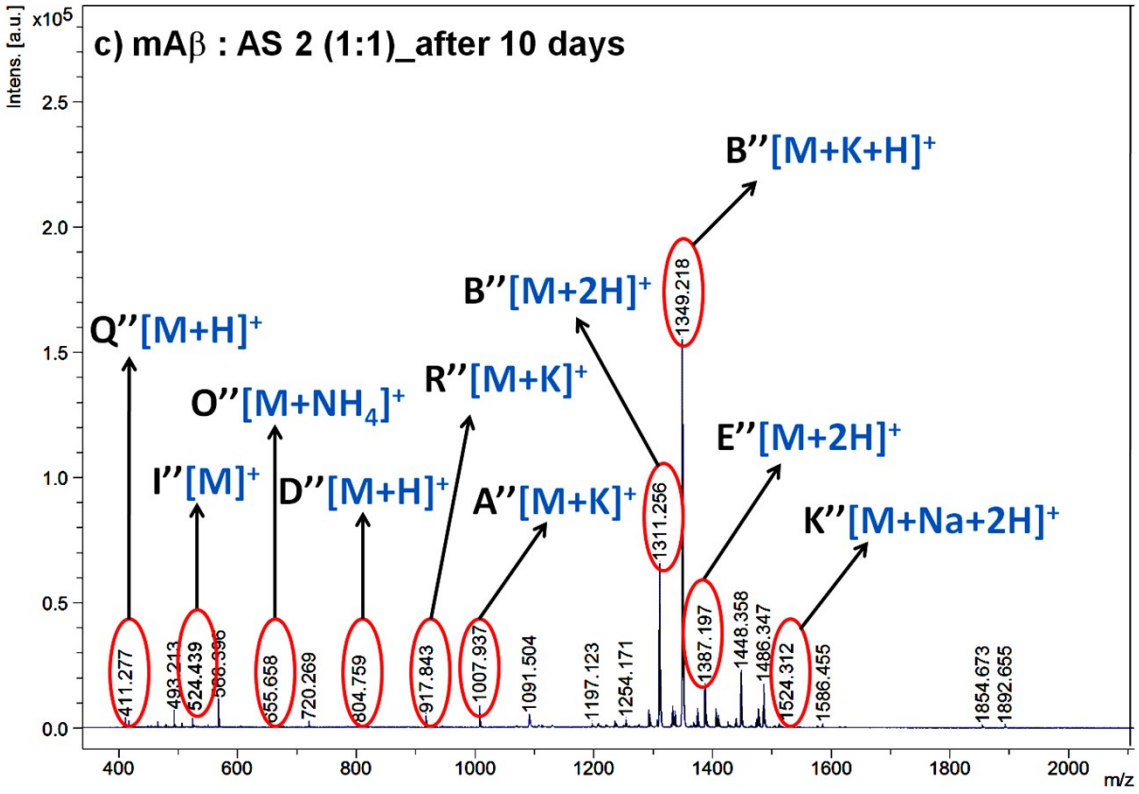

Figure S41. MALDI mass spectrum of mAβ in presence of AS2 (1:1) after 10 days of incubation in PBS.

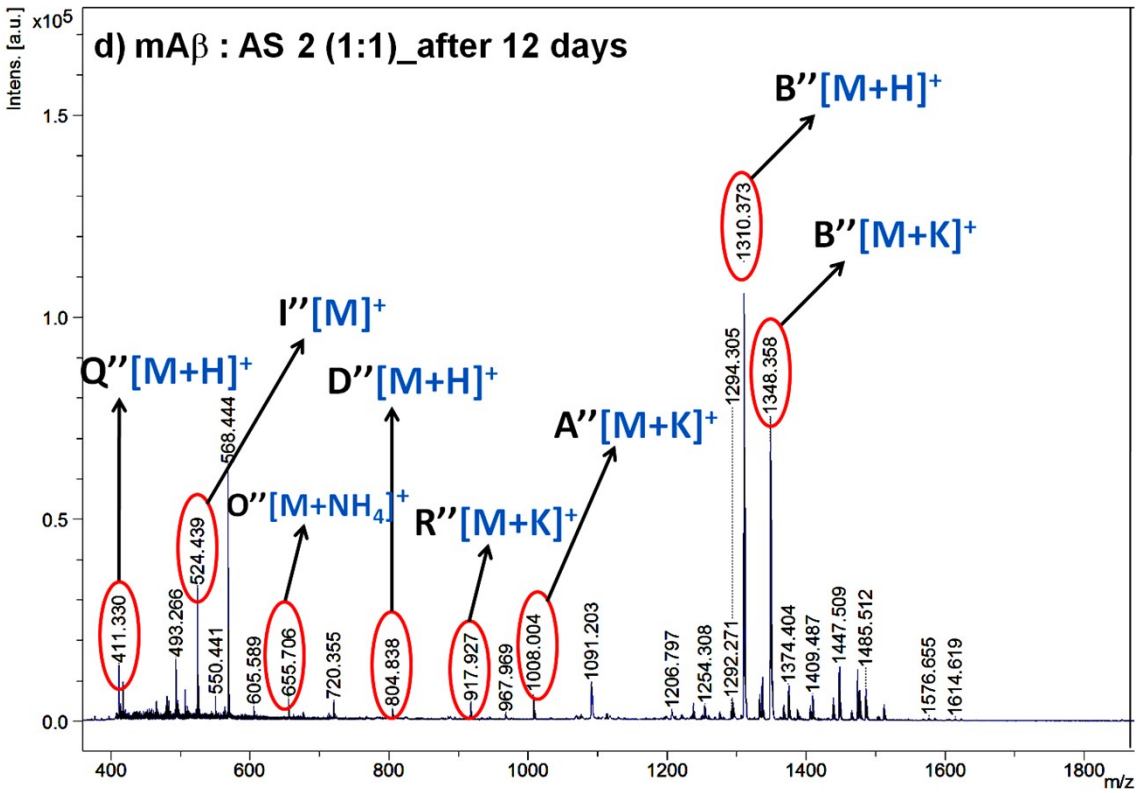

Figure S42. MALDI mass spectrum of mAβ in presence of AS2 (1:1) after 12 days of incubation in PBS.

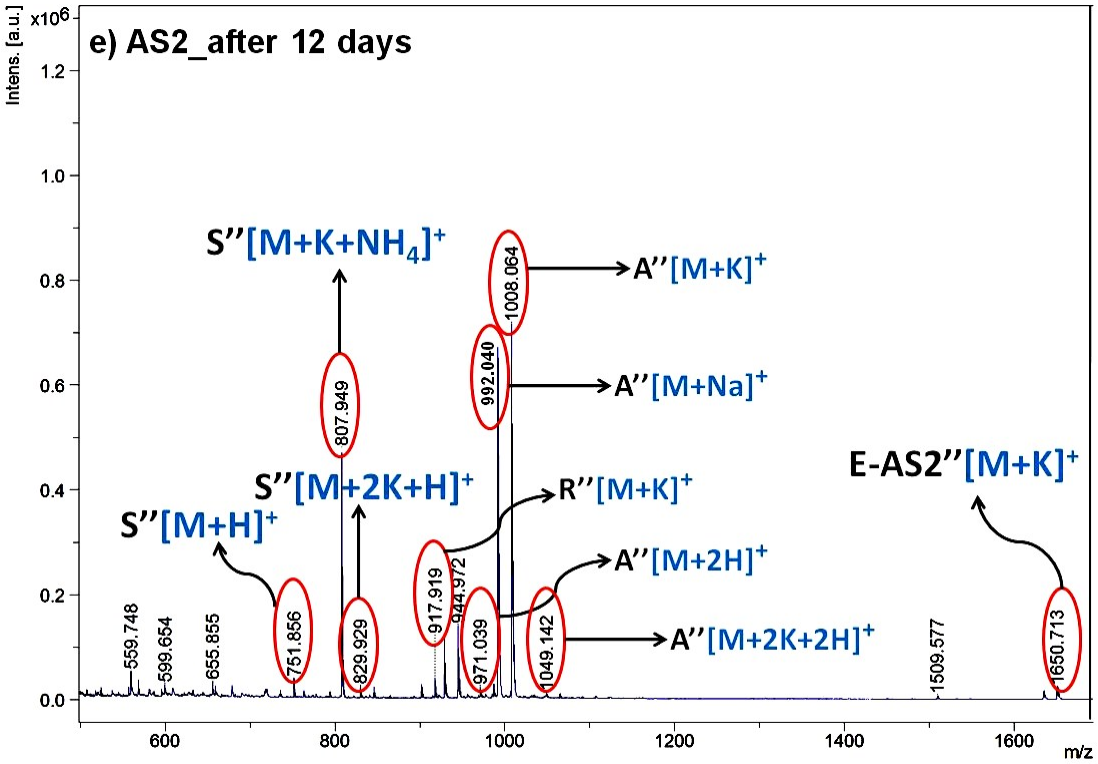

Figure S43. MALDI mass spectrum of AS2 alone after 12 days of incubation in PBS.

10. Plausible routes of the proteolytic activity of AS3 on mAβ:

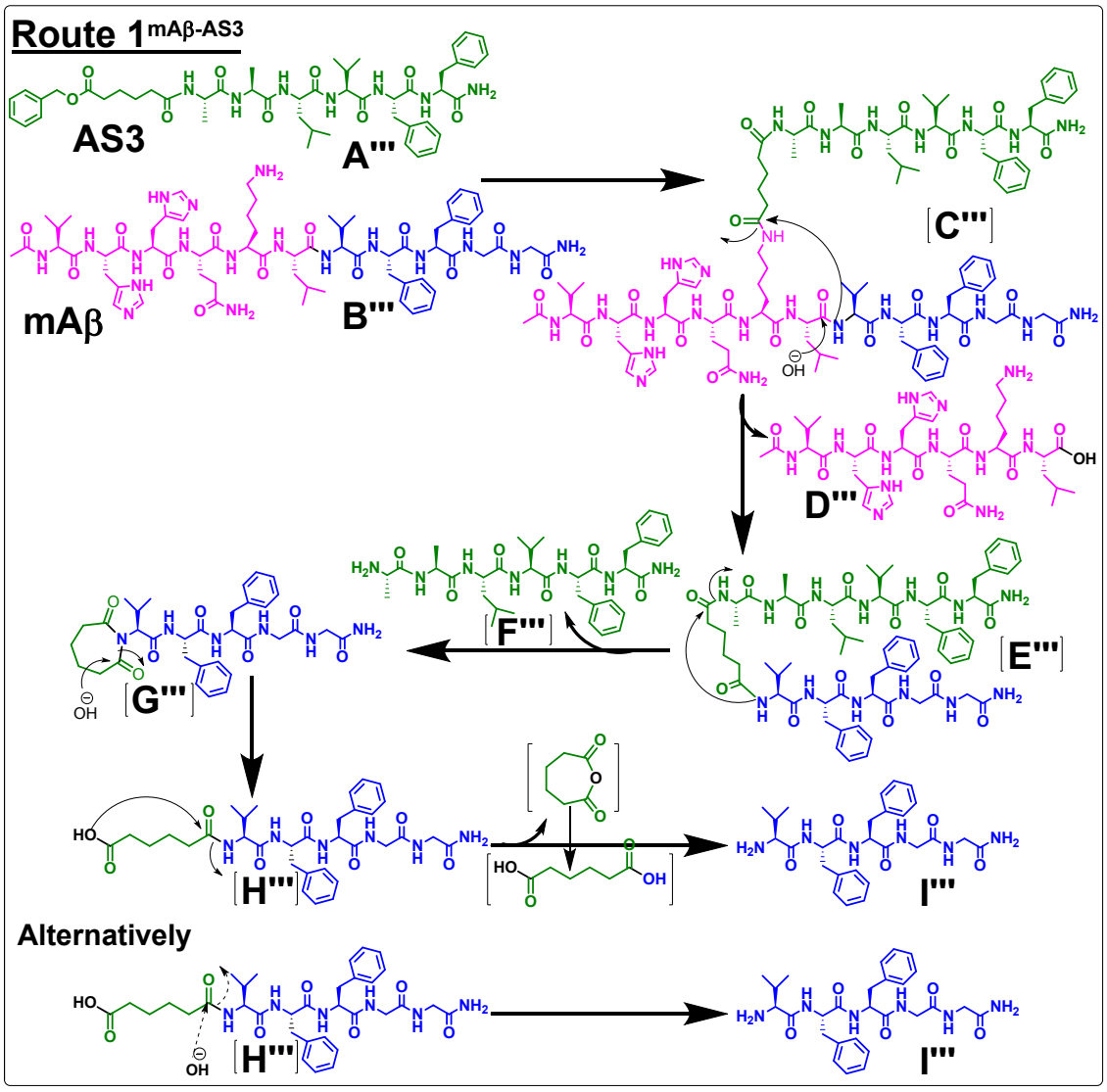

Figure S44. Plausible route of proteolysis of mAβ into various fragments by AS3 (Route 1$^{mAβ-AS3}$).

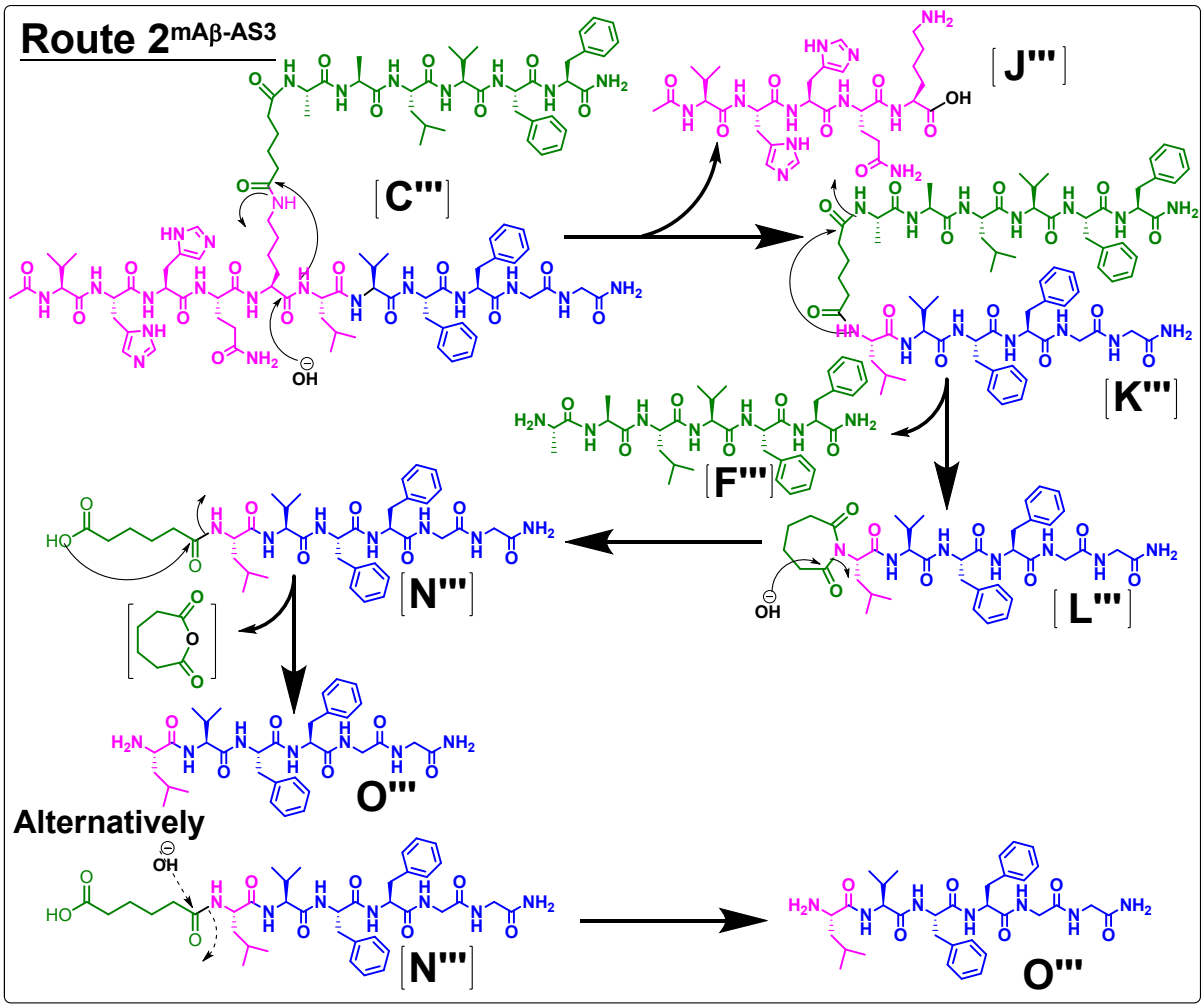

Figure S45. Plausible route of proteolysis of mAβ into various fragments by AS3 (Route 2$^{mAβ-AS3}$).

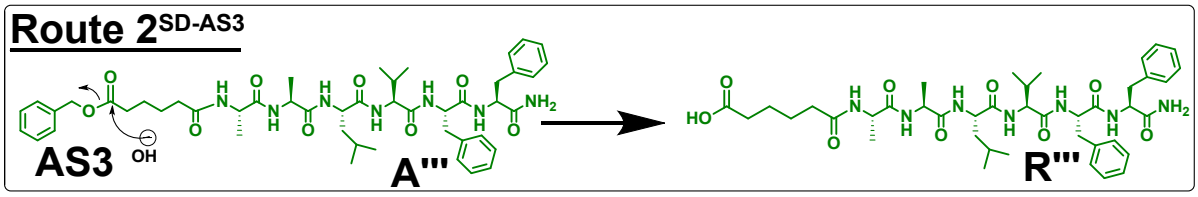

Figure S46. Plausible route of self degradation of AS3 (Route 2^{SD-AS3}).

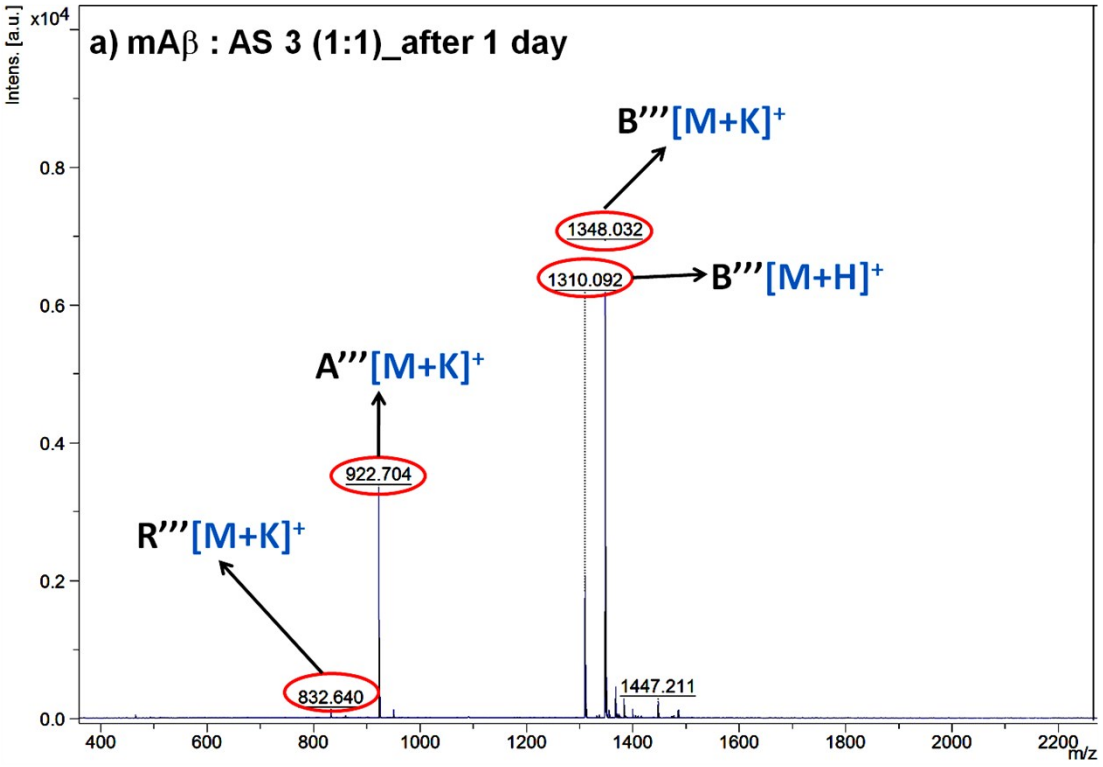

Figure S47. MALDI mass spectrum of mAβ in presence of AS3 (1:1) after 1 day of incubation in PBS pH 7.4 at 37°C.

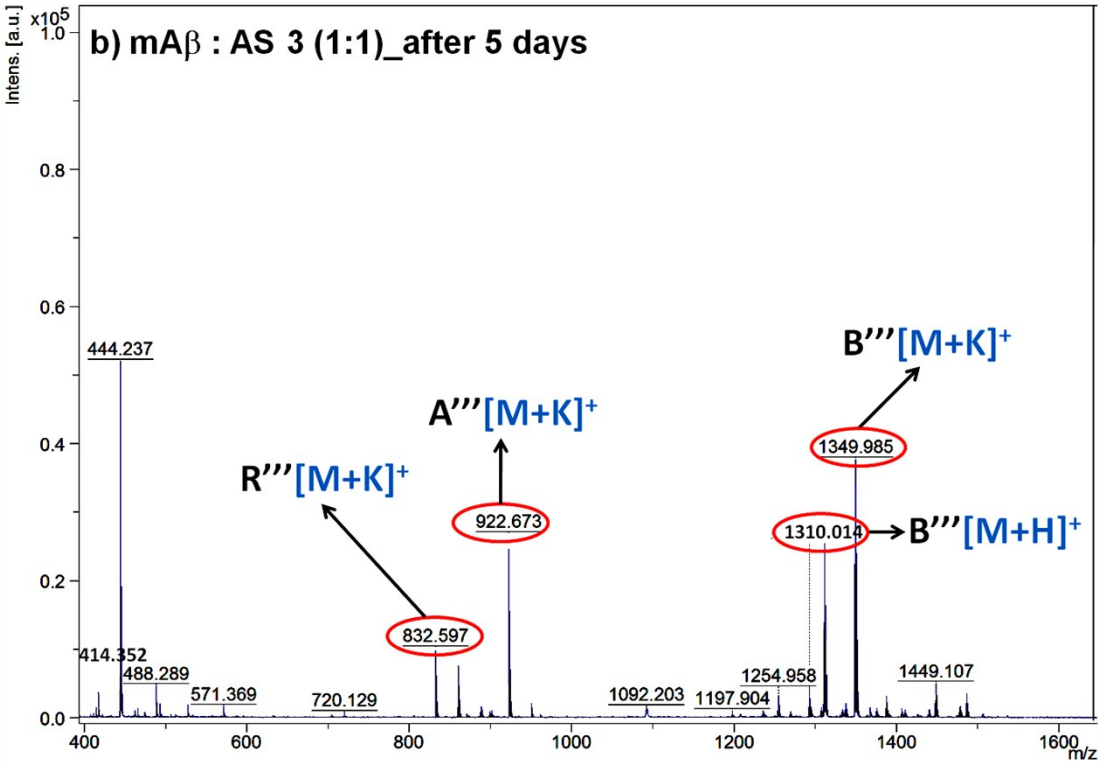

Figure S48. MALDI mass spectrum of mAβ in presence of AS3 (1:1) after 5 days of incubation in PBS.

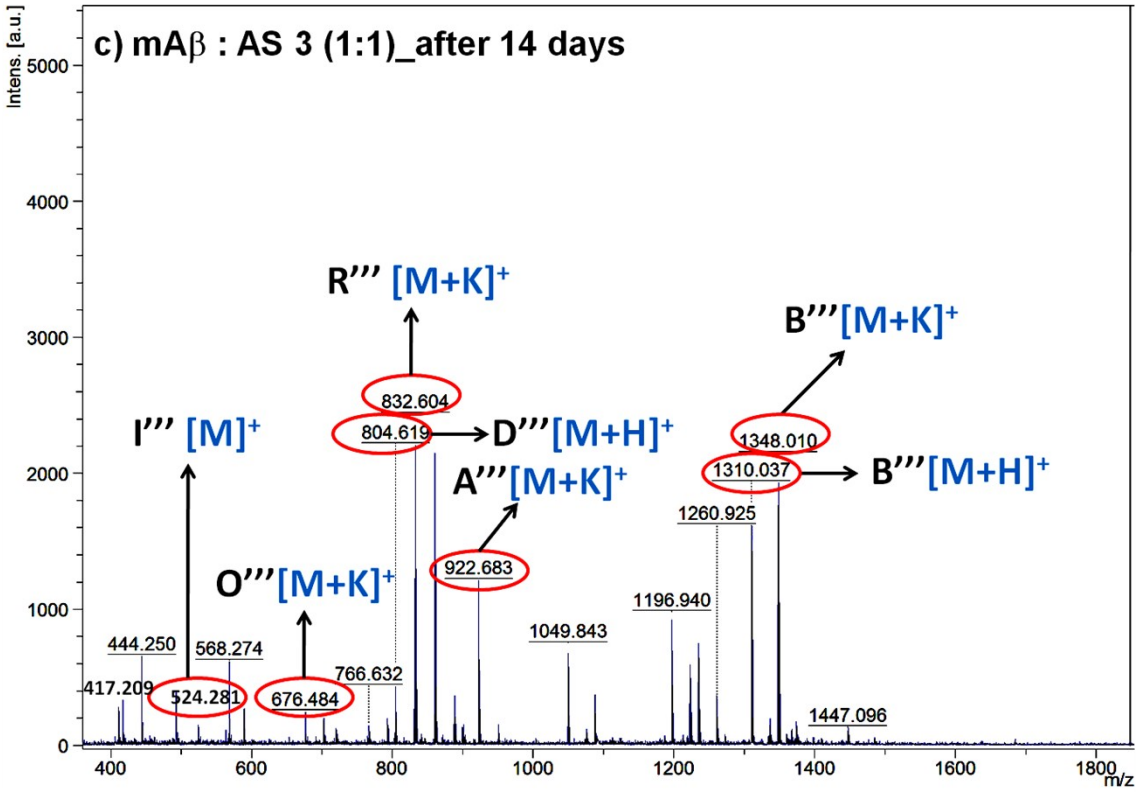

Figure S49. MALDI mass spectrum of mAβ in presence of AS3 (1:1) after 14 days of incubation in PBS.

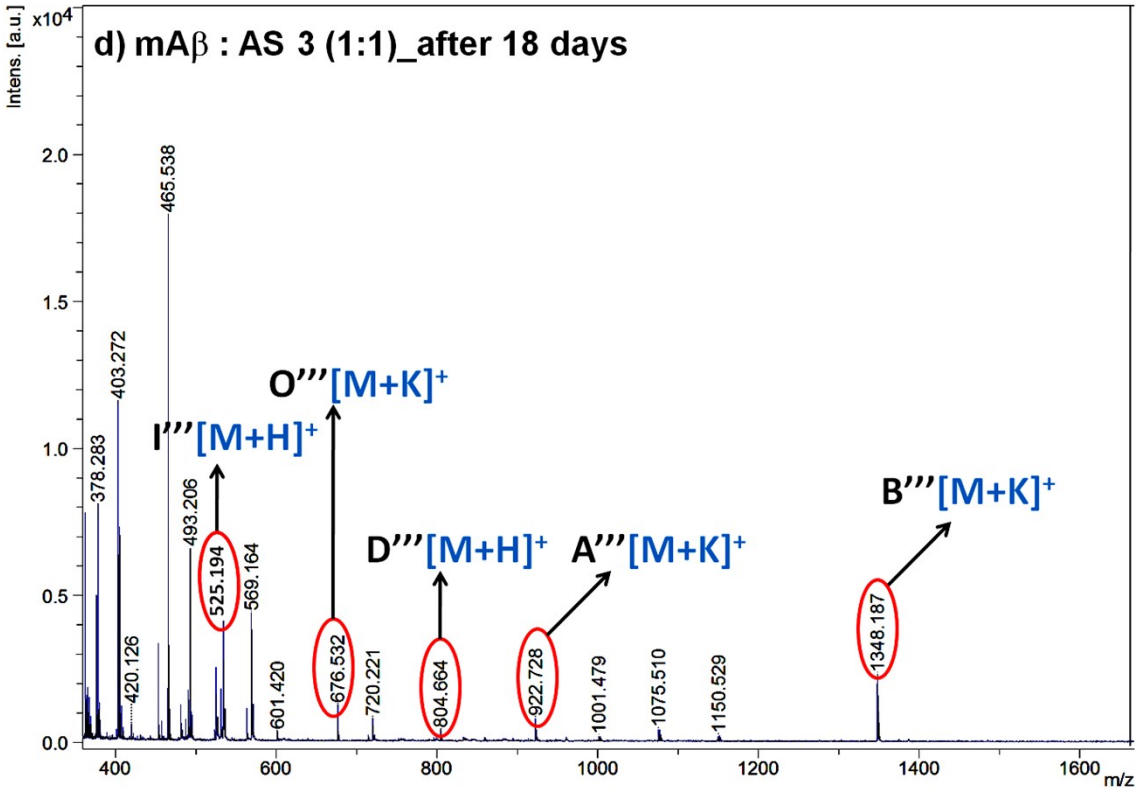

Figure S50. MALDI mass spectrum of mAβ in presence of AS3 (1:1) after 18 days of incubation in PBS.

11. Plausible routes of the proteolytic activity of AS4 on mAβ:

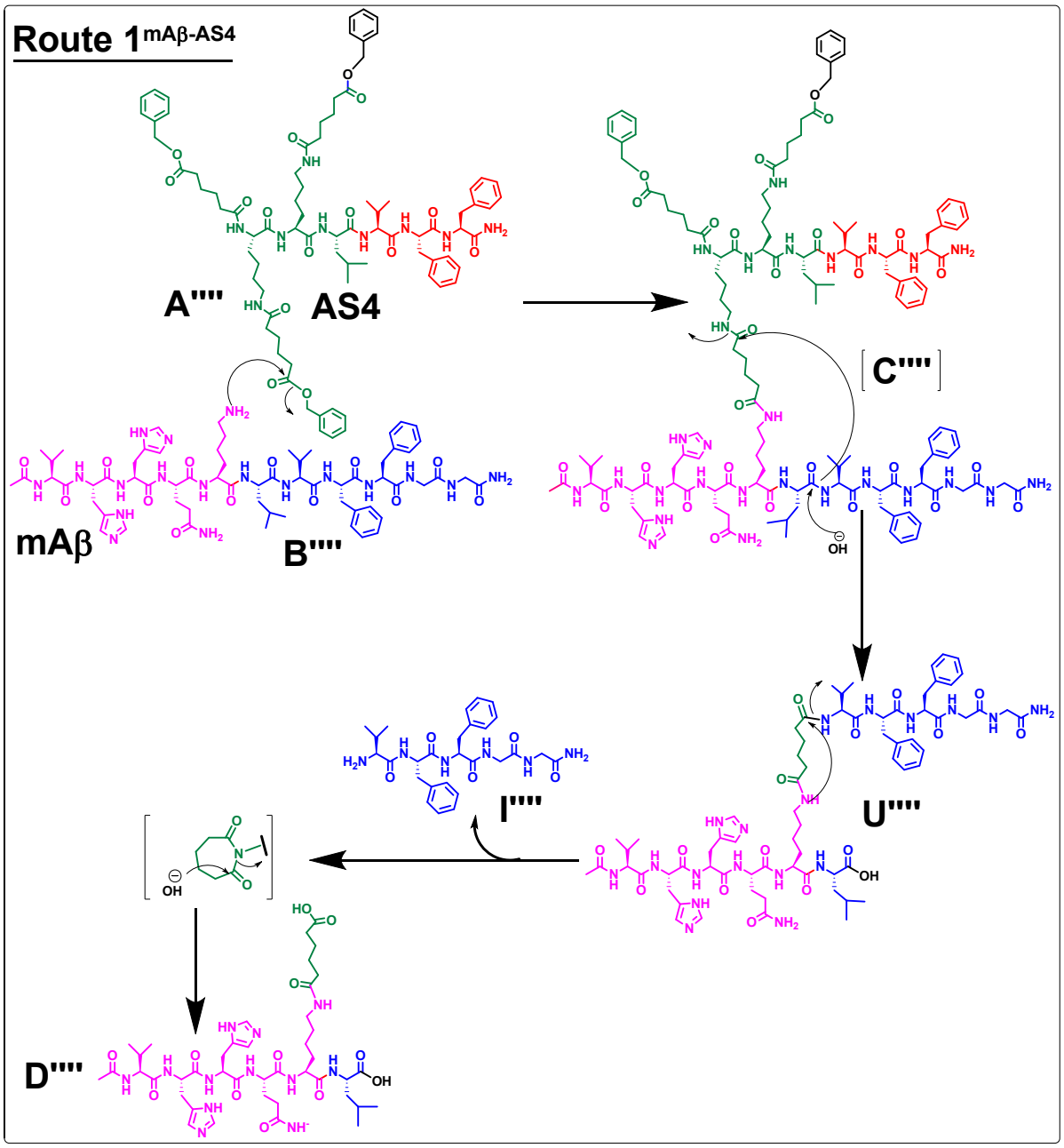

Figure S51. Plausible routes of proteolysis of mAβ into various fragments by AS4 (Route 1$^{mAβ-AS4}$).

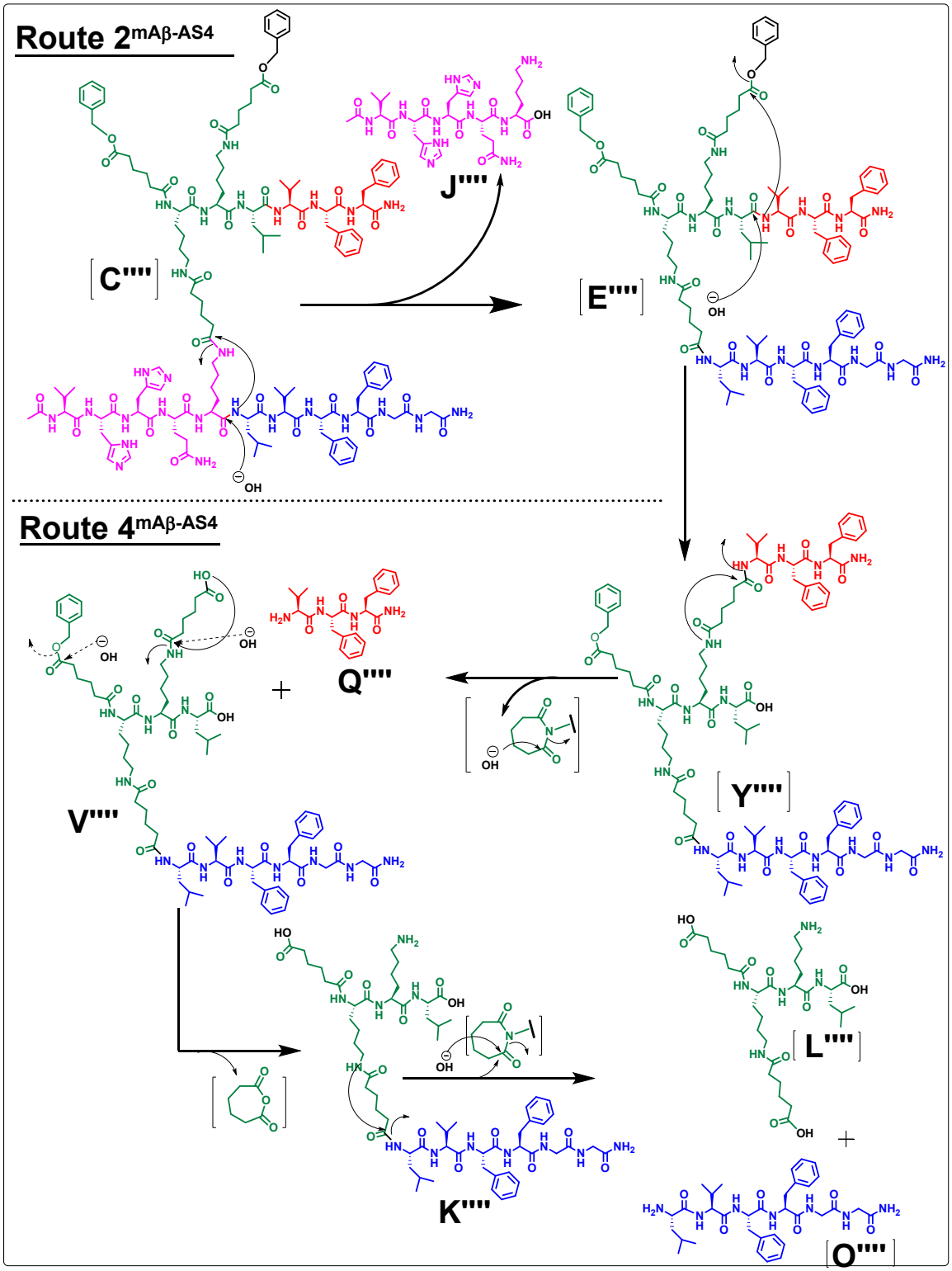

Figure S52. Plausible routes of proteolysis of mAβ into various fragments by AS4 (Route 2$^{mAβ-AS4}$ and Route 4$^{mAβ-AS4}$).

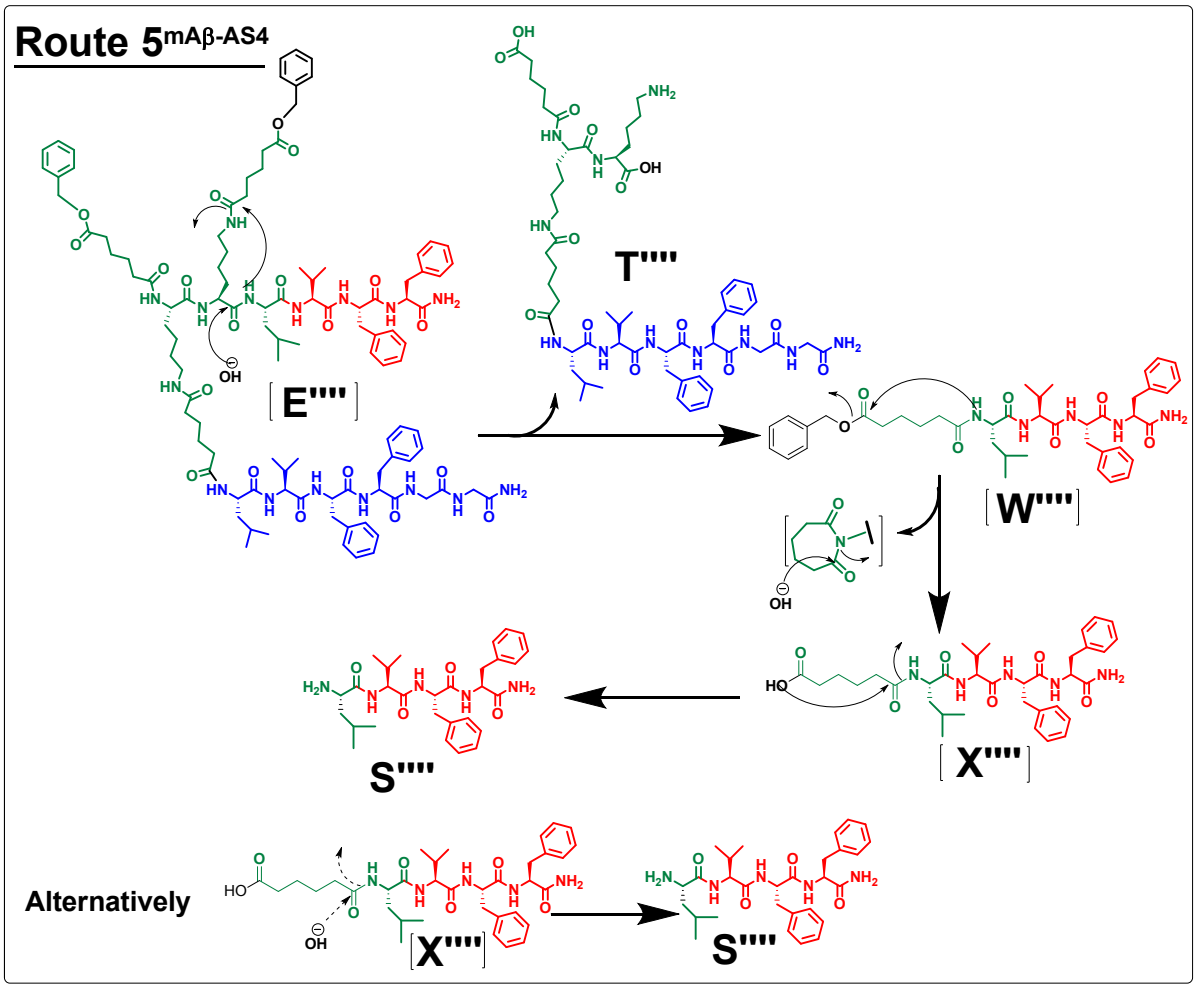

Figure S53. Plausible routes of proteolysis of mAβ into various fragments by AS4 (Route 5$^{mAβ-AS4}$).

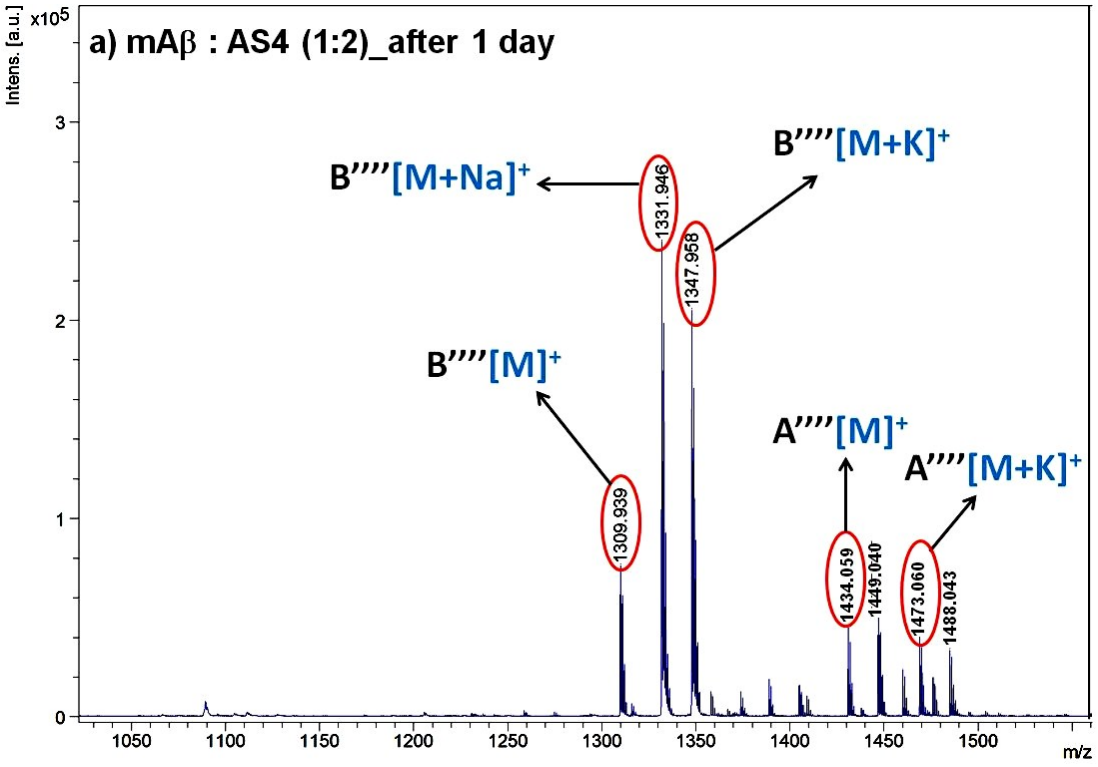

Figure S54. MALDI mass spectrum of mAβ in presence of AS4 (1:2) after 1 day of incubation in PBS pH 7.4 at 37°C.

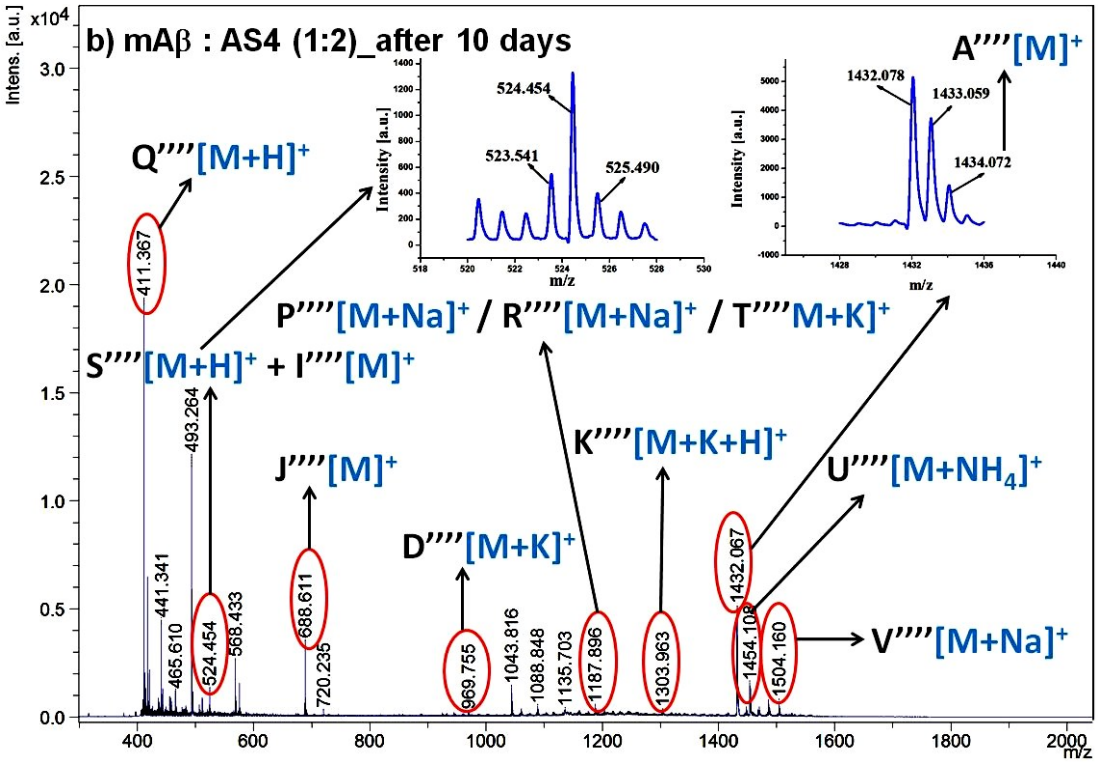

Figure S55. MALDI mass spectrum of mAβ in presence of AS4 (1:2) after 10 days of incubation in PBS.

12. Comparative map of the existence of mAβ:

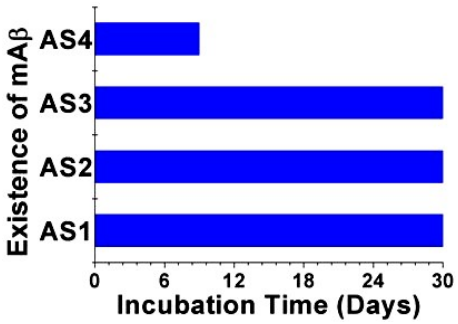

Figure S56. Existence of mAβ up to 30 days co-incubated with ASs.

13. Plausible routes of self degradation of AS4 (SD-AS4):

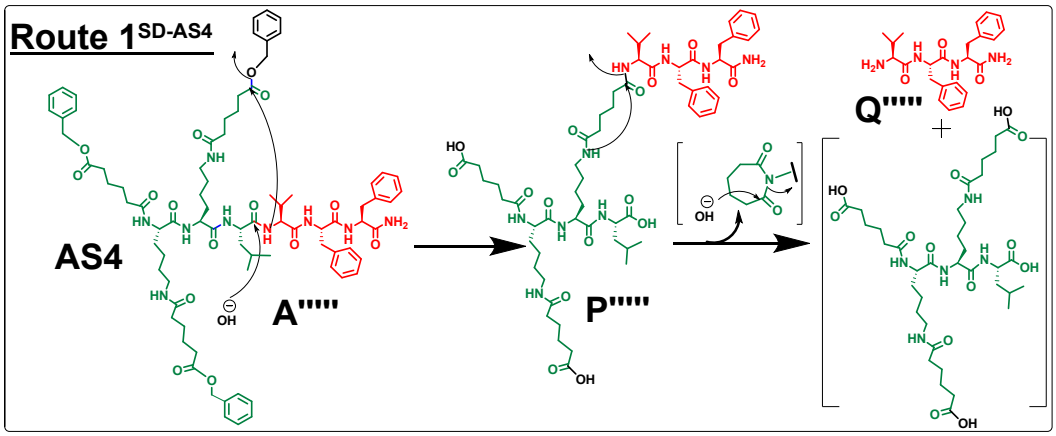

Figure S57. Plausible route of self degradation of AS4 into various fragments in absence of mAβ (Route $1^{SD\text{-}AS4}$).

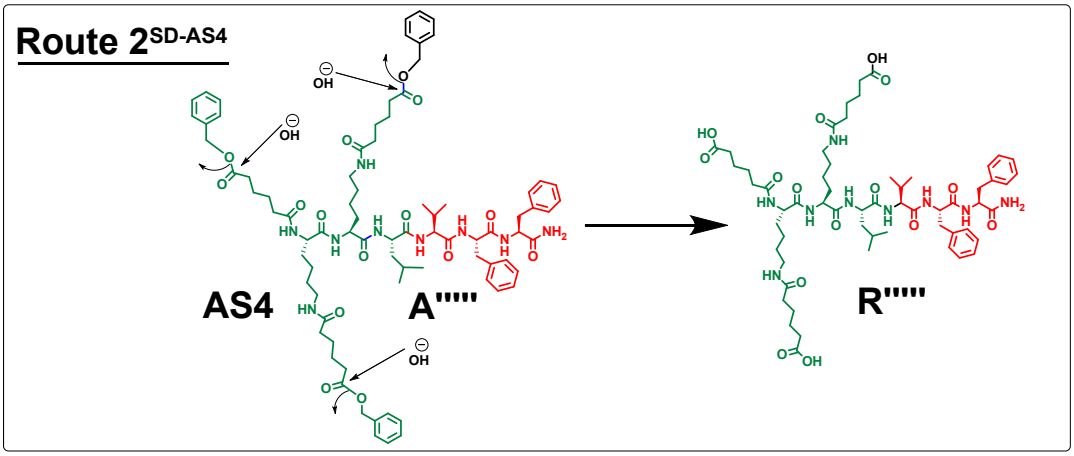

Figure S58. Plausible route of self degradation of AS4 into various fragments in absence of mAβ (Route $2^{SD\text{-}AS4}$).

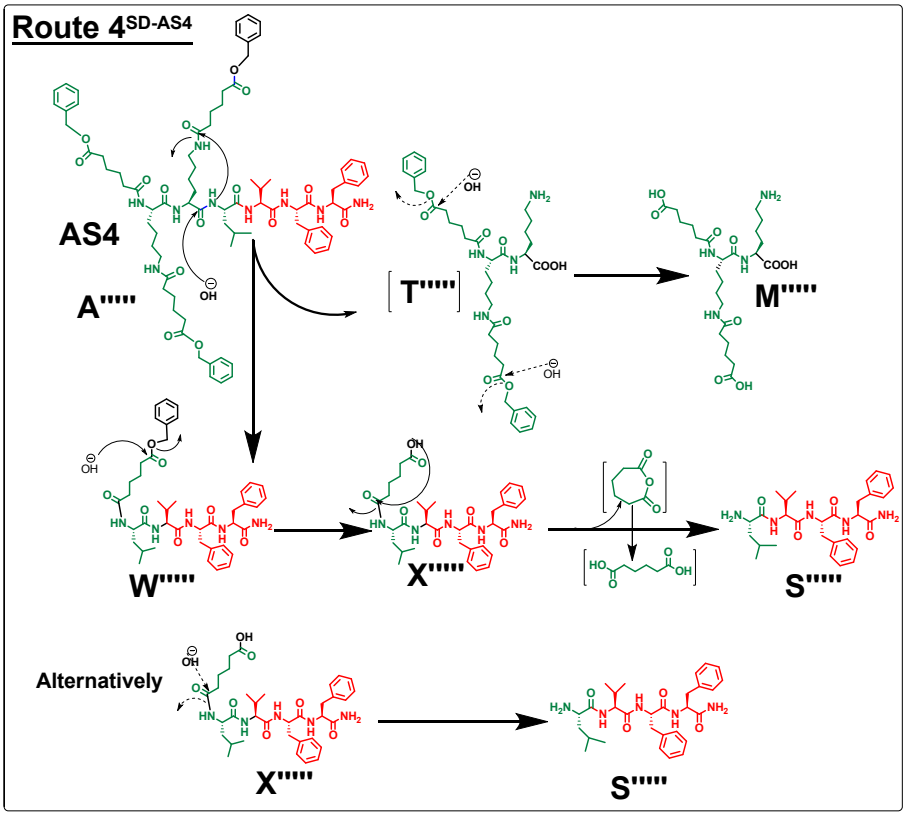

Figure S59. Plausible routes of self degradation of AS4 into various fragments in absence of mAβ (Route $4^{SD\text{-}AS4}$).

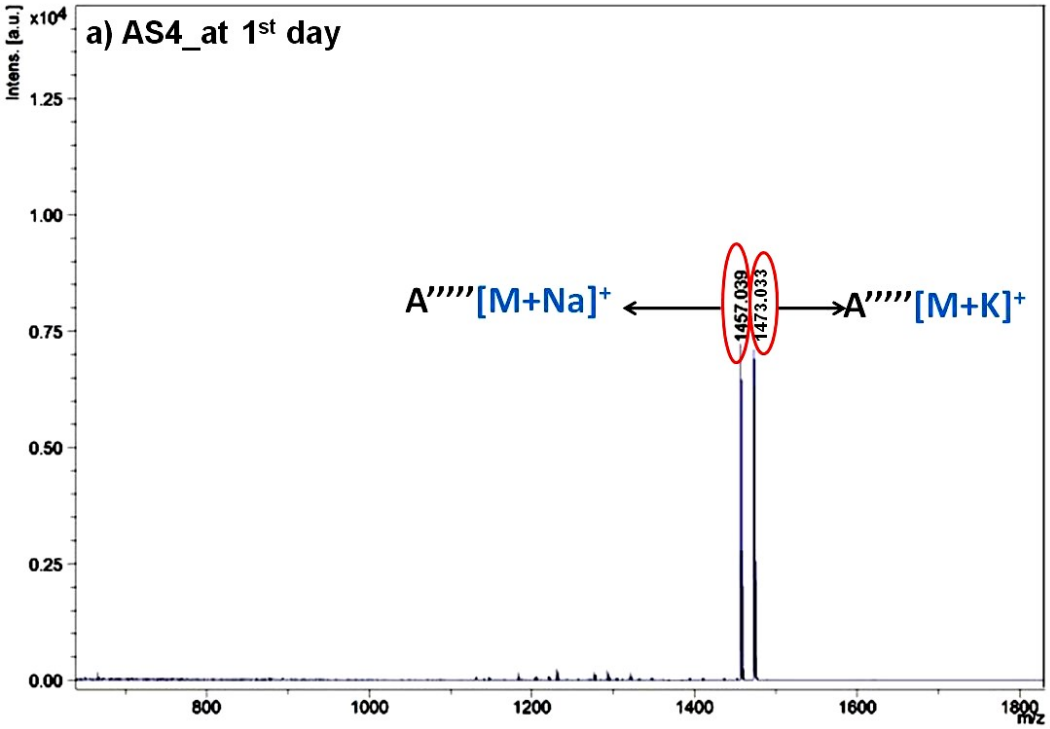

Figure S60. MALDI mass spectrum of AS4 at 1st day of incubation in PBS pH 7.4 at 37°C.

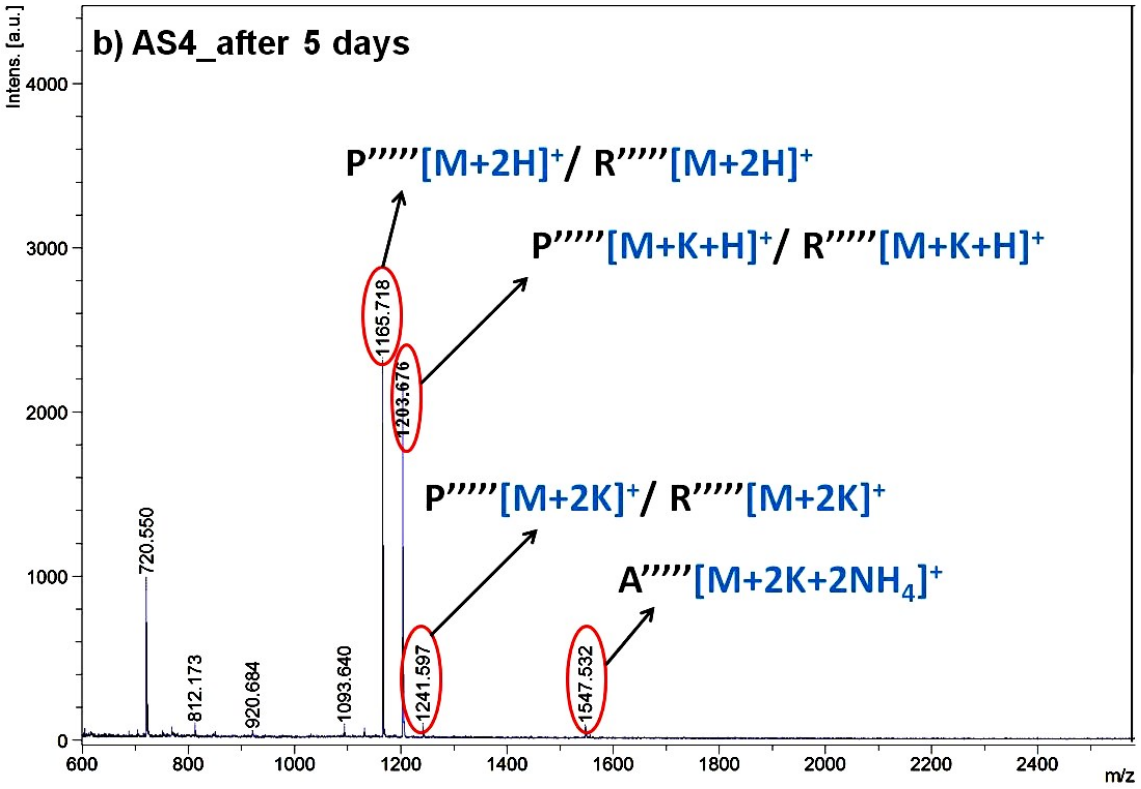

Figure S61. MALDI mass spectrum of AS4 after 5 days of incubation in PBS.

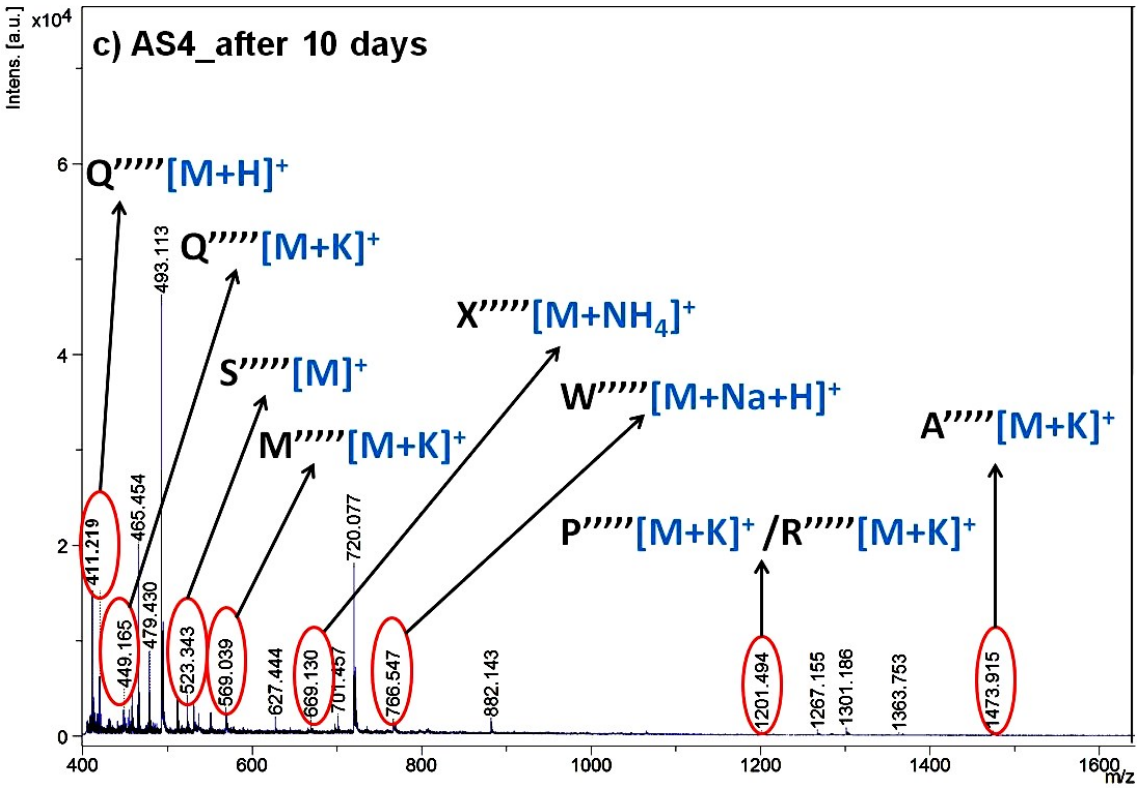

Figure S62. MALDI mass spectrum of AS4 after 10 days of incubation in PBS.

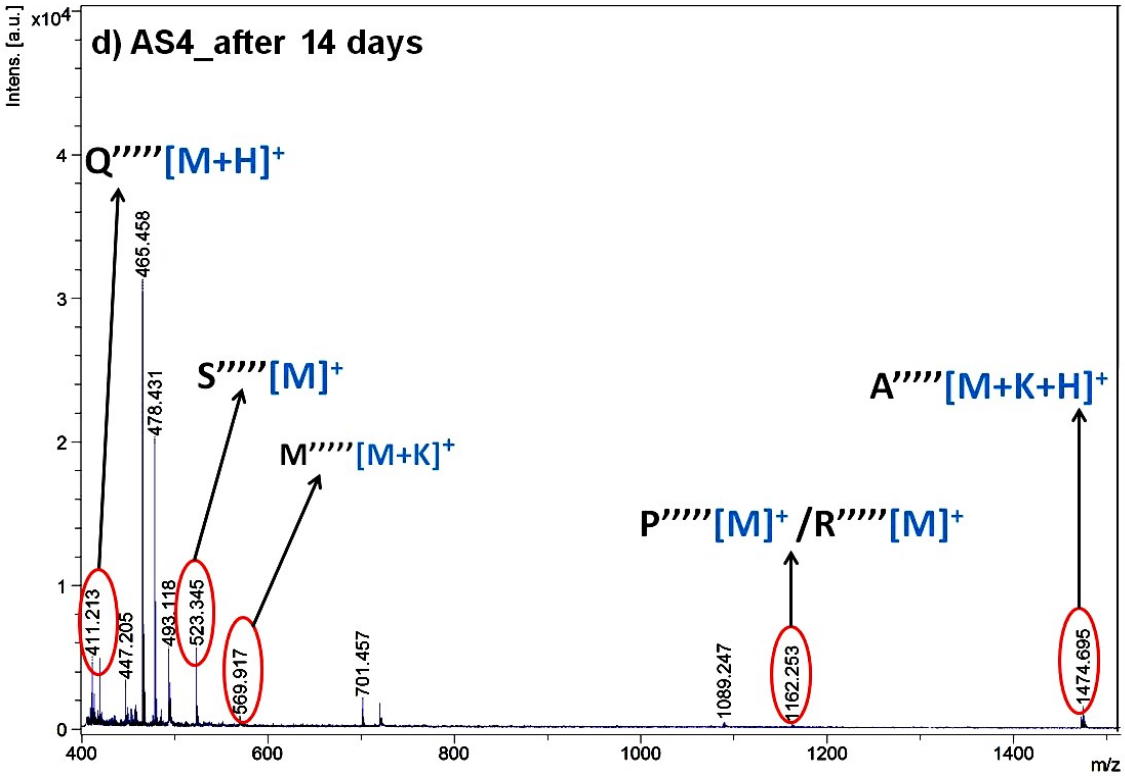

Figure S63. MALDI mass spectrum of AS4 after 14 days of incubation in PBS.

14. Self degradation of mAβ:

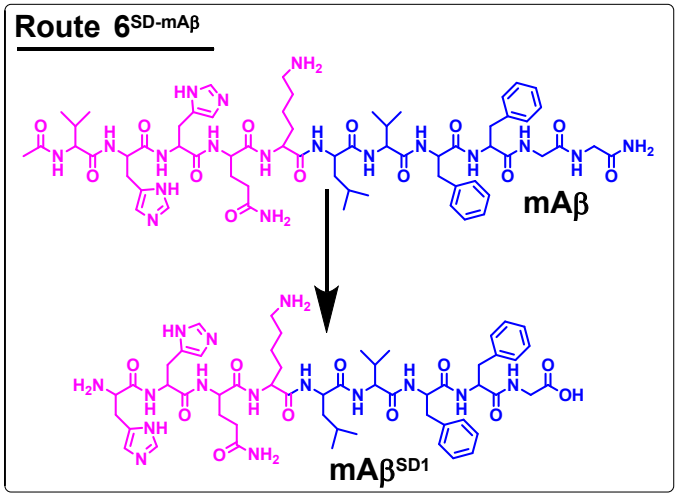

Figure S64. Plausible route of self degradation of mAβ into various fragments in absence of ASs (Route $5^{SD\text{-}mA\beta}$).

During sample preparation of mAβ for MALDI-MASS experiments, 2 µL of 10% TFA in water was added to break aggregation and to check self degraded fragments.

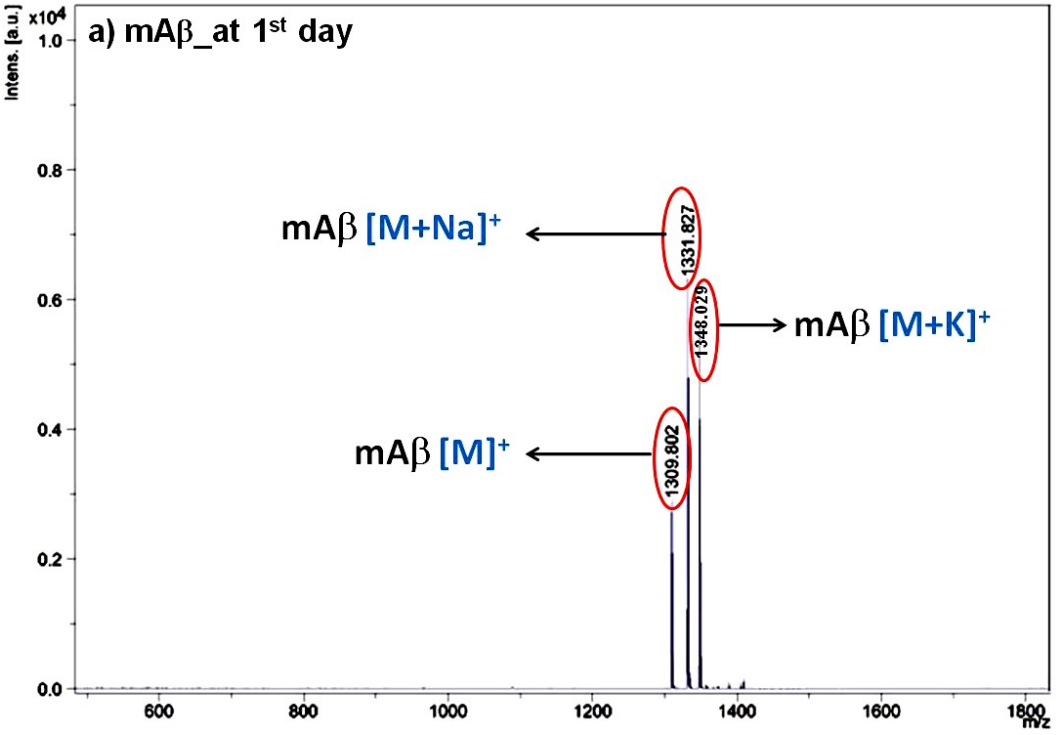

Figure S65. MALDI mass spectrum of mAβ at 1st day of incubation in PBS pH 7.4 at 37°C.

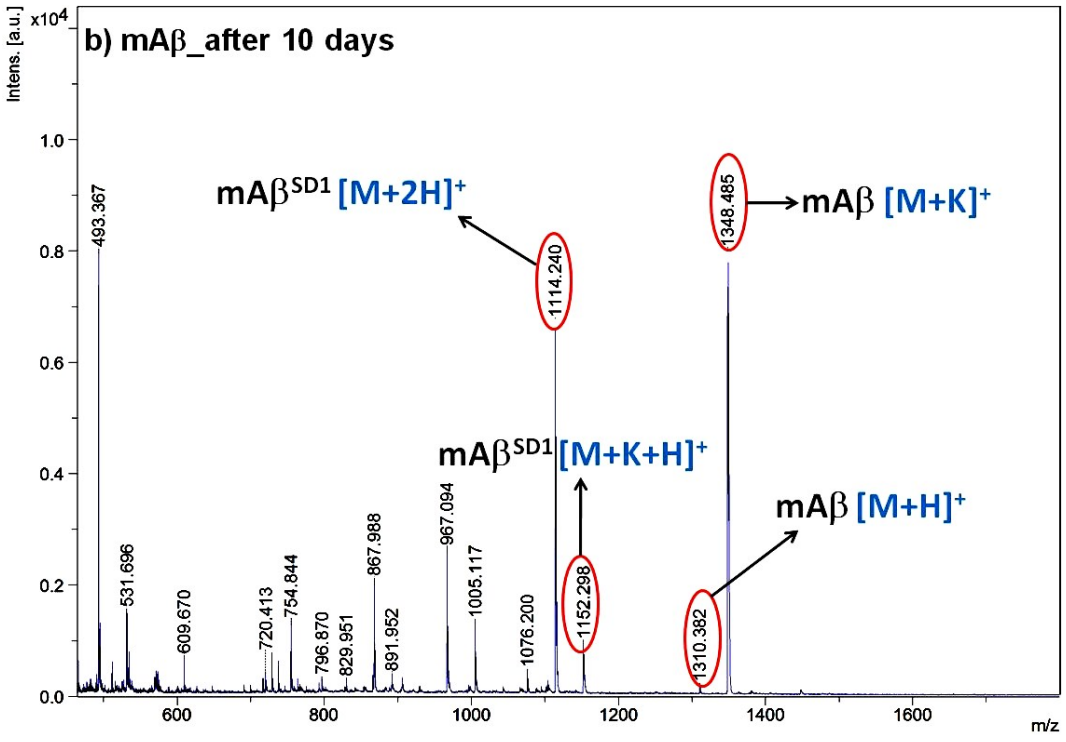

Figure S66. MALDI mass spectrum of mAβ after 10 days of incubation in PBS.

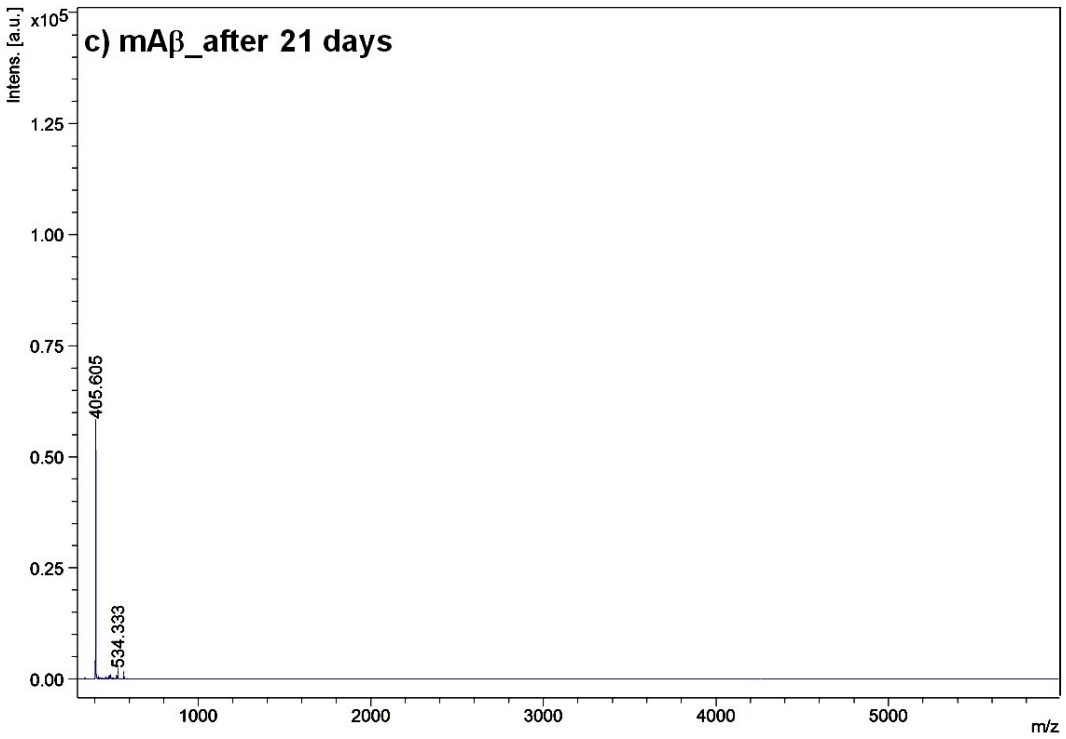

Figure S67. MALDI mass spectrum of mAβ after 21 days of incubation in PBS.

15. DFT calculation of the intermediate C’’’’:

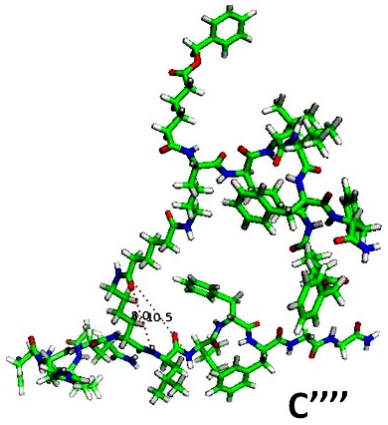

Figure S68. The most stable conformation of the intermediate C’’’’ (image generated by PyMOL) obtained from DFT calculation (Calculation Method: B3LYP, Basis Set: 6-31G, and Energy: -8804.41665341 a.u.).

16. Kinetics Study by HPLC and ESI-MS of mAβ in presence of AS2 (1:1):

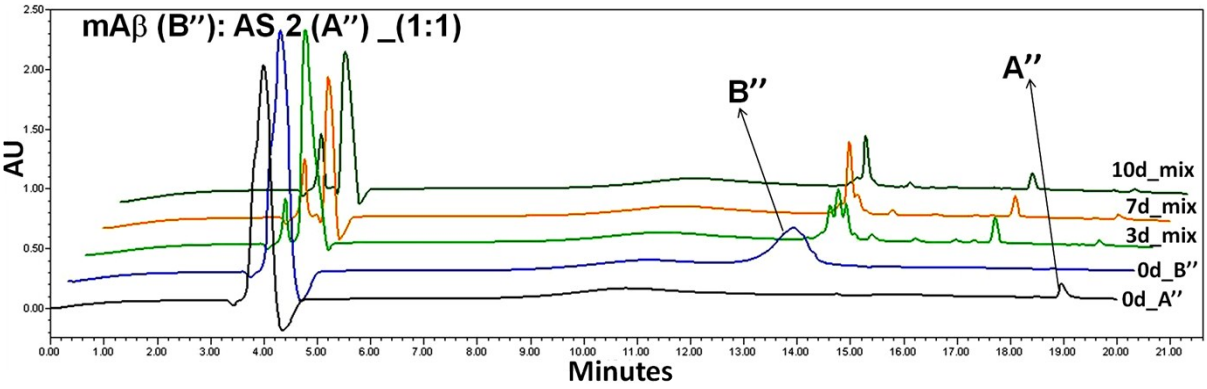

Figure S69. Time dependent kinetics study of mAβ in presence of AS2 (1:1), upto 10 days of incubation in PBS pH 7.4 at 37°C by RP-HPLC (Kinetics study was done using Waters 600E analytical HPLC system. An Ascentis C18 analytical column, flow rate of 0.8 ml/min, linear gradient of 5-50-100% CH_3CN over 0-10-18 minutes in a total run time of 20 min were used. Dual wavelength was selected at 214 nm and 254 nm).

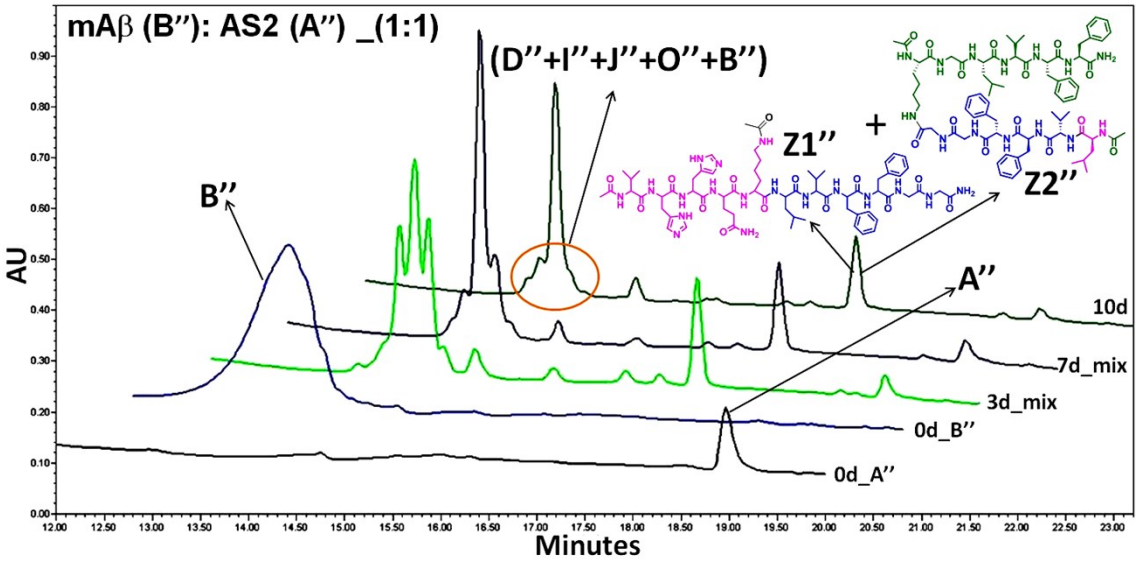

Figure S70. Expanded portion of the kinetics study of mAβ in presence of AS2 (1:1), upto 10 days of incubation in PBS pH 7.4 at 37°C.

Collected sample (from 10d_mix) was run further in Agilent-Q-TOF 6500 LCMS instrument, at ESI-positive mode. Agilent eclipse plus C18 analytical column, flow rate of 0.3 ml/min, linear gradient of 5-100% CH_3CN over 6 minutes in a total run time of 7 min were used. Wavelength was selected at 214 nm.

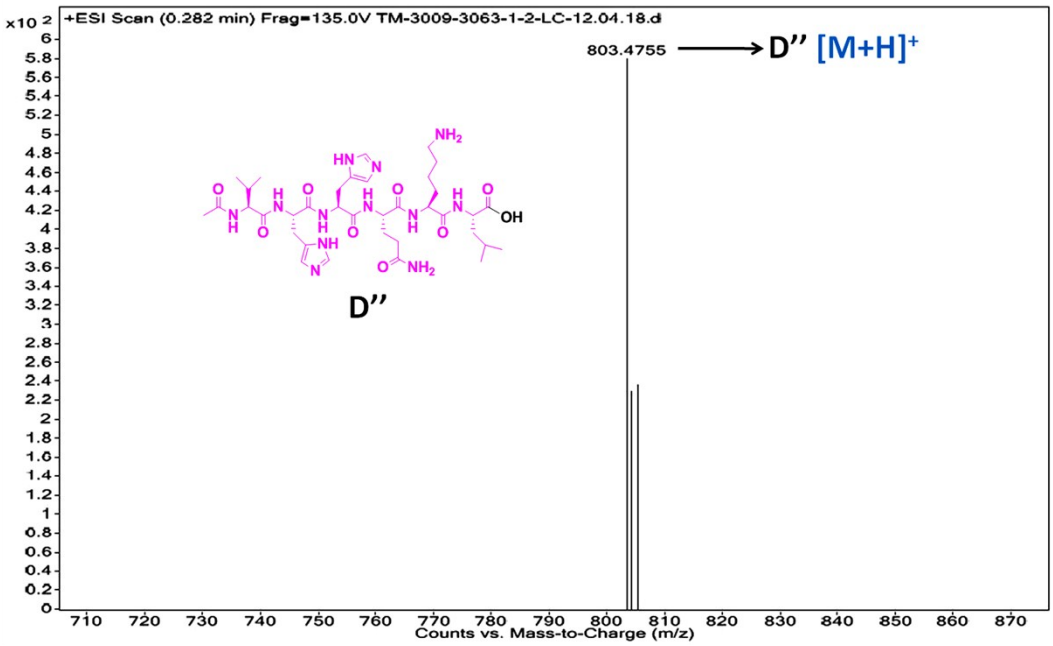

Figure S71. ESI-MS profile picture of the mAβ fragment D''. Calculated m/z for $C_{36}H_{58}N_{12}O_9$ $[M+H]^+$ is 803.4450, observed 803.4755.

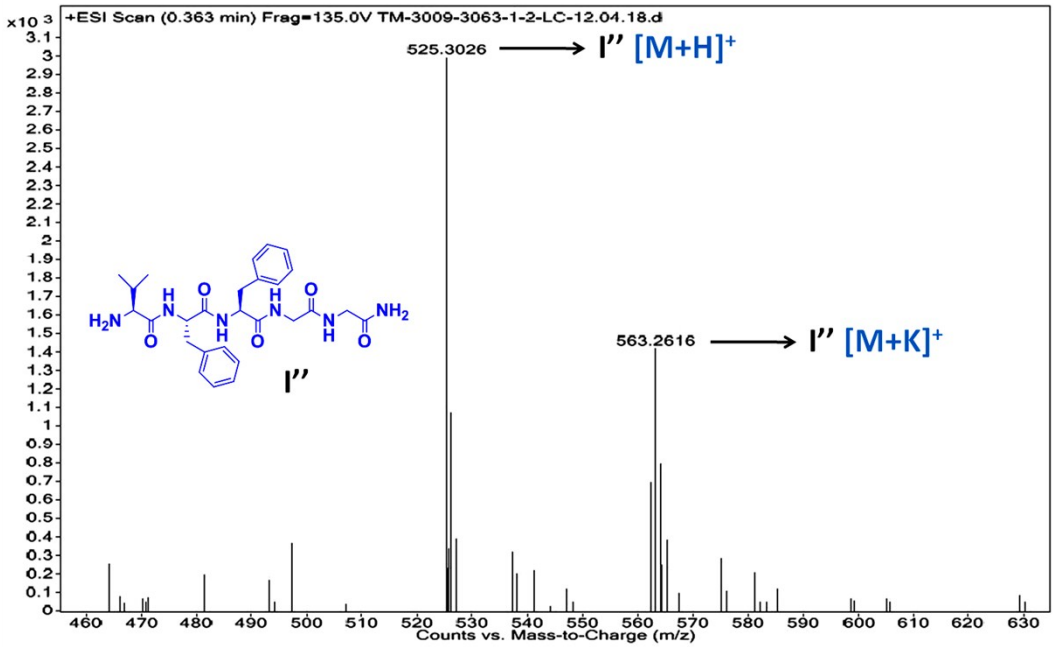

Figure S72. ESI-MS profile picture of the mAβ fragment I''. Calculated m/z for $C_{27}H_{36}N_6O_5$ $[M+H]^+$ is 525.2747, observed 525.3026; calculated m/z for $C_{27}H_{36}N_6O_5$ $[M+K]^+$ is 563.2747, observed 563.2616.

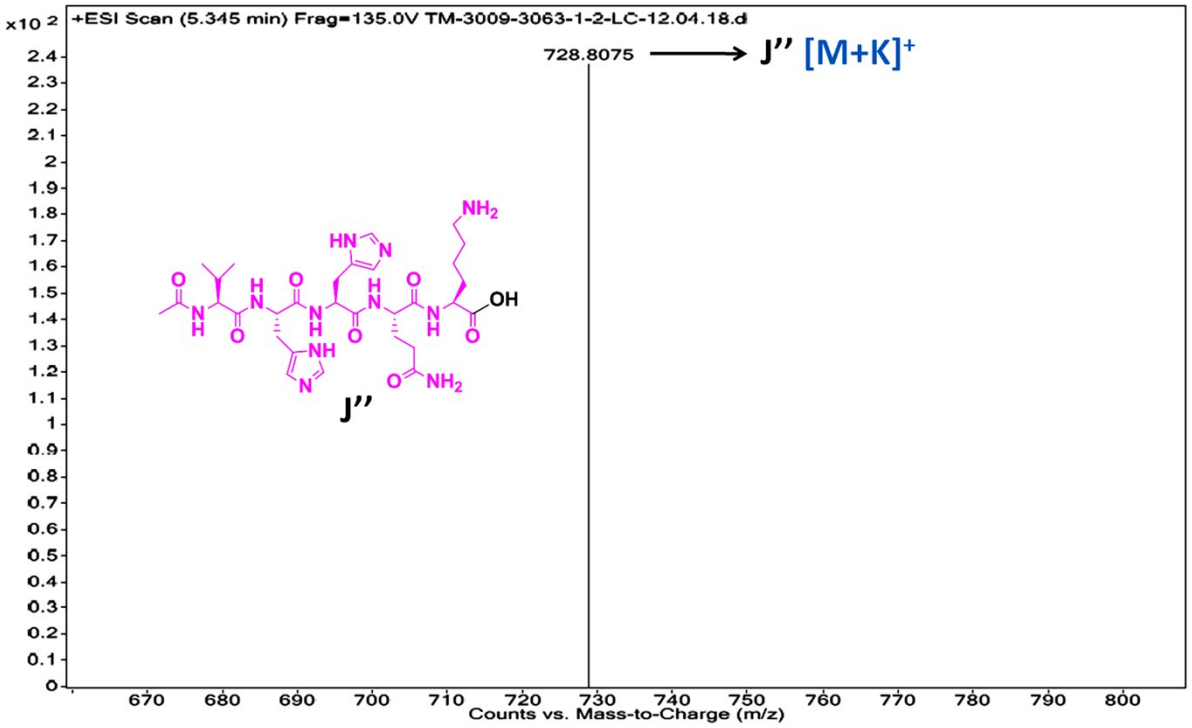

Figure S73. ESI-MS profile picture of the mAβ fragment J''. Calculated m/z for $C_{30}H_{47}N_{11}O_8$ $[M+K]^+$ is 728.7631, observed 728.8075.

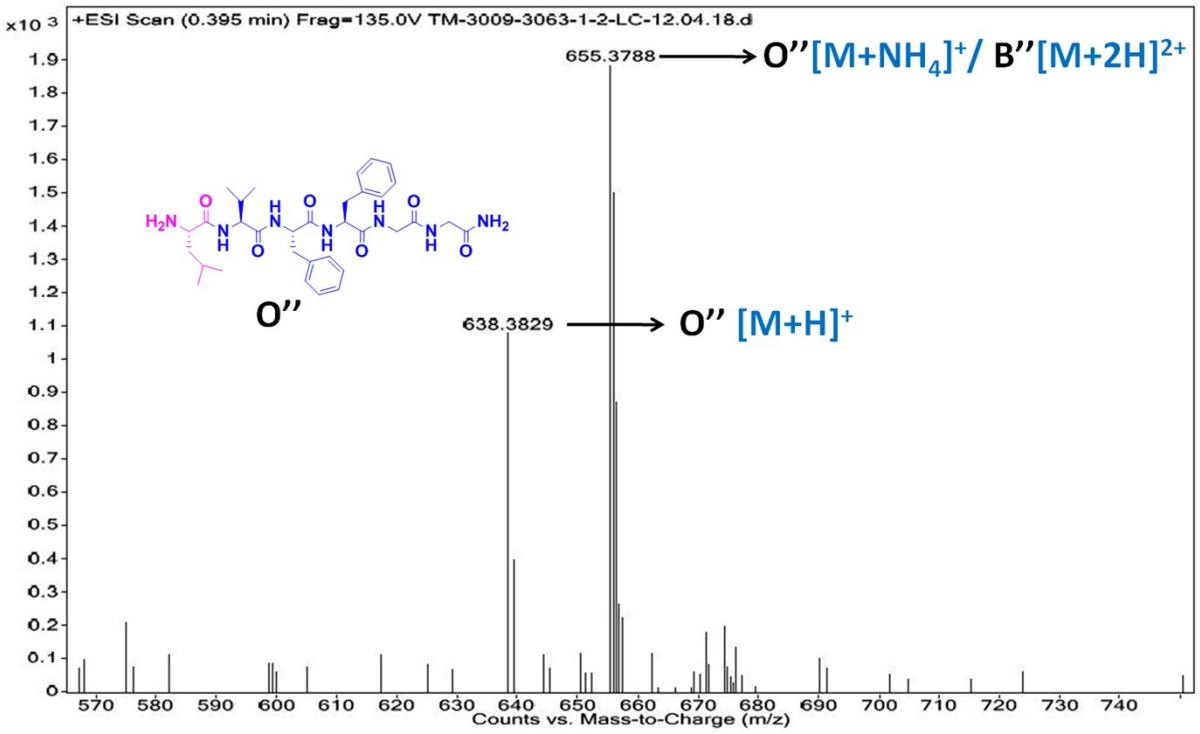

Figure S74. ESI-MS profile picture of the mAβ fragment O''. Calculated m/z for $C_{33}H_{47}N_7O_6$ $[M+H]^+$ is 638.3588, observed 638.3829; calculated m/z for $C_{33}H_{47}N_7O_6$ $[M+NH_4]^+$ is 655.3588, observed 655.3788. Calculated m/z for $C_{63}H_{92}N_{18}O_{13}$ $[M+2H]^{2+}$ is 655.3548, observed 655.3788.

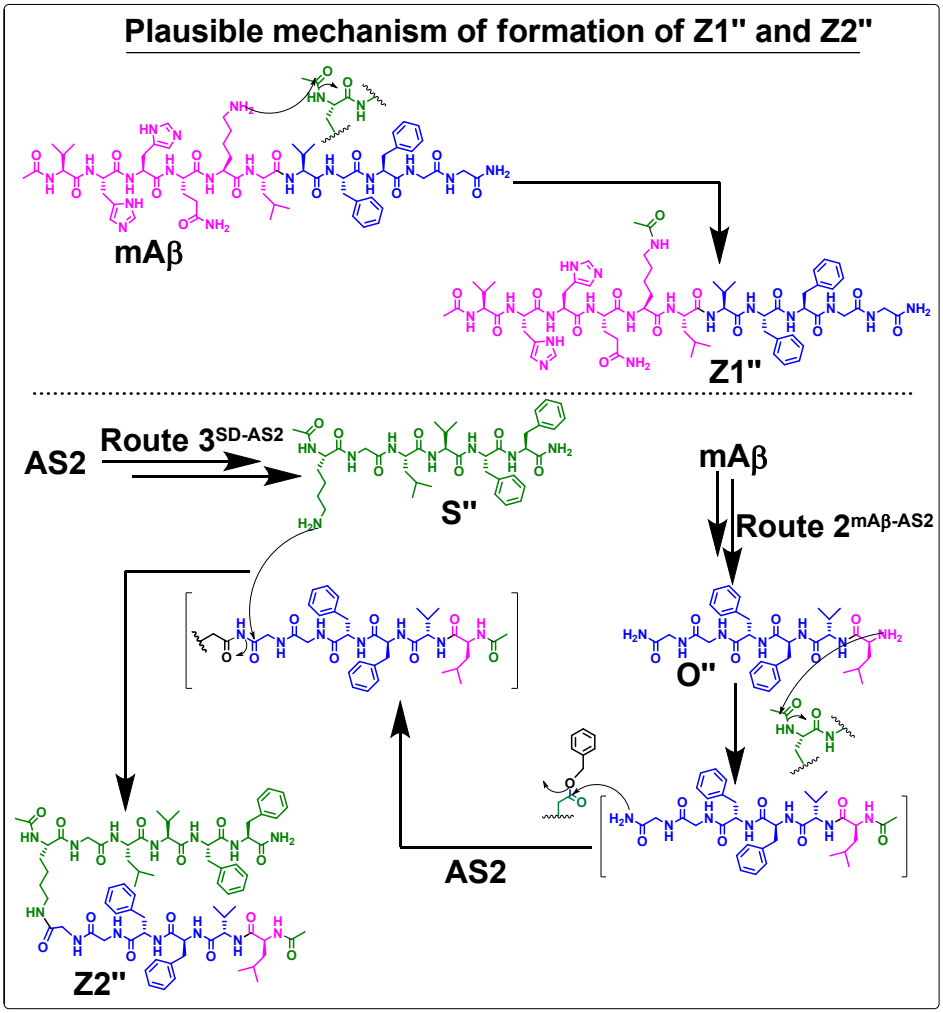

Figure S75. Plausible mechanism of formation of Z1'' and Z2''.

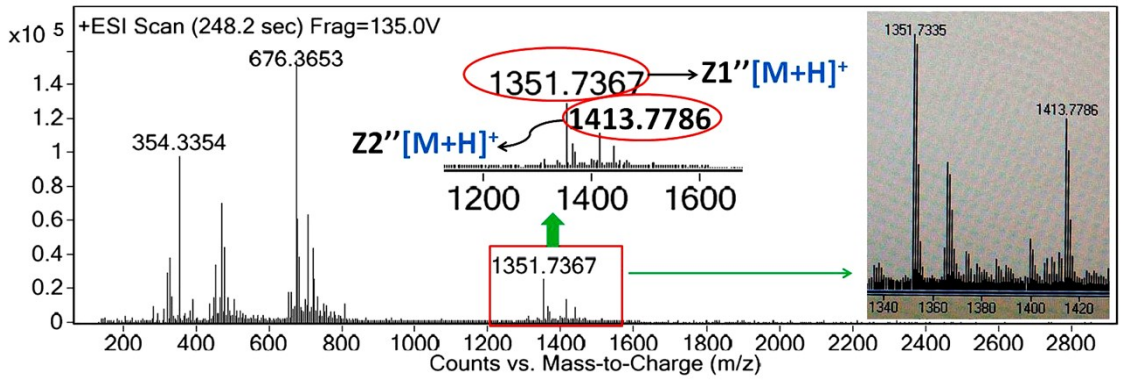

Figure S76. ESI-MS of Z1'' and Z2''. Calculated m/z for $C_{65}H_{94}N_{18}O_{14}$ $[M+H]^+$ is 1351.7197, observed 1351.7367 and calculated m/z for $C_{74}H_{104}N_{14}O_{14}$ $[M+H]^+$ is 1413.7856, observed 1413.7786.

17. Plausible routes of the proteolytic activity of AS4 on $A\beta_{1-40}$:

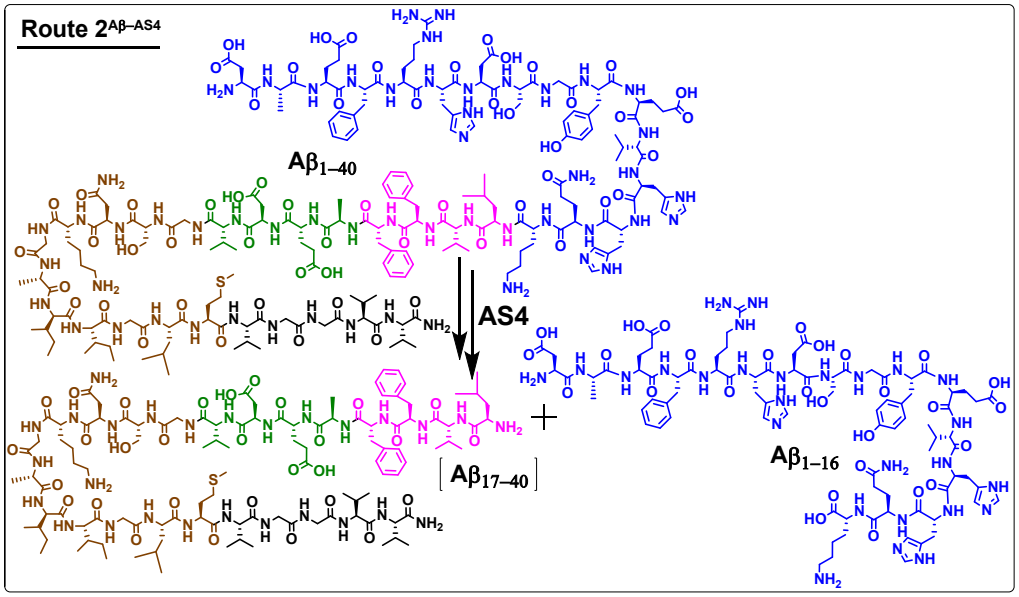

Figure S77. Plausible routes of proteolytic cleavage of $A\beta_{1-40}$ into various fragments by AS4 (Route $2^{A\beta-AS4}$). IM stands for Intermediate.

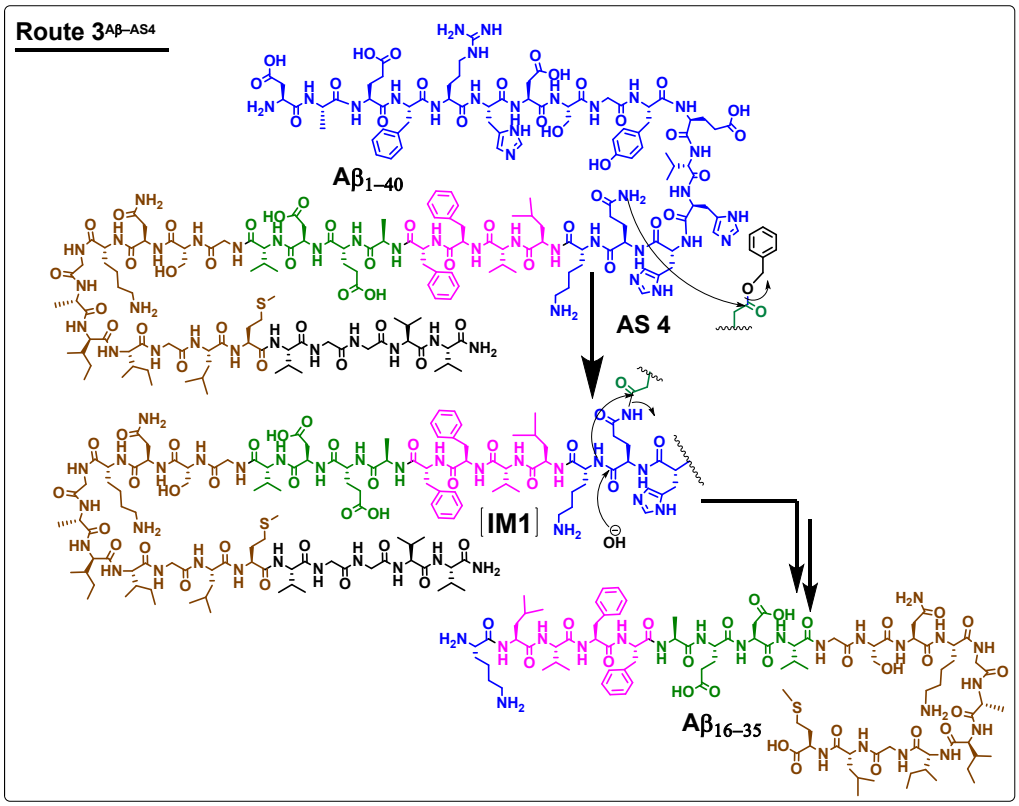

Figure S78. Plausible routes of proteolytic cleavage of $A\beta_{1-40}$ into various fragments by AS4 (Route $6^{A\beta-AS4}$).

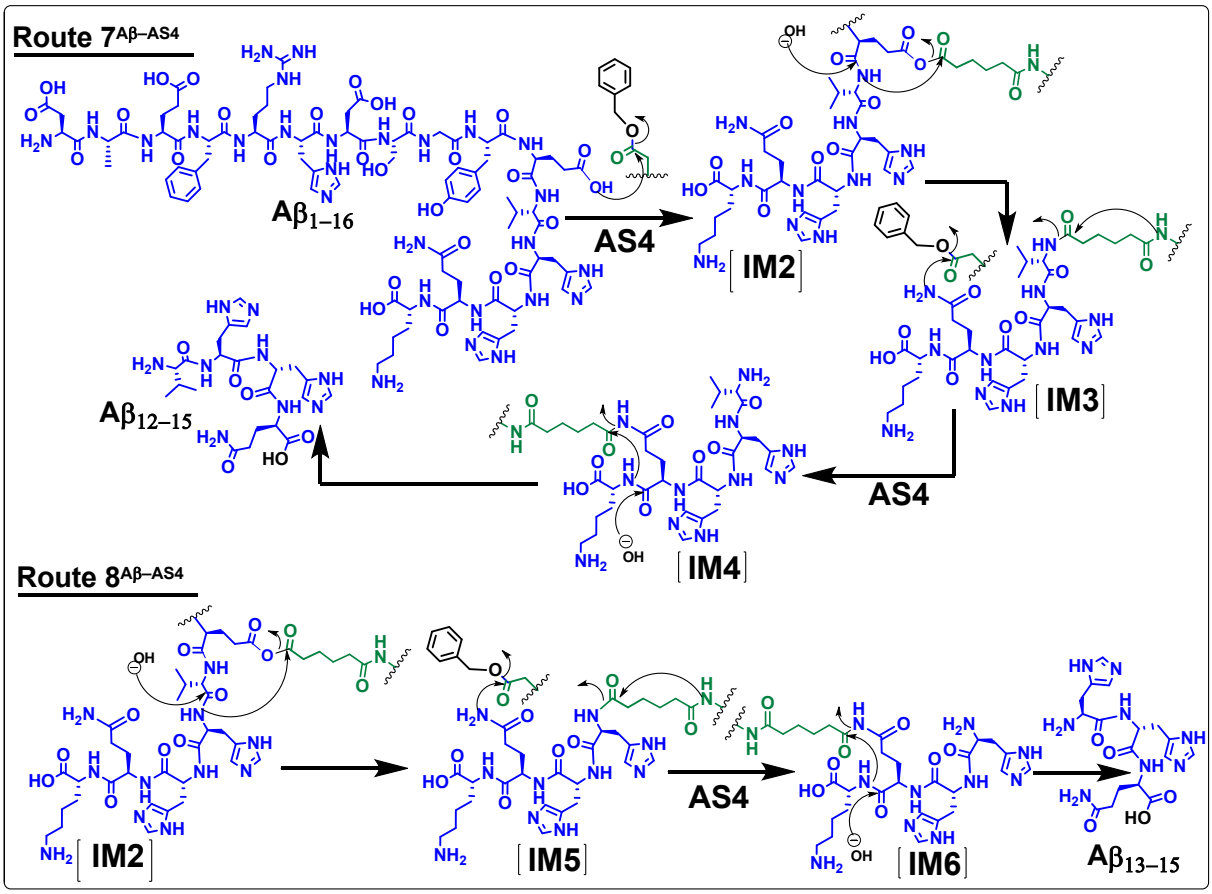

Figure S79. Plausible routes of proteolytic cleavage of $A\beta_{1-40}$ into various fragments by AS4 (Route $7^{A\beta-AS4}$ and Route $8^{A\beta-AS4}$).

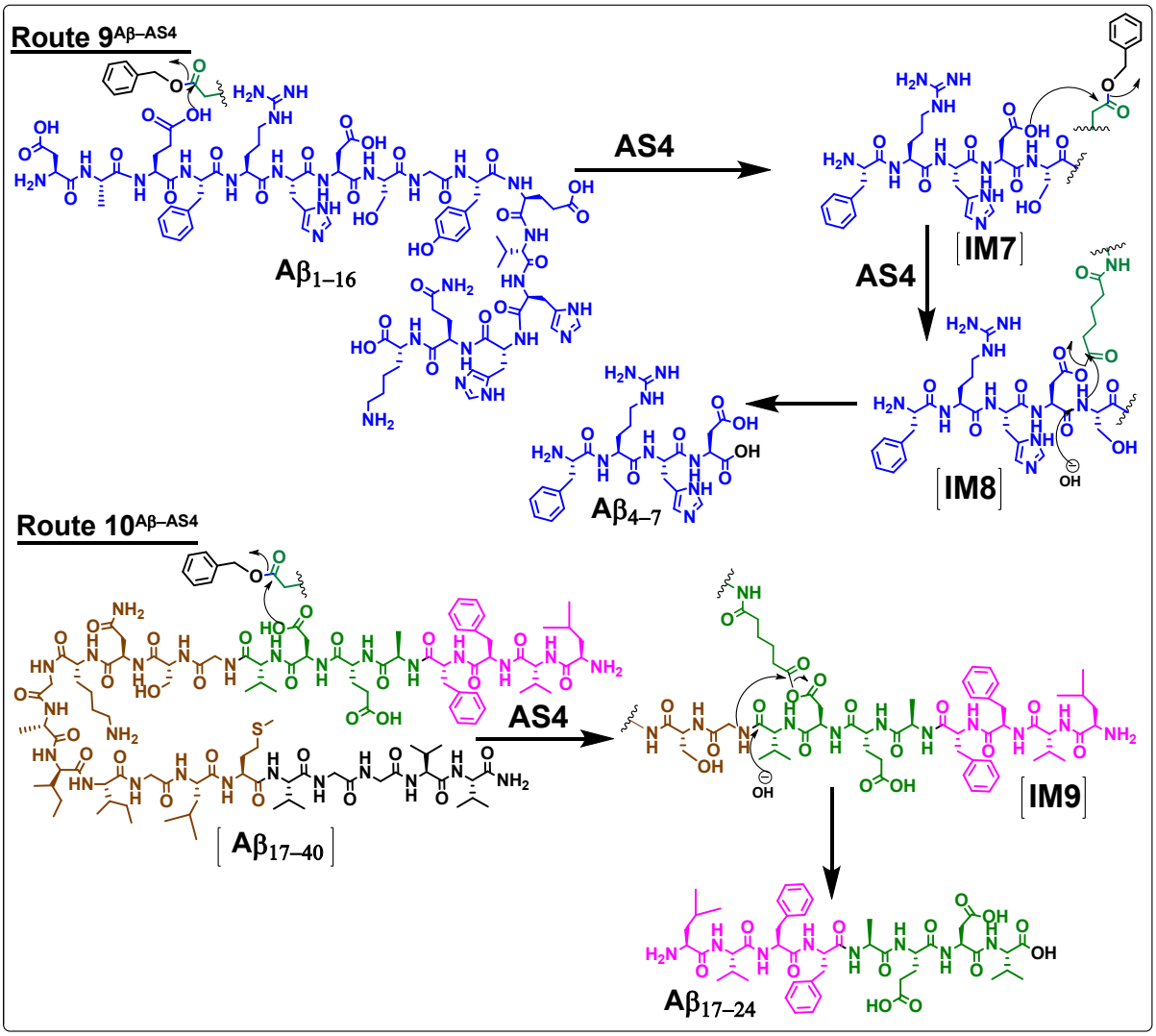

Figure S80. Plausible routes of proteolytic cleavage of $A\beta_{1-40}$ into various fragments by AS4 (Route $9^{A\beta\text{-}AS4}$ and Route $10^{A\beta\text{-}AS4}$).

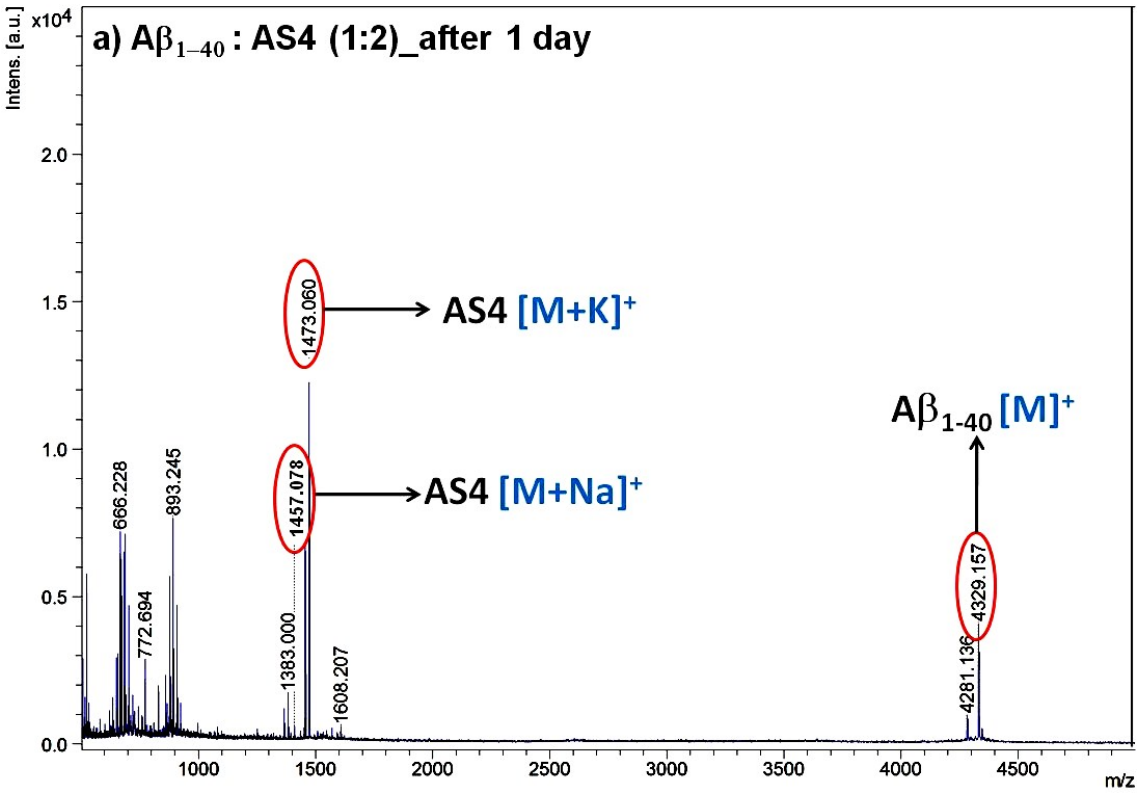

Figure S81. MALDI mass spectrum of Aβ in presence of AS4 (1:2) after 1 day of incubation in PBS pH 7.4 at 37°C.

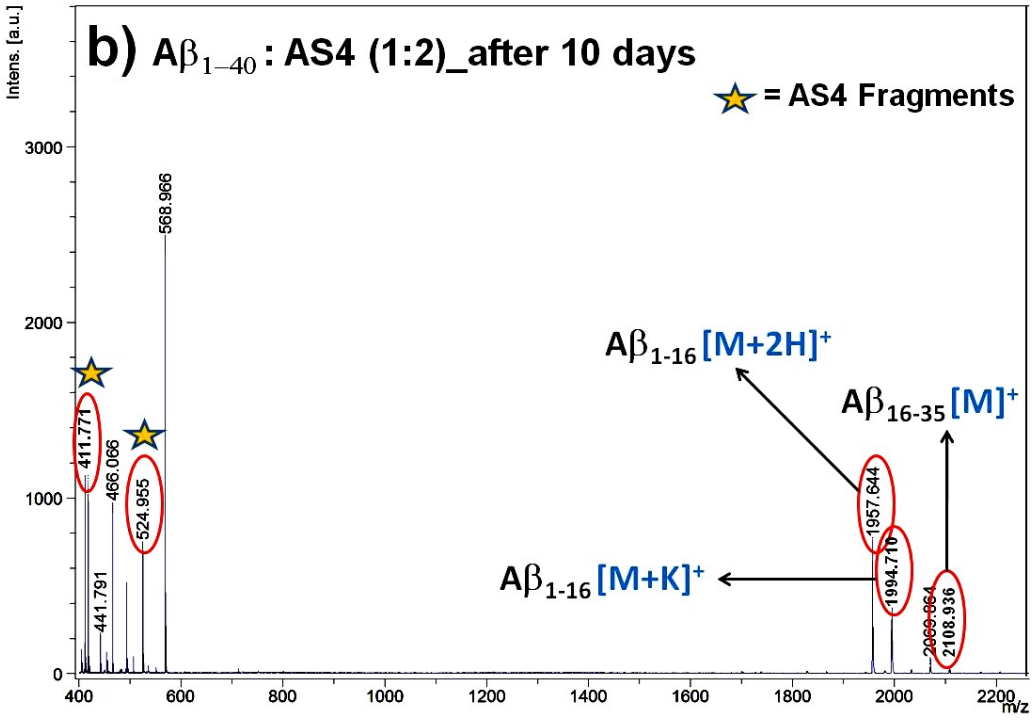

Figure S82. MALDI mass spectrum of Aβ in presence of AS4 (1:2) after 10 days of incubation in PBS.

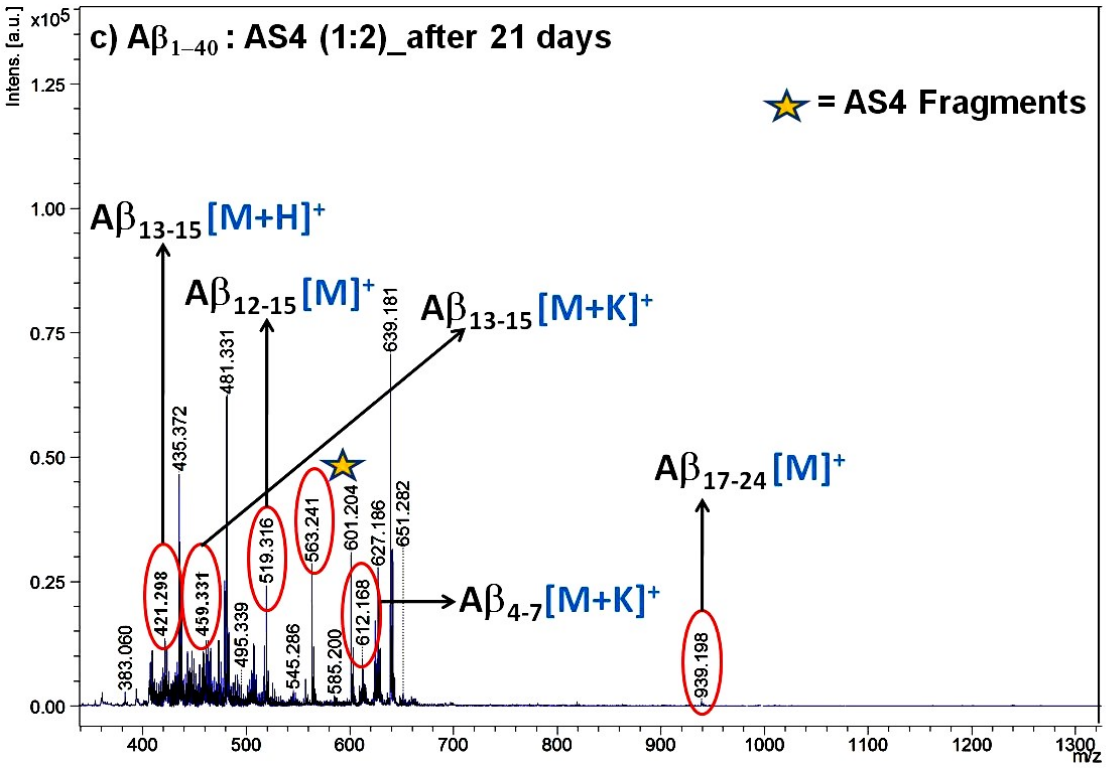

Figure S83. MALDI mass spectrum of Aβ in presence of AS4 (1:2) after 21 days of incubation in PBS.

18. MALDI mass spectra of $A\beta_{1-40}$:

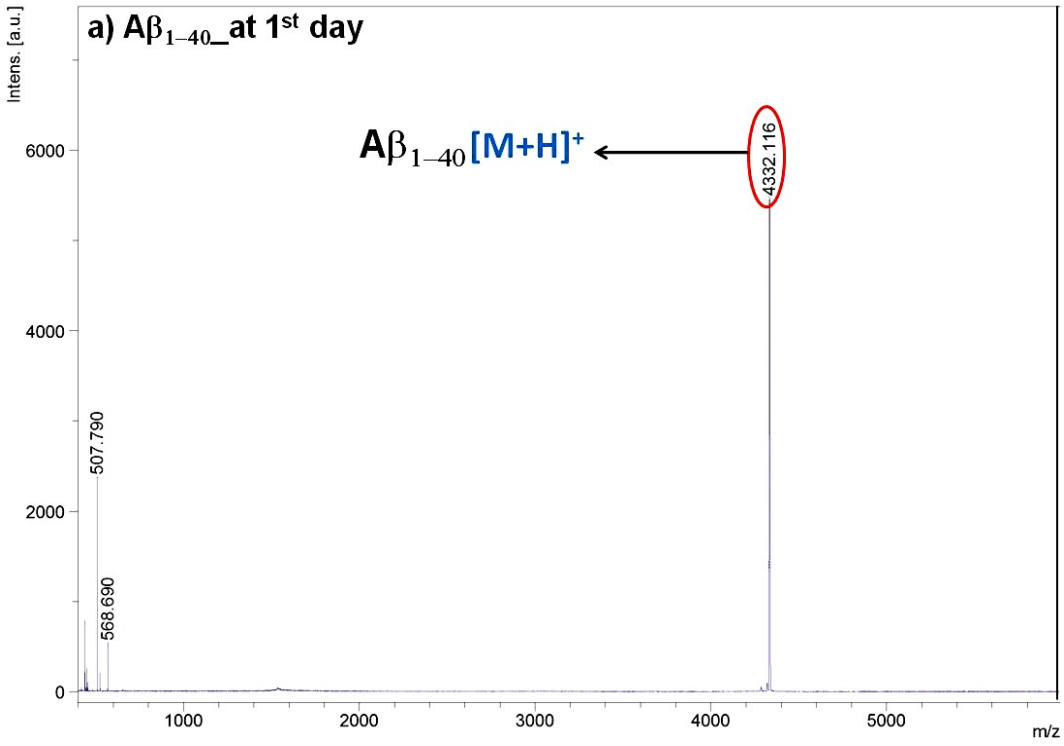

Figure S84. MALDI mass spectrum of Aβ in absence of AS4 at 1st day in PBS.

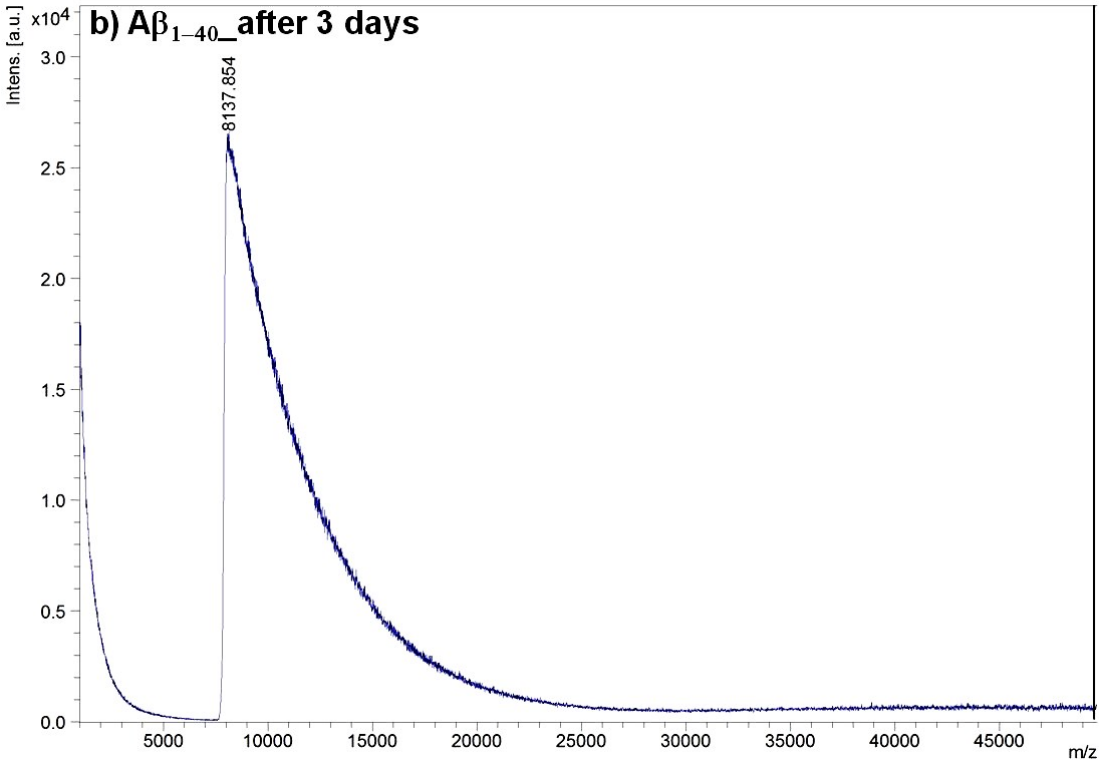

Figure S85. MALDI mass spectrum of Aβ in absence of AS4 after 3 days of incubation in PBS.

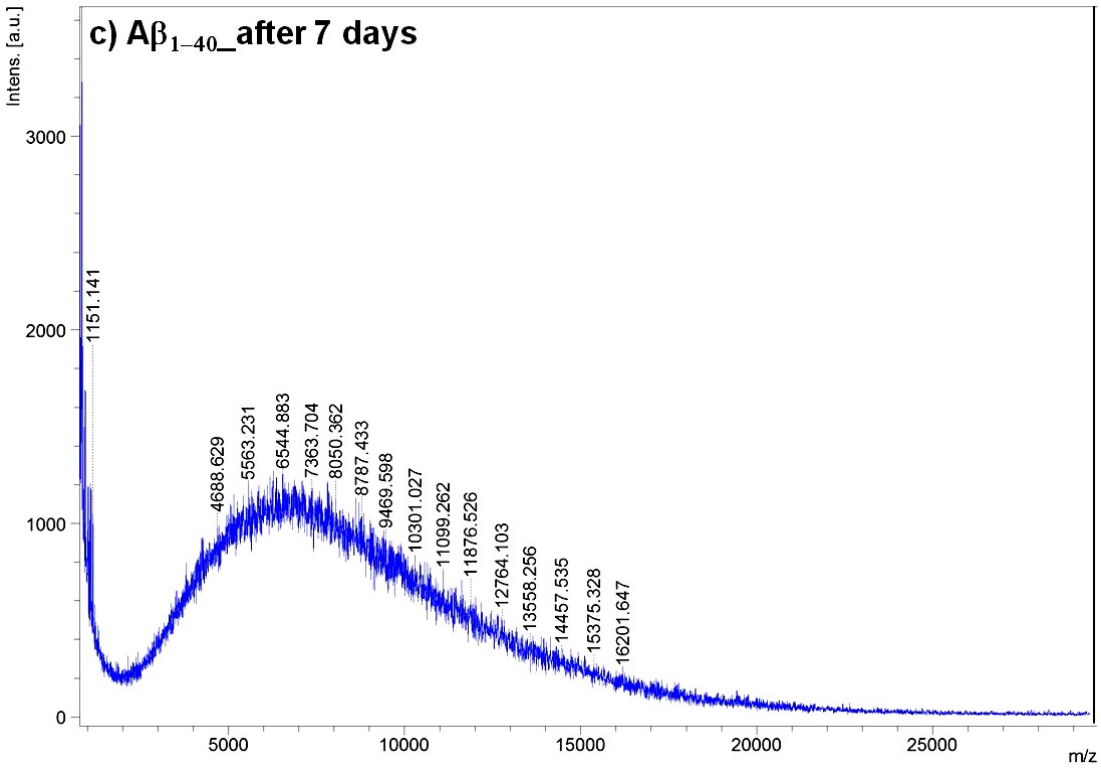

Figure S86. MALDI mass spectrum of Aβ in absence of AS4 after 7 days of incubation in PBS.

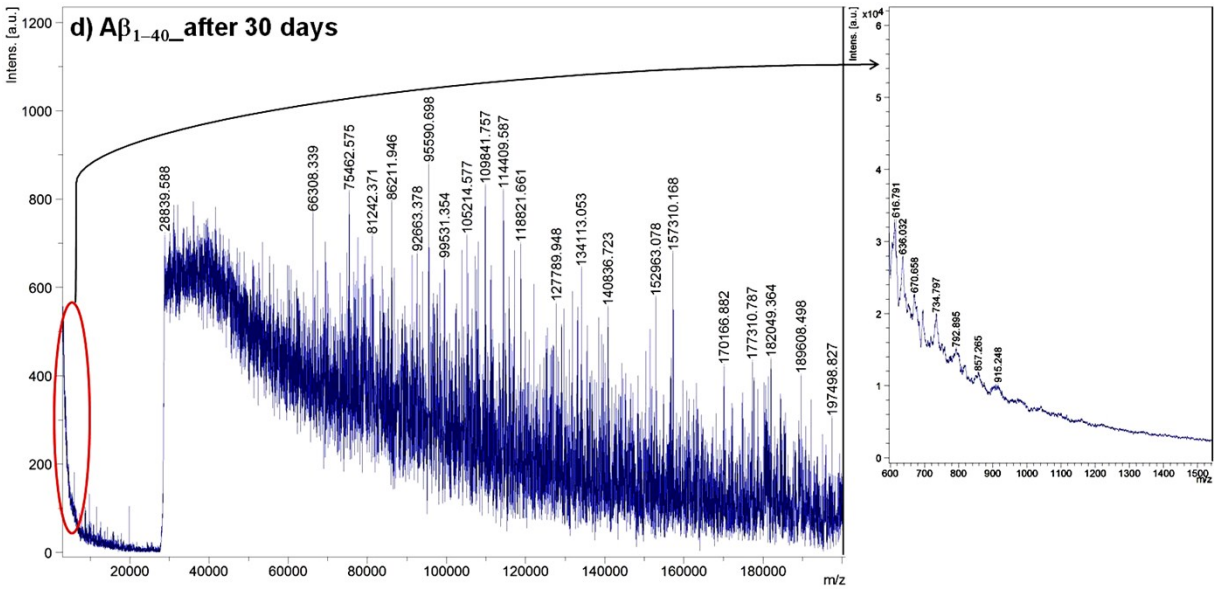

Figure S87. MALDI mass spectrum of Aβ in absence of AS4 after 30 days of incubation in PBS.

19. Plausible routes of the proteolytic activity of AS4 on mutant DTP 28, the negative control (NC) peptide):

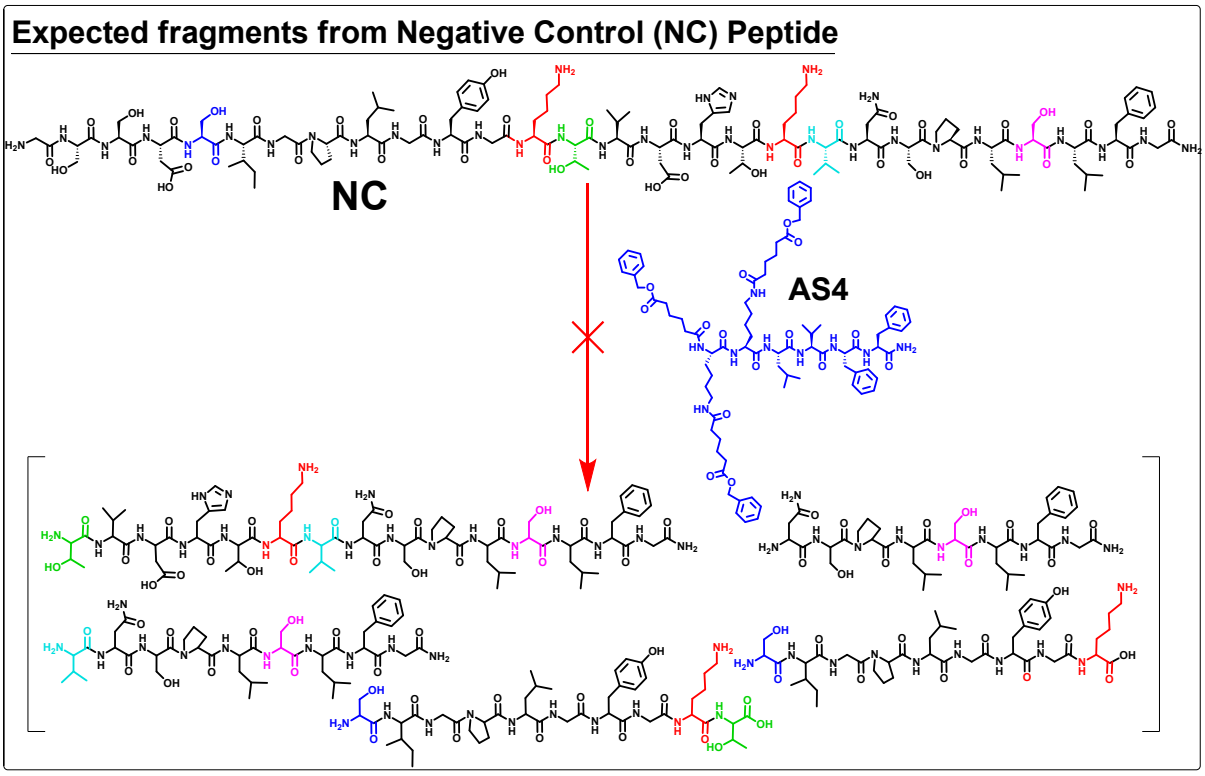

Figure S88. Negative control (NC) peptide didn't give expected fragments in presence of AS4.

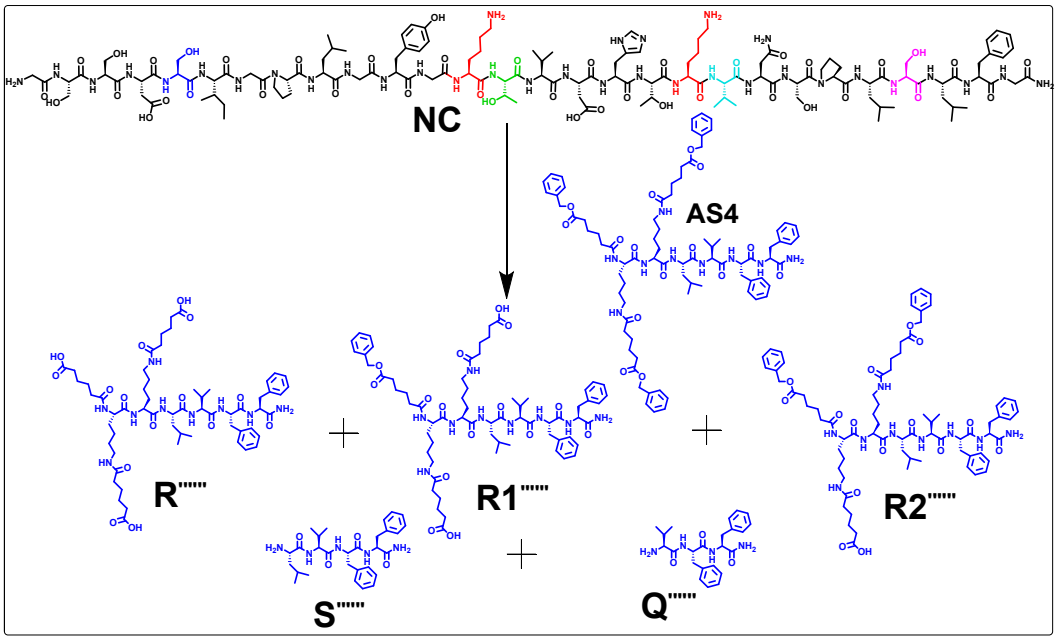

Figure S89. Observed self degradation products of AS4 in presence of NC peptide (Route $1^{SD\text{-}AS4}$, Route $4^{SD\text{-}AS4}$and Route $5^{SD\text{-}AS4}$).

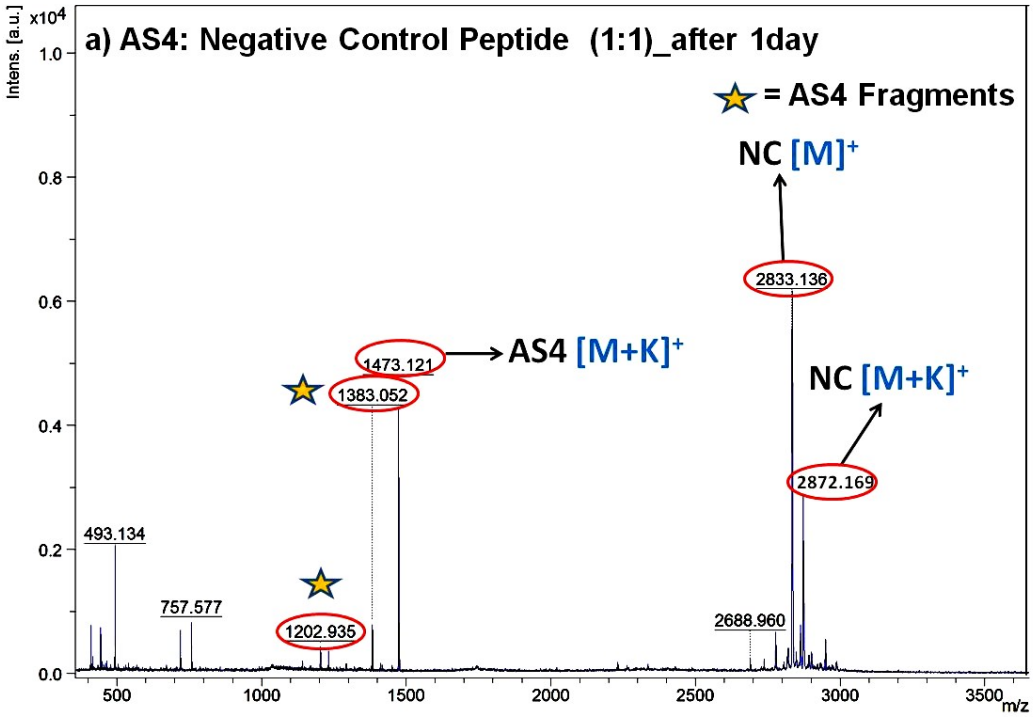

Figure S90. MALDI mass spectrum of negative control peptide in presence of AS4 (1:1) after 1 day of incubation in PBS pH 7.4 at 37°C.

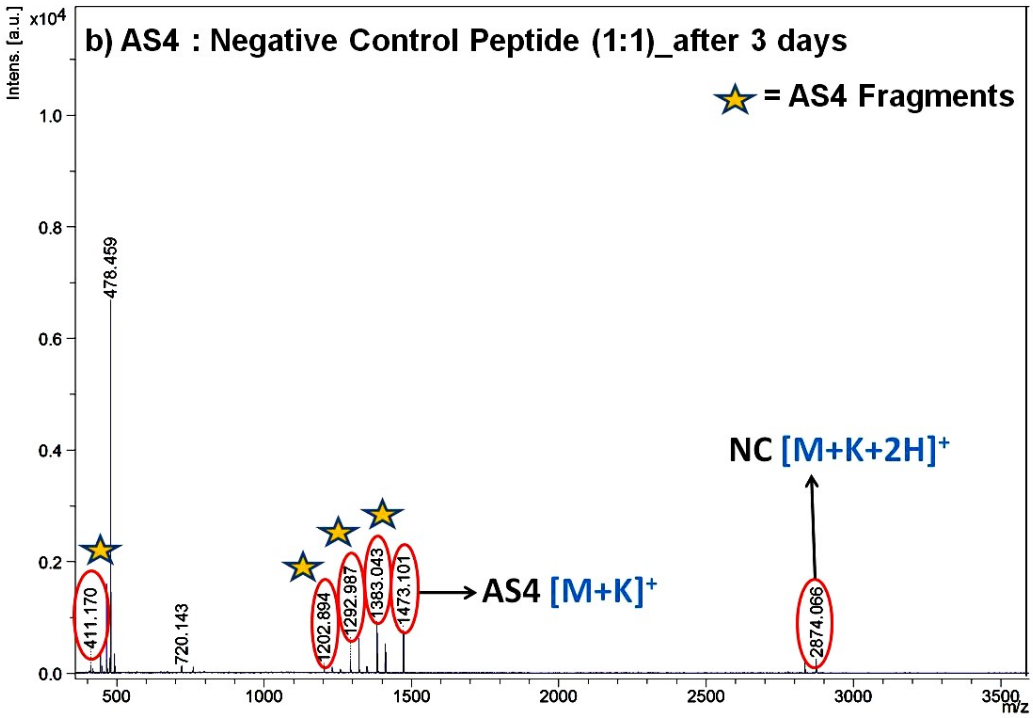

Figure S91. MALDI mass spectrum of negative control peptide in presence of AS4 (1:1) after 3 days of incubation in PBS pH 7.4 at 37°C.

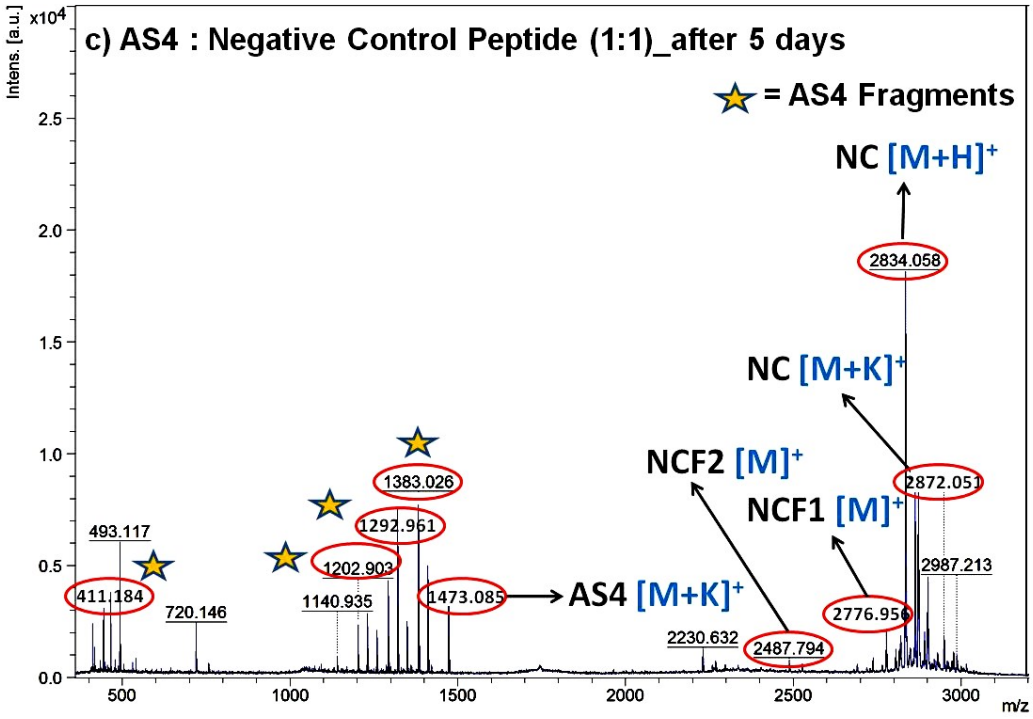

Figure S92. MALDI mass spectrum of negative control peptide in presence of AS4 (1:1) after 5 days of incubation in PBS pH 7.4 at 37°C.

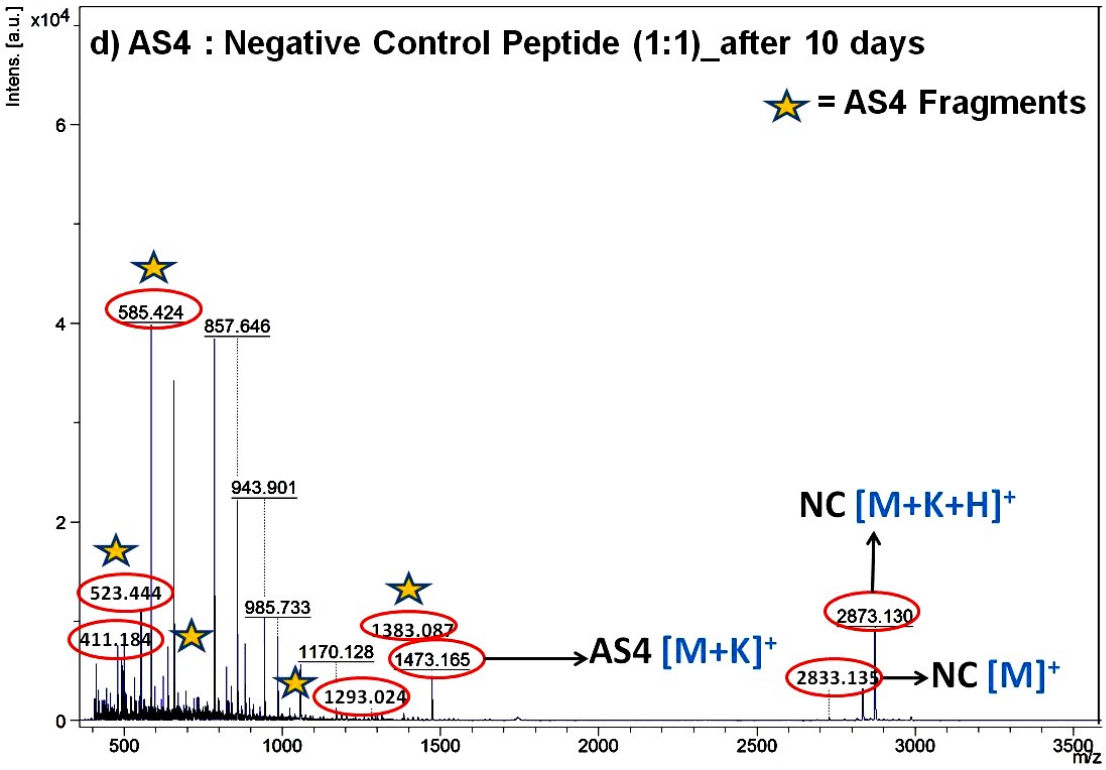

Figure S93. MALDI mass spectrum of negative control peptide in presence of AS4 (1:1) after 10 days of incubation in PBS pH 7.4 at 37°C.

20. Self degradation of mutant DTP 28 (NC):

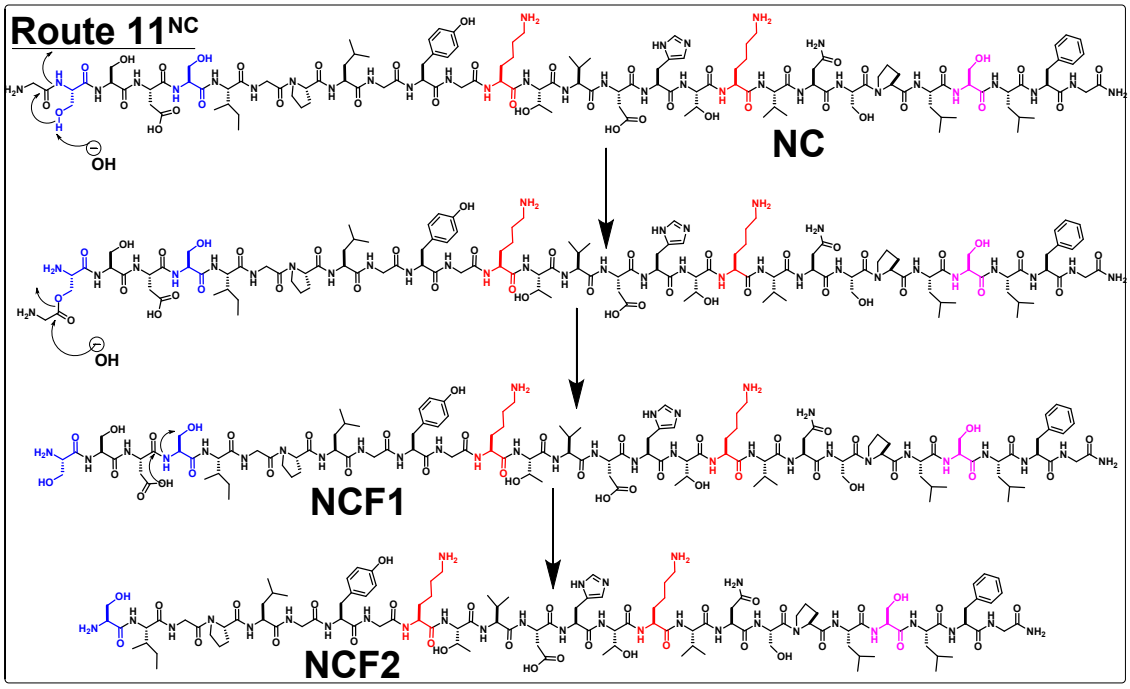

Figure S94. Plausible routes of cleavage of NC peptide into various fragments in absence of AS4 (Route 11^{NC}). NCF stands for negative control peptide fragments.

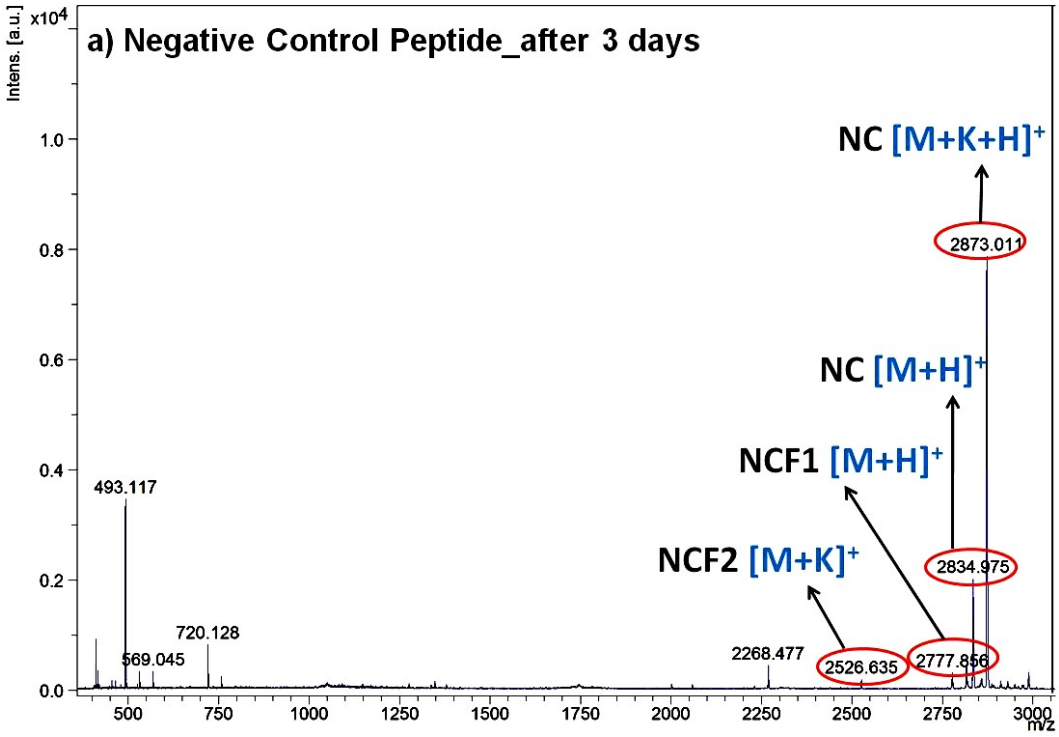

Figure S95. MALDI mass spectrum of NC peptide in absence of AS4 after 3 days of incubation in PBS pH 7.4 at 37°C.

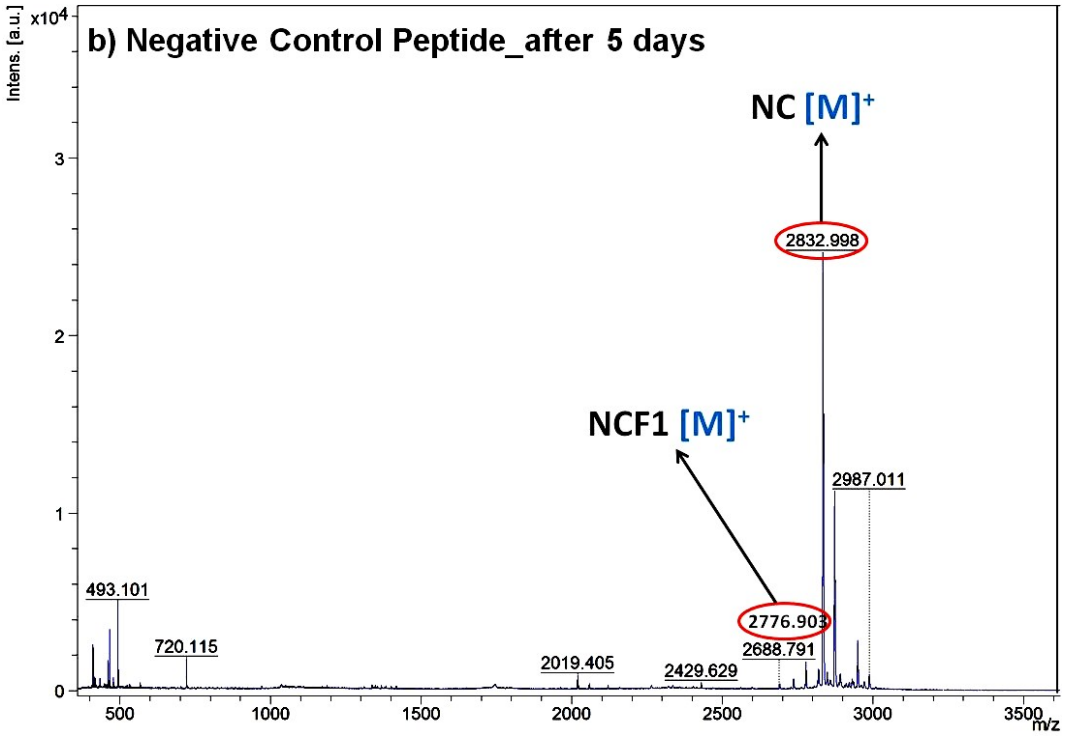

Figure S96. MALDI mass spectrum of NC peptide in absence of AS4 after 5 days of incubation in PBS pH 7.4 at 37°C.

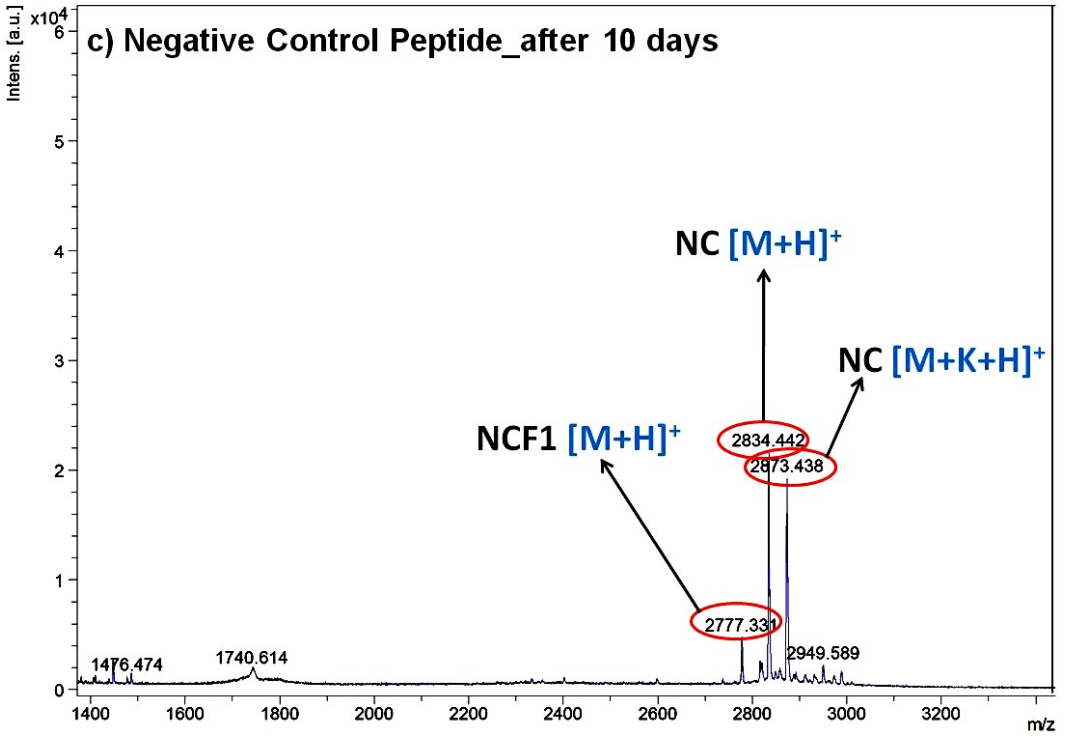

Figure S97. MALDI mass spectrum of NC peptide in absence of AS4 after 10 days of incubation in PBS pH 7.4 at 37°C.

21. Inhibition of amyloid accumulation of $A\beta_{1-40}$ by AS4:

21.1. ThT fluorescence assay and CD experiments of $A\beta_{1-40}$:

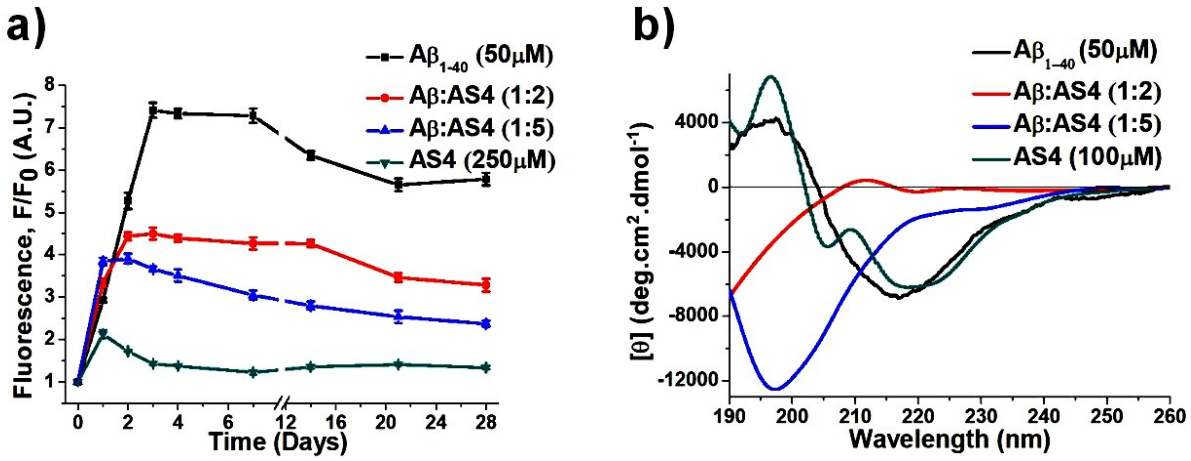

Figure S98. Normalized profiles of dose dependent (a) ThT fluorescence assay, and (b) CD experiments. Spectra of $A\beta_{1-40}$ in absence (black), presence of 2 fold AS4 (red), 5 fold AS4 (blue), and AS4 alone (dark cyan). CD Spectra were recorded after 28 days of incubation. Error bars represent standard deviations of at least three independent measurements. All the peptide solutions were incubated in PBS pH 7.4 (50 mM) at 37°C in parallel.

21.2. FTIR spectra of $A\beta_{1-40}$:

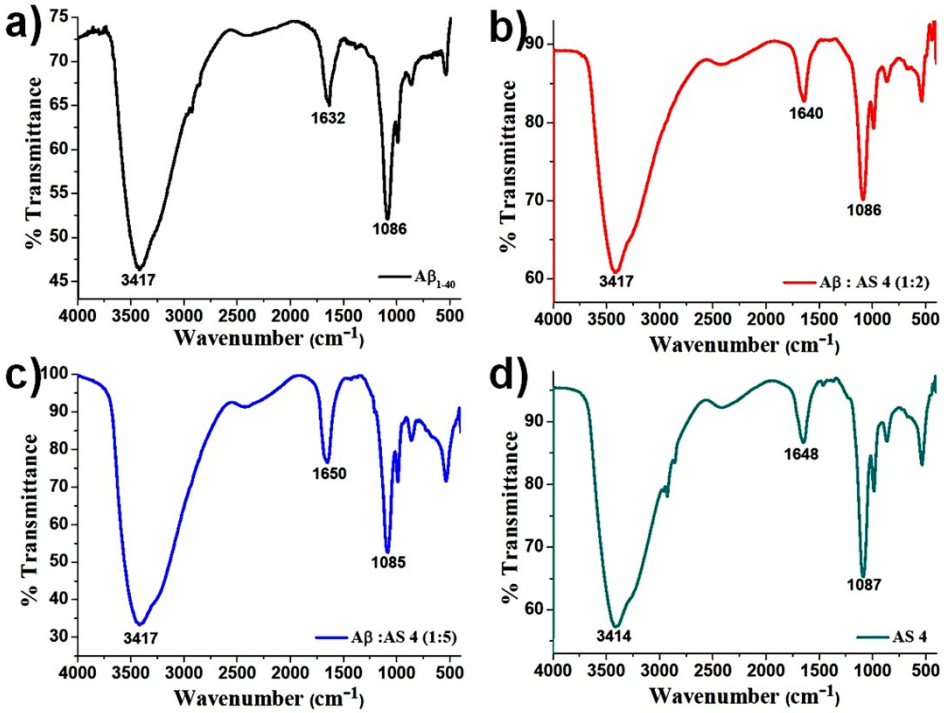

Figure S99. FTIR spectra of $A\beta_{1-40}$ (black, a) in absence, presence of (red, b) 2 fold AS4, (blue, c) 5 fold molar excess of AS4, and AS4 alone (dark cyan red, d). Spectra were recorded after 28 days of incubation. All the peptide solutions were incubated in PBS pH 7.4 (50 mM) at 37°C.

21.3. TEM images, Congo red stained birefringence images, and AFM images of $A\beta_{1-40}$:

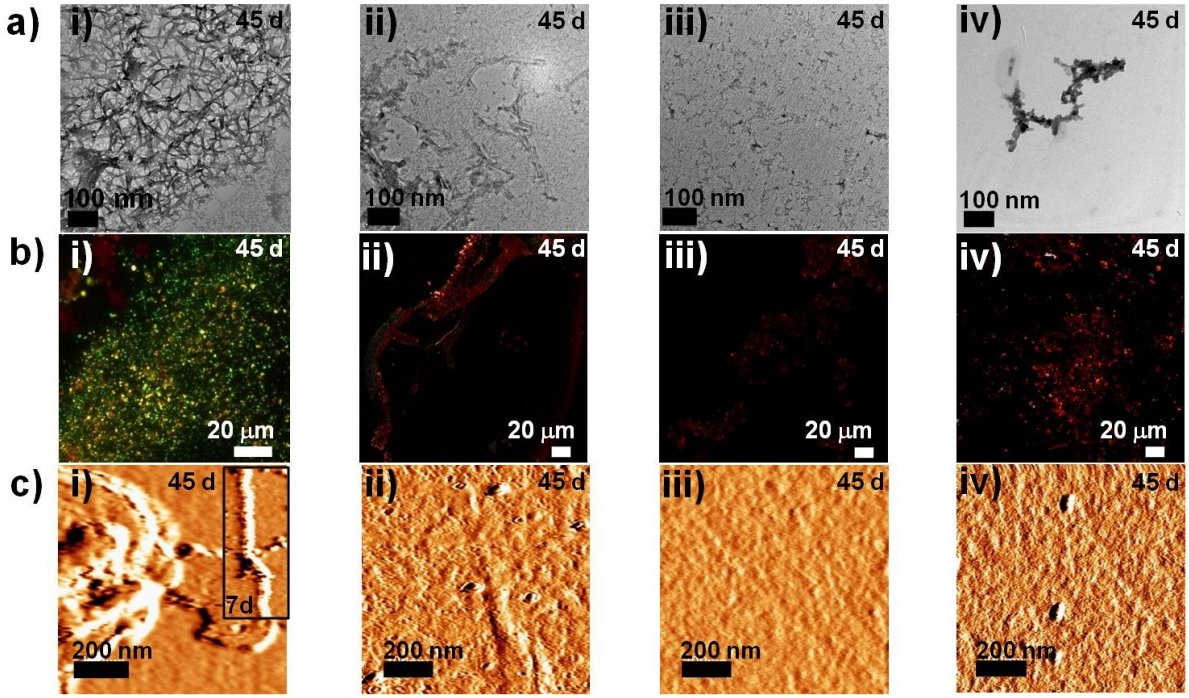

Figure S100. (a) TEM images, (b) Congo red stained birefringence images, and (c) AFM images of $A\beta_{1-40}$ (i) in absence, and presence of (ii) 2 fold AS4, (iii) 5 fold AS4, and (iv) AS4 alone. Images that were captured after 45 days are displayed. Scale bars are indicated as 200 nm for TEM and AFM images and 20 μm for birefringence images. All the peptide solutions were incubated in PBS pH 7.4 (50 mM) at 37°C in parallel.

22. Disruption of preformed $A\beta_{1-40}$ fibril by AS4:

22.1. ThT fluorescence assay and CD experiments of $A\beta_{1-40}$:

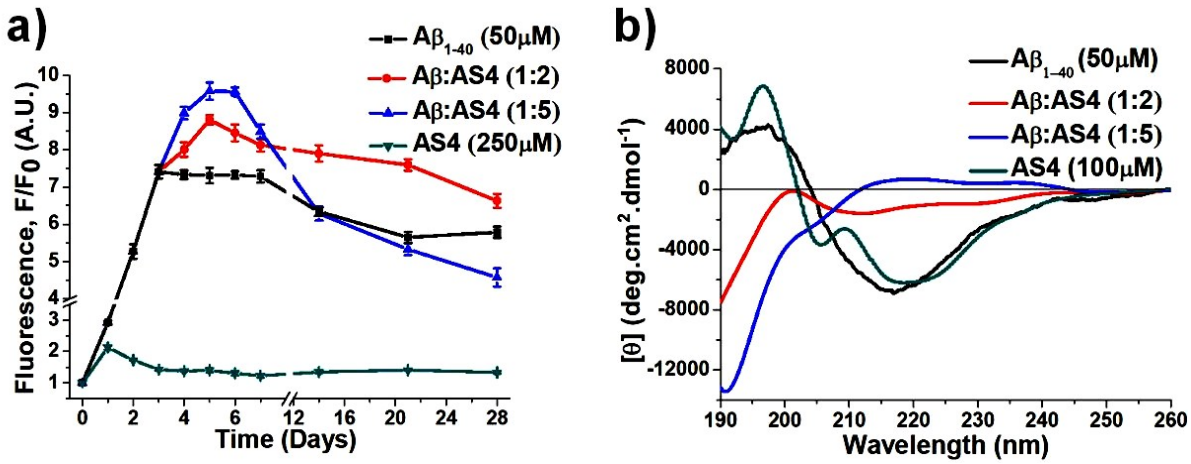

Figure S101. Normalized profiles of dose dependent (a) ThT fluorescence assay, and (b) CD experiments. Spectra of $A\beta_{1-40}$ in absence (black), presence of 2 fold AS4 (red), 5 fold AS4 (blue), and AS4 alone (dark cyan). CD Spectra were recorded after 28 (3+25) days of incubation. Error bars represent standard deviations of at least three independent measurements. All the peptide solutions were incubated in PBS pH 7.4 (50 mM) at 37°C in parallel.

22.2. FTIR spectra of $A\beta_{1-40}$:

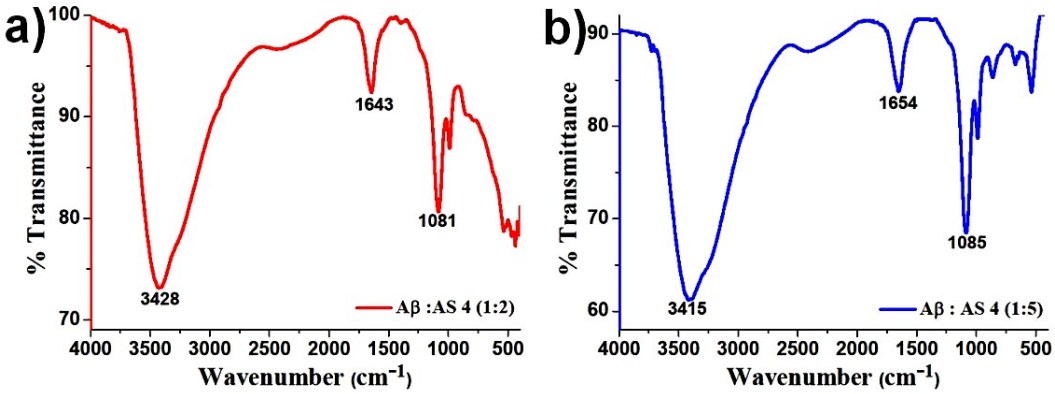

Figure S102. FTIR spectra of preformed $A\beta_{1-40}$ fibril disruption in presence of (red, a) 2 fold AS4 and (blue, b) 5 fold molar excess of AS4. AS4 added to $A\beta_{1-40}$ after 3 days of its incubation. Spectra were recorded after (3+25) days of incubation. All the peptide solutions were incubated in PBS pH 7.4 (50 mM) at 37°C.

22.3. TEM images and Congo red stained birefringence images of $A\beta_{1-40}$:

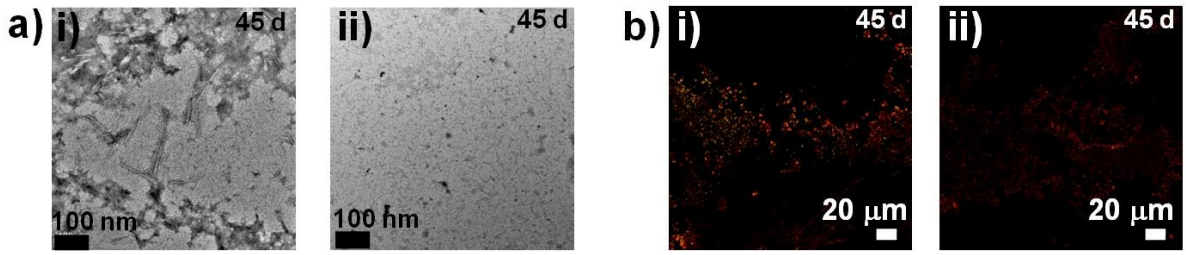

Figure S103. (a) TEM images, and (b) Congo red stained birefringence images of $A\beta_{1-40}$ (i) in absence, and presence of (i) 2 fold AS4, (ii) 5 fold AS4. Images that were captured after 45 (3+42) days are displayed. Scale bars are indicated as 200 nm for TEM images and 20 μm for birefringence images. All the peptide solutions were incubated in PBS pH 7.4 (50 mM) at 37°C in parallel.

23. DLS analysis of inhibiting $A\beta_{1-40}$ fibril formation by AS4:

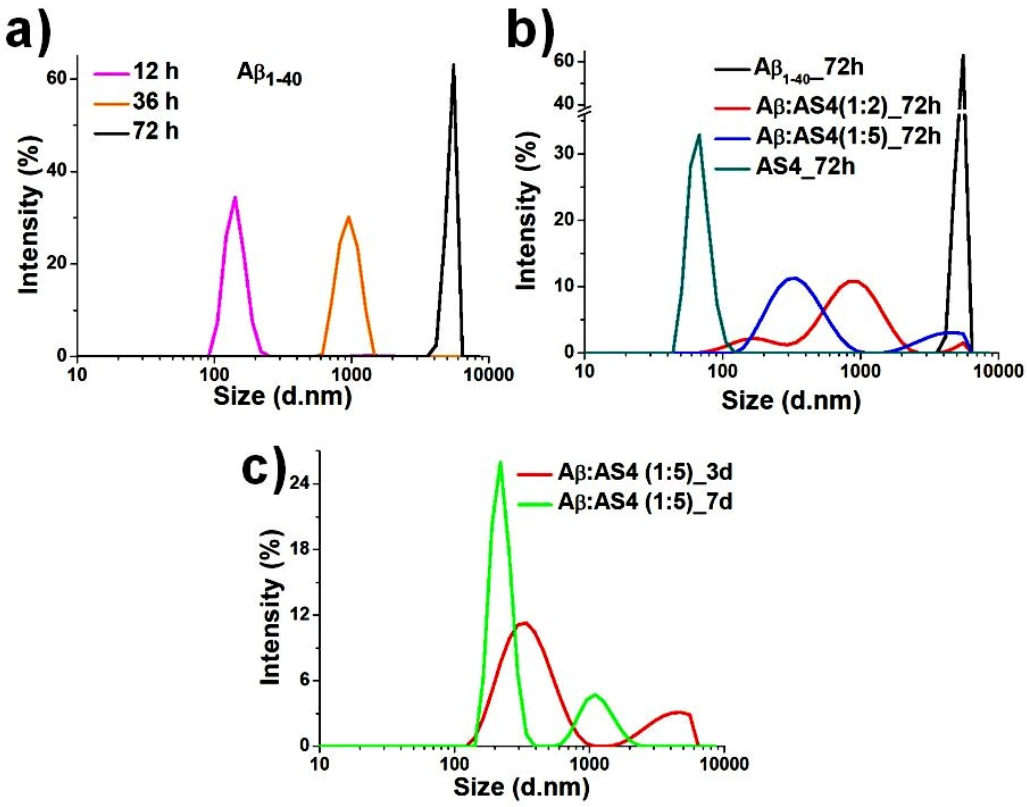

Figure S104. Overlay of DLS profiles of (a) $A\beta_{1-40}$ at various time points, (b) $A\beta_{1-40}$ (black), in presence of 2 fold (red), 5 fold (blue) molar excess of AS4, and AS4 (dark cyan) at 72h, and (c) $A\beta_{1-40}$ (black) in presence of 5 fold molar excess of AS4 after 3 days (red) & 5 days (green).

24.Preparation of large unilamellar vesicles (LUVs) and carboxyfluorescein entrapment:

Large unilamellar vesicles (LUVs) were prepared by mixing three different lipids; DPPC, Cholesterol and GM1 with 68:30:2 molar ratios. At first, lipids were solubilized in chloroform and methanol (2:1) to make 2 mM stock solution in a glass vial and solvents were evaporated completely using nitrogen gas followed by vacuum to make lipid films. The lipid films were hydrated with carboxyfluorescein (200 μM, 500 μL) in 50 mM HEPES buffer of pH 7.4. After that, the solution was vortexed vigorously for 30 min for emulsification. Then, the glass vial was dipped into liquid nitrogen for instant cooling and after 5 min the frozen solution was dipped into water bath at 50-60 °C, and the procedure is known as thawing process which was repeated for five times. Excess dye was removed by ultracentrifugation at 20000 rpm for 30 min at 10ºC. Supernatant dye solution was discarded and the lipid pellet was re-hydrated with 50 mM HEPES buffer of pH 7.4. This step was repeated twice and the final lipid pellet was collected. Next, 500 μL of HEPES buffer of pH 7.4 was added to the lipid pellet and vortexed to obtain homogenous suspension, which was filtered through 0.45 μm polycarbonate membrane to obtain dye loaded LUVs (2 mM). The formation of LUVs was characterized by transmission electron microscopy (TEM) from negatively stained sample over carbon coated copper grid using 2% uranyl acetate solution.

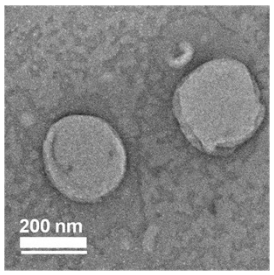

Figure S105. TEM image of negatively stained LUVs. The concentration of the sample was 100 μM. Scale bar is indicated as 200 nm.

25. Vesicle leakage study:

Three sets of peptide solutions were used for the vesicle leakage studies along with untreated LUVs: (A) $A\beta_{1-40}$ (incubated for 24 h), (B) $A\beta_{1-40}$ (incubated for 10 days), (C) $A\beta_{1-40}$ and AS 4 (1:5, AS 4 was added to the preformed fibrillar aggregates after 72 h and incubated for 10 days). Peptides and lipid were taken in 1:20 molar ratios and the entrapped dye (carboxyfluorescein) release was monitored by fluorescence emission. Emission was recorded for each 20 min interval up to 120 min, and then 12 h interval up to 72 h. Emission and excitation were measured at 516 nm and 485 nm respectively, using 5 nm of band width on a Fluoromax-4, Horiba instrument. Finally 10 μL of Triton X-100 was added to obtain complete dye release from the vesicle and the final fluorescence was measured. Untreated LUVs (natural dye leakage) were studied and used as control. The % dye release was calculated as,

% Leakage = {(Observed fluorescence −initial fluorescence) / (Total fluorescence −initial fluorescence)} × 100%

The graph was plotted using Origin Pro 8 software from text file, and average was taken with observed standard deviation of three independent measurements for each data point.

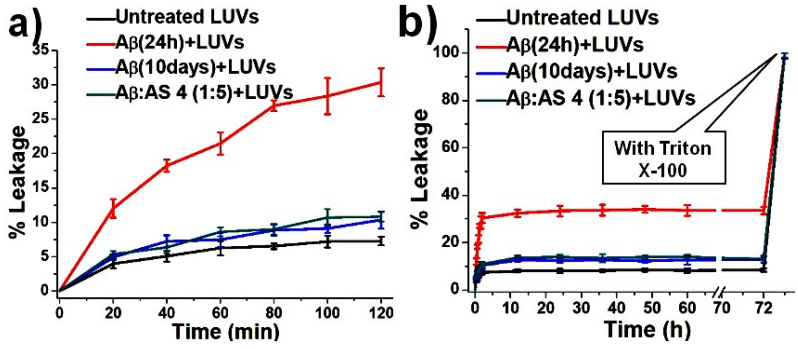

Figure S106. % dye (carboxyfluorescein) leakage from LUVs up to (a) 120 min and (b) up to 72 h; by untreated LUVs (black), LUVs treated with 24 h old Aβ protofibril (red), LUVs treated with 10 days old mature Aβ fibril (blue), and LUVs treated with 10 days old Aβ:AS4 sample (green).

References

[1] Coin, I.; Beyermann, M.; Bienert, M. *Nat. Protoc.* **2007**, 2, 3247-3256.

[2] Nilsson, M. R. *Methods* **2004**, 34, 151–160.

[3] Manavalan ,P.; Johnson, W. C. *Nature* **1983**, 305, 831–832.

[4] Peng, J. et al. *Sci. Rep.* **2015**, 5, 10171.

[5] Larson, M. E.; Lesne, S.E. *J. Neurochem.* **2012**, 120, 125–139.

[6] Trott, O.; Olson, A. J. *J. Comput. Chem.* **2010**, 31, 455-461.

[7] O. Crescenzi *et al*. *Eur. J. Biochem*. 2002, **269** , 5642−5648.